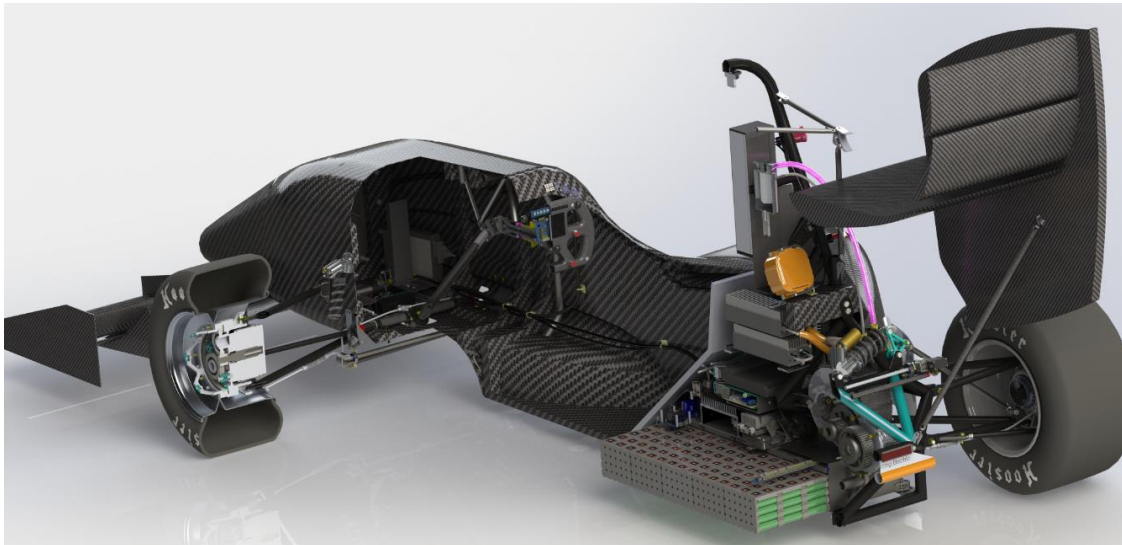


ME 351 - Formula Electric In-Hub Motor System for Formula SAE Electric



WISCONSIN
UNIVERSITY OF WISCONSIN-MADISON



University of Wisconsin - Madison

Authors: William Kucinski, Rocky Liang, Chad Davis, Matt Masucci

Issue 1.1 – 02/10/2017

Foreword

This report is written to present the collaborative efforts of a motivated group of individuals, determined to improve upon Wisconsin Racing's legacy of excellence in design, manufacturing and teamwork. Wisconsin Racing has entered the field of sustainable transportation with the development of the team's first fully electric vehicle set to compete in 2017. The WR-217e project began in early 2016 with a group of six motivated combustion members and has grown to become a full second branch of Wisconsin Racing.

A senior design team has been created to assist in the research, design and implementation of the front in-hub motor package for the WR-217e. This team is tasked with determining the optimal solution for Wisconsin Racing that meets the design specifications and sets the team up for continued success.

Abstract

This report details the development phase of the WR-217e architecture. First, an in-depth analysis of the key performance metrics for the system is performed. Once the key parameters for the vehicle were obtained, various concepts were developed and compared to select the final design decisions. The transmission system was designed in Solidworks and analyzed with student developed analysis tools, Solidworks finite element analysis and KISSsoft. The combination of three analysis techniques resulted in an in-depth investigation along with multiple verifications. The manufacturing design and documentation is provided for each component in the assembly. The report ends with the discussion of the possible impact on the FSAE Electric competition and commercial industry.

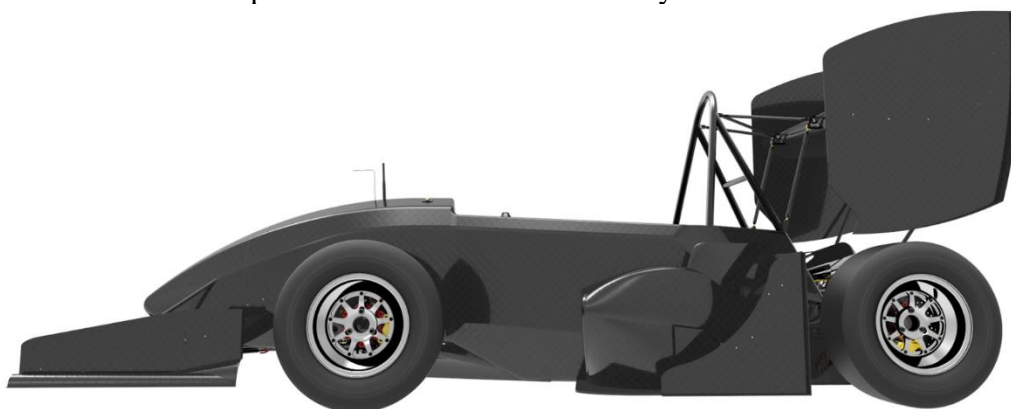




Table of contents

The Authors

Acknowledgements

Background

Motor Analysis

Transmission Ratio

Drivetrain Concepts

Planetary System

KISSsoft

System Design

Upright Design

Wheel Center Design

Brake System Design

Brake Caliper Design

Final Design

Manufacturing Design

Commercial Viability

Sources

Appendix



The Authors

The authors of this report are four students enrolled in the University of Wisconsin-Madison's Mechanical Engineering Capstone Design course. This is one of two design projects given to students with a deep interest in sustainable transportation and a motivation to develop a novel solution capable of pushing the Formula SAE Electric competition in the United States to another level.

The primary goal of these projects is to give the Wisconsin Racing team the design support necessary to develop the electric vehicle within one academic year. The secondary motivation of this project is to provide a well-documented report of the development of a high voltage powertrain capable of competing at the international level. The team saw a large gap in the level of design between Formula Student and Formula SAE and is therefore developing an open platform to aid in the development for Formula SAE Electric.



William Thomas Kucinski
Project Leader
Architecture Design and Analysis
Technical Director Formula SAE Electric

Education Focus

Billy's focus has been on structural and machine element design with a co-focus on engineering management. Through four years of Formula SAE on the Wisconsin Racing team, he has worked in nearly every area of vehicle design, manufacturing, testing, procurement, sponsorship, graphic/digital design and management.



Matt Masucci
Communicator
Brake Design and Analysis Support

Education Focus

Matt's focus has been on powertrain development. He has worked as a member of the combustion car for the last 3 years and has worked in several powertrain development positions in industry. The work with the electric brake system provided him with valuable design experience through an interesting design challenge.



Chad Davis
Admin
Planetary Design and Analysis Support

Education Focus

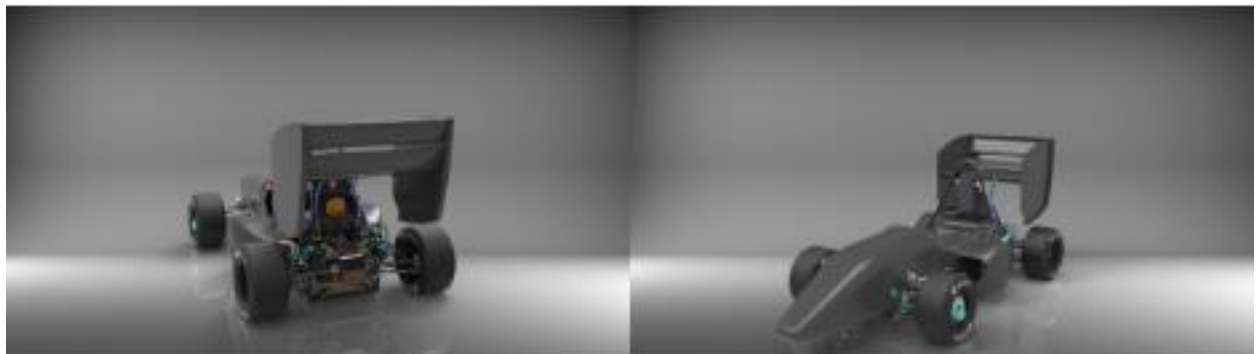
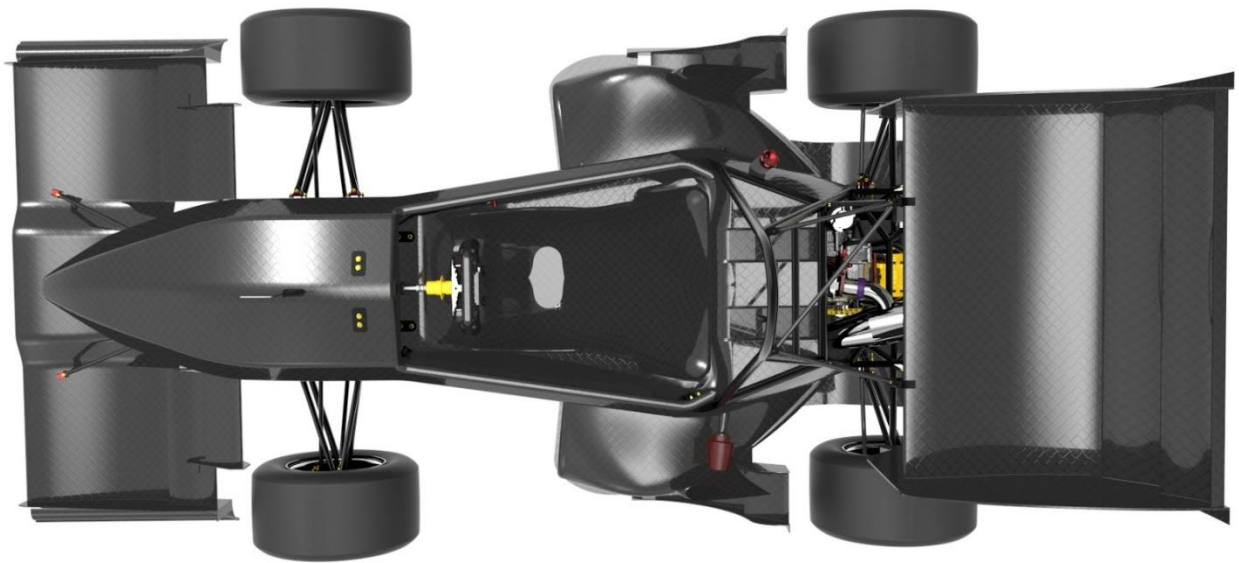
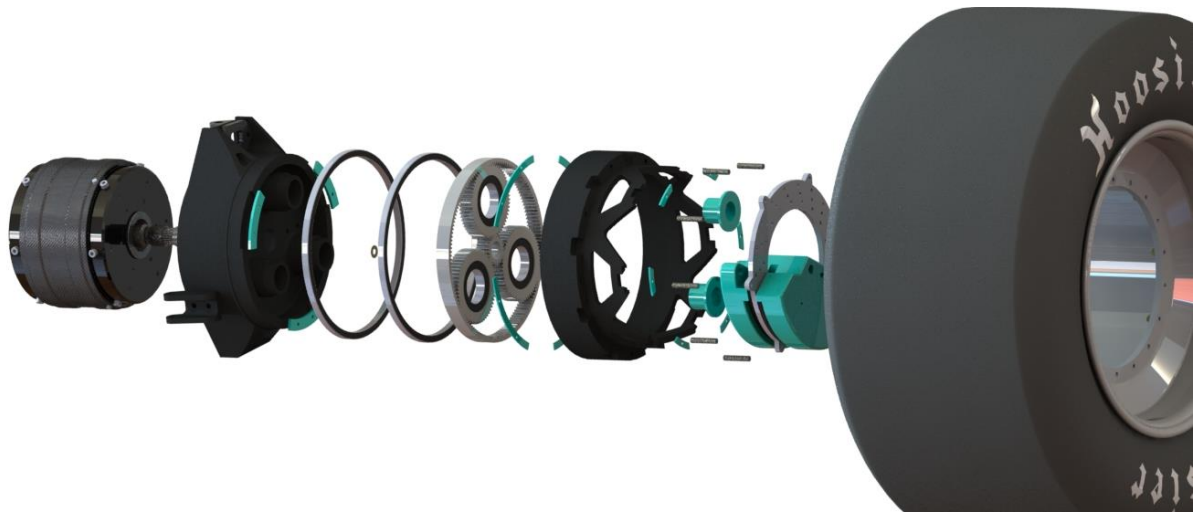
Chad's interested in electric motors and electric vehicle design with a sub-interest in green energy sources. He is currently an undergraduate research assistant with WEMPEC and a proud member of the Formula SAE Electric Team.



Rocky Liang
Accountant
Wheel Center Design and Analysis Support

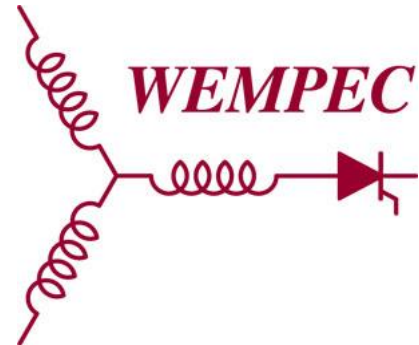
Education Focus

Rocky intends to specialize in controls and automation, as well as electrification of vehicles. He has conducted research in fuel spray visualization and is currently a member of UW's manufacturing lab.





Acknowledgements



Concept

Formula SAE is based on building a team and acquiring the resources necessary to create a fictional manufacturing company that is contracted to develop a small Formula-style race car. The teams compete to show their prototype has the highest potential for production. The target market for these vehicles alters slightly from team to team but is majorly based on the non-professional weekend autocross racer. Each student team researches, designs, builds, tests and competes with their prototype at multiple events around the globe. The vehicles are designed to a series of rules, whose purpose is to ensure on-track safety and promoting well developed engineering principles and problem solving.

Wisconsin Racing Mission

The mission of Wisconsin Racing is to take the knowledge gained through coursework and work with industry partners and apply that knowledge to the development of innovative formula-style vehicles. Wisconsin Racing is dedicated to pushing the status quo, developing broadly experienced students and having fun in the process. The team consists of nearly one hundred members who apply their knowledge to various aspects of the design, manufacturing and business aspects of the team. To a Wisconsin Racing team member, FSAE is valuable platform to develop their skills and express their creativity.





Events

The Formula SAE competition incorporates both static and dynamic events to test the engineering principles applied to the vehicle, the manufacturing quality, and the overall performance of the vehicle in relation to the competitors.

Static Events

Business presentation: The business presentation is an event structured to pitch the prototype design and manufacturing techniques to potential investors. Each team is allowed ten minutes to entice the investors in the business and explain the marketing plan to manufacture one thousand vehicles per year.

Cost Event: The cost event requires each team to document the cost associated with each vehicle component as well as the methods used to manufacture and assemble the vehicle. The event challenges students to present the correct documentation and answer questions focused on manufacturing and sustainability.

Design: The design event is the pinnacle event to many of the teams as you are allotted forty minutes to explain the theory and analysis behind the design and development of the car to a panel of world class engineering judges. Winning this event directly highlights the team's superiority of engineering knowledge. A first place in vehicle design is almost as prestigious as an overall competition victory.

Dynamic Events

Acceleration: A seventy-five meter drag race event designed to prove the car's longitudinal acceleration capability.

Autocross: This event is a one lap time trial and is the most technically challenging of all the dynamic events. The driver must use proper driving technique and show superior skill over the other teams. This is the most prestigious of the dynamic events as it provides a method to show which vehicle and driver combination best utilized their understanding of vehicle dynamics and testing.

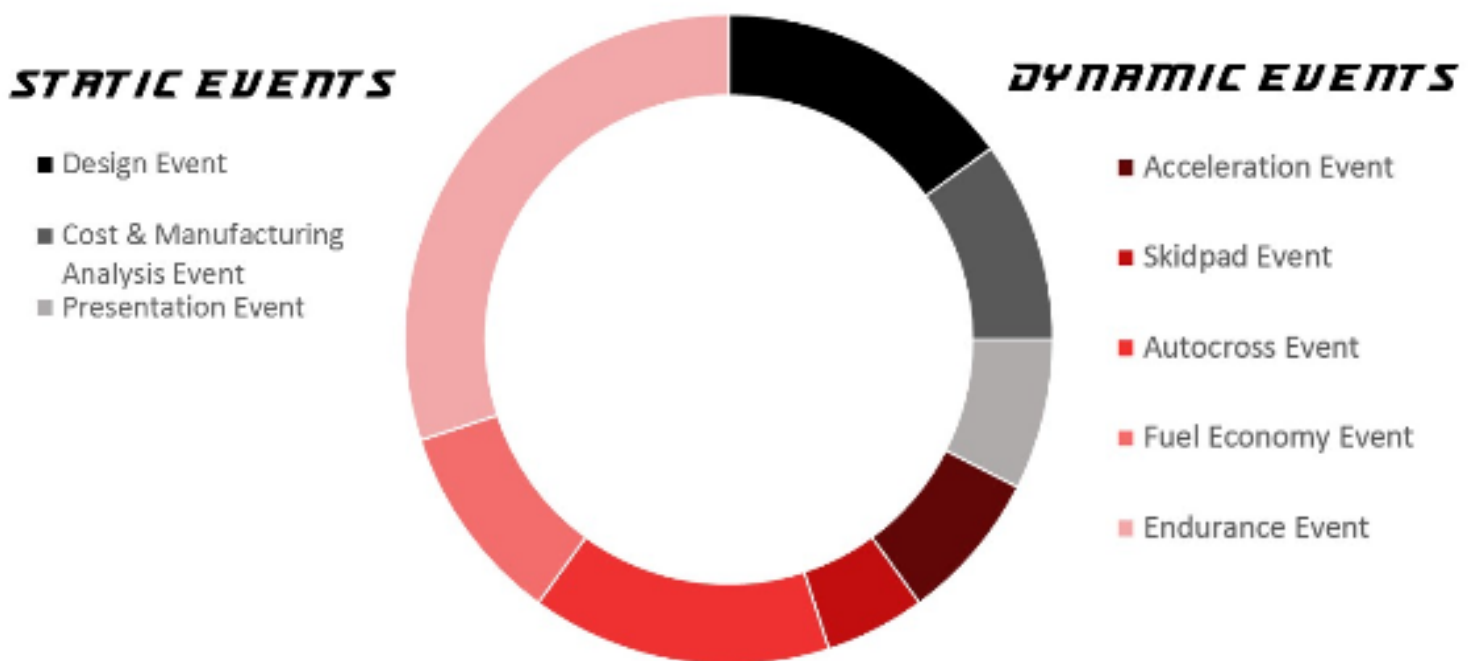
Endurance: The endurance event is by far the most demanding event on the vehicle as it consists of 20 laps with a pit stop and driver change totaling a twenty-two kilometer race. This event tests the reliability, fuel economy and race strategy of the teams. This event has by far the highest failure rate of any event in the competition. Nearly fifty percent of the vehicles will not complete this event at the World Championship held in Brooklyn, Michigan.



Skid pad: This event consists of a right and left hand circle and tests the steady state cornering ability of the vehicle.

Efficiency: This event scores the team on the amount of consumed fuel or energy during the endurance event. The winning team shows a deep understanding of the losses incurred in the operation of a vehicle and a superior ability to efficiently utilize their fuel or energy.

THE COMPETITION



Project Overview

Since the automotive industry is desperately searching for alternative propulsion solutions to non-renewable fossil fuels, electric vehicles have grown in popularity. As an automotive design training program, the University Of Wisconsin chapter of the Society of Automotive Engineers has become increasingly dedicated to finding solutions to the growing environmental issues related to the pollution of our atmosphere. Currently the UW-Madison SAE Chapter runs ethanol (E85, supplied by the Diamond Sponsor UWGP) in the Formula Combustion vehicle and in the Clean Snowmobile and Hybrid vehicle.

In light of the growing market for electric vehicles, the chapter made the bold decision to build two FSAE vehicles starting in 2017. One high efficiency turbocharged combustion vehicle and one all-wheel drive fully electric vehicle. The addition of electric vehicle allows for a massive expansion of engineering challenges for the UW-Madison Automotive students.

The students on the team are now exposed to the design of custom batteries and electrical circuitry, both high and low voltage systems, as well as electric motor controls and calibration, electric motor design, transmission design and many other electrical and mechatronic design projects. This exposure will not only prepare the students for the ever-growing automotive market, but will also place them at the forefront of that design.

Wisconsin Racing's early move into the Formula Electric competition will also allow the organization to get a jump on the competition in an effort to stay ahead and drive innovation. Wisconsin Racing has always prided itself on a devotion to pushing the boundaries and will continue to do so through a modular platform chassis allowing both the electric and combustion vehicle to utilize the same aerodynamics package and monocoque chassis along with many low level components. Wisconsin Racing, "One Team | Two Cars", 2017.





- 1 The in-hub motor design must comply with 2017 - 2018 FSAE Electric Rules
- 2 The in-hub motor system must incorporate Plettenberg Nova 15 Motors this year
- 3 The system must decrease the output speed of the motor by a minimum of 6 to 1 while staying within the geometric design space allotted by the suspension kinematics.
- 4 The system must minimize the unsprung mass of the corner assembly while achieving a minimum safety factor of 1.5 and a design life minimum of 69 hours.
- 5 The system must be designed within the manufacturing and funding limitations of the Wisconsin Racing team and Wisconsin Racing Sponsors.
- 6 The system must last the entirety of the 2017 season, while the motors must last for a minimum of 4 seasons.
- 7 Dedicated year - to - year sponsors must be obtained to ensure the sustainability of the addition of a second vehicle to the Wisconsin Racing Team.
- 8 Full documentation and adequate knowledge transfer of all design, manufacturing, assembly and testing must be provided to the rising team members to ensure future success.
- 9 Documentation must be made public for reference to Formula Electric teams looking to enter the competition.
- 10 The system must be designed to allow torque vectoring and regenerative braking.



Target Market

The primary target market is the Wisconsin Racing team including the driver and engineering students. The secondary target market is the fictional weekend auto-cross enthusiast as specified by the competition.

Driver

The in-hub motor system must be designed for a symbiotic relationship with the driver. Due to the added mass of the front corner a detailed analysis of the steering force must be conducted. The driver must also be able to operate the vehicle seamlessly with the torque vectoring and regenerative braking algorithms. Extensive on-track testing must be conducted to properly tune the vehicle for each individual driver to ensure minimum lap times and energy consumption.

Team Members

The in-hub motor design must be designed to work within the kinematic constraints of the vehicle to ensure the optimal dynamic behavior of the vehicle. The upright incorporates an adjustable pillow block on the upper A-arm to allow chamber variation adjustments. This addition allows the race engineer to test multiple set ups for the vehicle. The system must also be designed with an ease of inspection and adjustment as to not delay testing time.

Weekend Auto-Cross Enthusiast

Based on a survey of 500 potential customers who attended various events at Road America in Elkhart Lake, Wisconsin, it was determined that the three most important factors in our target consumer's purchasing decision are performance, reliability, and cost. It has also been determined that there is a clear place for the WR-217e in the existing market of autocross/track-day vehicles in the price and performance gap between shifter karts and single seat open-wheelers. Electronic surveys were also sent LMP1, WEC racing and Formula E enthusiasts in the Midwest.





Vehicle Dynamics

The brief introduction to vehicle dynamics is necessary due to the sensitivity of the drivetrain to the kinematic design of the vehicle. At the most basic level vehicle dynamics studies the motion of the vehicle based on the forces and torques acting on the chassis. The torque created by the motor must travel through the transmission system and into the tire through the wheel. The tire then reacts the torque through the contact patch and accelerates the vehicle.

In order to select the motors for the vehicle, a study to determine vehicle sensitivity to available torque and grip at the tire was conducted. The vehicle is operating in one of three states. At the traction limit, torque limited or perfectly riding the traction limit. Oversizing the motors to be traction limited at all times results in excessive weight, whereas under sizing the motors results in increased lap times due to underutilization of the available grip of the tire. Therefore the motors and transmission system must be designed based on the available grip of the tires.

The available grip of the tires can be estimated based on test data provided by Calspan for the Hoosier tires used in Formula SAE, specifically the LCO and R25B tires. The testing data provides the available grip of the tire based on the load case and geometric relation of the tire to the ground and velocity of the vehicle. With a student developed lap time simulation tool in Matlab, a quasi-steady state two track model is utilized to calculate the available grip and therefore aid the selection of the motor and necessary gearbox.

The lap simulator takes in various vehicle parameters such as the vehicle mass, motor torque speed diagram, accumulator (battery) parameters, vehicle center of gravity, estimated coefficient of friction for the tires and runs a time based simulation of the vehicle moving through a competition-representative track. For each time step, the model calculates the available grip of each tire and the available torque. The default is to ride the traction limit whenever possible to minimize lap time.

This model was run with a multiple motor combinations to determine the optimal power split between the four wheels. Due to the competition regulations the vehicle is never allowed to use more than 80 kW. Therefore a series of simulations were conducted to select the most efficient and lowest lap time.

This resulted in a power split of twenty-five percent to the front wheels and seventy-five percent to the rear wheels. This split makes sense with even the most basic understanding of load transfer. In short, during acceleration seventy-five percent of the normal load will be on the rear tires and therefore seventy-five percent of the available power will be usable at the rear wheels.

The reverse load transfer occurs during braking, and to maximize the amount of possible regenerative braking it would be intuitive to desire seventy-five percent of the available power at the front. However, based on the design of the accumulator, the split of seventy-five percent rear

and twenty-five percent front is capable of charging the battery at its peak charge rate and therefore the larger motor is not necessary for the front wheels under braking.

Torque Vectoring

Perhaps the most beneficial performance gains of the electric vehicle are the ability to control all four wheels independently through a novel torque vectoring algorithm. Torque vectoring is a method of distributing power to the four tires of the vehicle based on current vehicle state determined from the use of multiple sensors. The use of electric motors is particularly suited for torque vectoring due to the more instantaneous torque response of the motor versus a combustion engine.

The major vehicle dynamics parameter that benefits is the ability to “yaw” or rotate the vehicle. The ability to quickly change the vehicle’s direction of travel allows the driver to brake later when entering a corner and rotate the car out of the corner quicker. The vehicle will have a steady state maximum grip capability which cannot be increased by the algorithm but the vehicle can reach this steady state quicker, therefore allowing the car to keep a higher average speed.

A second major benefit of torque vectoring is that it allows the electric powertrain to compensate for imperfections in the setup of the chassis. Due to errors in manufacturing or vehicle setup, the car may exhibit understeer or oversteer tendencies at different speeds. This can now be corrected as the onboard computer can artificially balance the car during steering maneuvers. These corrections are achieved through the application of positive or negative (acceleration or braking) torque.

These benefits are the key driving forces behind the development of the all-wheel drive architecture for the WR-217e. The report defines the driving decisions and constraints imposed on the design of the vehicle and the analysis behind each component in the front in-hub assembly.



Collaboration



Max Liben
Powertrain Architecture, Vehicle Dynamics Simulation & Controls
Team President Formula SAE Electric



Nils Justin
Brake System Support



Will Sixel
Controls, Thermal Modeling



Motor Analysis

This report highlights the investigation of three motors which are viable for the application to an FSAE Electric vehicle. The first of the three motors is produced by a small company in Southern California that specializes in custom motor design. They offered to investigate designing a custom motor for the Wisconsin Racing team. The second two companies are both located in Germany. Plettenberg designs motors within the 300V max voltage limit for the competition, whereas AMK designs a 600V system but sells a package specifically for Formula Student.

A quality function deployment chart was created to compare the three motors and aid in the selection of the best suited solution. The categories were created based on the motor parameters, financial limitations of the team, reliability of the system and the availability of the motor and replacement components.

From this study, the AMK package proved to be the best suited motors for the application. However due to the voltage regulation of the U.S competition, the team was unable to utilize those motors for the WR-217e. The second place motor was the Plettenberg Nova series.

The Plettenberg Nova series are brushless DC surface permanent magnet motors that come in either liquid cooled or air cooled versions and have paired inverters. While the Plettenberg motors do not provide the desired flux field weakening, they operate within the voltage limit, are extremely power dense and provide both the desired power distribution and maximum torque.

The major contributor to the downgrade of the NeuMotors was due to the availability, reliability and inverter availability. While the company was willing to work with the team to design custom motors, their engineering support did not provide the confidence necessary to go through with the relationship. Secondly, the company did not specialize in inverter design and the inverter companies willing to sponsor the team were not willing to do the work necessary to pair the controller.



Table1: Quality Function Deployment for Motor Selection

<u>Category</u>	<u>Multiplier</u>	<u>NeuMotors 4430</u>		<u>Plettenberg Nova Series</u>		<u>AMK</u>	
		<u>Score</u>	<u>w/Multiplier</u>	<u>Score</u>	<u>w/Multiplier</u>	<u>Score</u>	<u>w/Multiplier</u>
<u>Cost</u>	<u>2</u>	<u>10</u>	<u>20</u>	<u>3</u>	<u>6</u>	<u>3</u>	<u>6</u>
<u>Cooling Jacket</u>	<u>4</u>	<u>1</u>	<u>4</u>	<u>9</u>	<u>36</u>	<u>9</u>	<u>36</u>
<u>Operating Voltage</u>	<u>5</u>	<u>10</u>	<u>50</u>	<u>6</u>	<u>30</u>	<u>1</u>	<u>5</u>
<u>Product Quality</u>	<u>3</u>	<u>6</u>	<u>18</u>	<u>8</u>	<u>24</u>	<u>9</u>	<u>27</u>
<u>Weight</u>	<u>3</u>	<u>8</u>	<u>24</u>	<u>7</u>	<u>21</u>	<u>7</u>	<u>21</u>
<u>Outside Diameter</u>	<u>4</u>	<u>7</u>	<u>28</u>	<u>6</u>	<u>24</u>	<u>9</u>	<u>36</u>
<u>Length</u>	<u>3</u>	<u>6</u>	<u>18</u>	<u>7</u>	<u>21</u>	<u>4</u>	<u>12</u>
<u>Lead Time</u>	<u>3</u>	<u>5</u>	<u>15</u>	<u>3</u>	<u>9</u>	<u>4</u>	<u>12</u>
<u>Available Testing Data</u>	<u>5</u>	<u>1</u>	<u>5</u>	<u>8</u>	<u>40</u>	<u>9</u>	<u>45</u>
<u>Peak Torque (post-transmission)</u>	<u>5</u>	<u>5</u>	<u>25</u>	<u>7</u>	<u>35</u>	<u>8</u>	<u>40</u>
<u>Max Motor Speed / Required Gear Reduction</u>	<u>4</u>	<u>8</u>	<u>32</u>	<u>8</u>	<u>32</u>	<u>3</u>	<u>12</u>
<u>Mounting Design</u>	<u>2</u>	<u>3</u>	<u>6</u>	<u>5</u>	<u>10</u>	<u>5</u>	<u>10</u>
<u>Reliability / System Complexity</u>	<u>5</u>	<u>3</u>	<u>15</u>	<u>8</u>	<u>40</u>	<u>6</u>	<u>30</u>
<u>Availability of Compatible Inverter</u>	<u>5</u>	<u>1</u>	<u>5</u>	<u>10</u>	<u>50</u>	<u>10</u>	<u>50</u>
<u>Inverter Flux Weakening Capability / FOC</u>	<u>2</u>	<u>3</u>	<u>6</u>	<u>1</u>	<u>2</u>	<u>9</u>	<u>18</u>
<u>Inverter Current Control</u>	<u>3</u>	<u>3</u>	<u>9</u>	<u>2</u>	<u>6</u>	<u>9</u>	<u>27</u>
<u>Inverter Communication</u>	<u>3</u>	<u>3</u>	<u>9</u>	<u>1</u>	<u>3</u>	<u>9</u>	<u>27</u>
<u>Peak Power</u>	<u>5</u>	<u>5</u>	<u>25</u>	<u>8</u>	<u>40</u>	<u>9</u>	<u>45</u>
	<u>Final Score</u>	<u>88</u>	<u>314</u>	<u>107</u>	<u>429</u>	<u>123</u>	<u>459</u>



Transmission Ratio

The transmission ratio for the in-hub motors was driven from three main sources, the geometric packaging limitations, the achievable acceleration time and the top speed of the vehicle.

1 The WR-217e in-hub motor design requires the system to be packaged within the suspension geometry and the exterior plane of the tire, as well as within an outside diameter equal to the bore in the Keizer 10" aluminum wheel shells.

2 Lap simulation for the vehicle showed that between a gear ratio of 6.5 and 7 there was a negligible loss in lap time. The final 6 to 1 was selected as it allowed for adequate material to be on the sun gear while the staying as close to possible to the desired transmission ratio range previously specified.

The vehicle acceleration is particularly important in the architecture trade analysis as it has a very high return on investment for points at competition. Implementing motors for the front wheels of the vehicle increases the capable acceleration by nearly thirty percent.

3 Setting a vehicle top speed also plays a significant role in the vehicle design pending the output speed of the motor. The vehicle top speed is designed at 70 mph due to the maximum speeds seen during the acceleration event as well as the vehicle averaging 35 mph during the autocross and endurance events.

Drivetrain Architecture

There are three main techniques used in the drivetrains of common transportation devices. These are the chain drive, belt drive and gear drive. Each device transfers the torque from the output shaft of the propulsion mechanism and transfers it to a second shaft either increasing or decreasing the torque and speed.

1 Formula SAE combustion heavily utilizes the chain drive architecture due to the common implementation of motorcycle engines, predesigned for chain sprockets. The chain drive system is very simple and much more inexpensive as compared to gears. However, if a large gear reduction is necessary, as with electric motors, the secondary sprocket size increases dramatically. The chain drive system also suffers from chain extension requiring constant maintenance for slack in the chain. Finally a chain drive system also has a backlash an order of magnitude larger than that of a gear drive. This backlash leads to a decrease in vehicle performance by slight delays in vehicle response to driver input. Of even more importance the backlash in the system will create “impact” loads on the sprocket teeth and chain. These impact forces occur each time the drive steps on and off the throttle which leads to fatigue of drivetrain components- this is a particular issue of interest due to most team utilizing an aluminum sprocket.

2 A belt drive system experiences nearly all of the same negative effects of the chain drive with slight decreases in the amount of backlash and impact loading. The operating noise of the belt drive is also lower than that of the chain driven system.

3 The final architecture is that of the gear. Either spur or helical gears can be utilized for a gearbox. While the helical gear can transmit higher torques than the straight cut spur gear, they have higher losses due to increased friction. Gears have the ability to be paired in multiple combinations to increase the gear ratio. The downfall to the gear architecture is the system becomes much more complex and cost increases substantially.

Even with the increased complexity and cost, gears are the optimal choice for many automotive applications due to their precision. The gearbox also allows for nearly seamless torque transmission decreasing the lag time in torque to the wheel from the driver input.

Gears have been selected for the use in the front in-hub motors since a chain or belt drive is particularly unfeasible and the reduction of backlash and a large deduction in a small area are necessary. Gears were also selected for the rear drivetrain for similar reasons.

Gear Drives

Due to the geometric constraints on the in-hub design, a planetary design is necessary; however, before this decision is made, a full investigation of the possible drivetrain configurations must be performed.

Configuration one

The first configuration investigated for the all-wheel drive system places two Plettenberg Nova 30 motors inboard in the rear with a two stage single speed reduction utilizing tripods and half shafts. The front utilizes two Plettenberg Nova 15 motors inboard with a ninety degree transmission box mounted to the side of the monocoque along with half shafts and tripods to get the torque to the wheels.

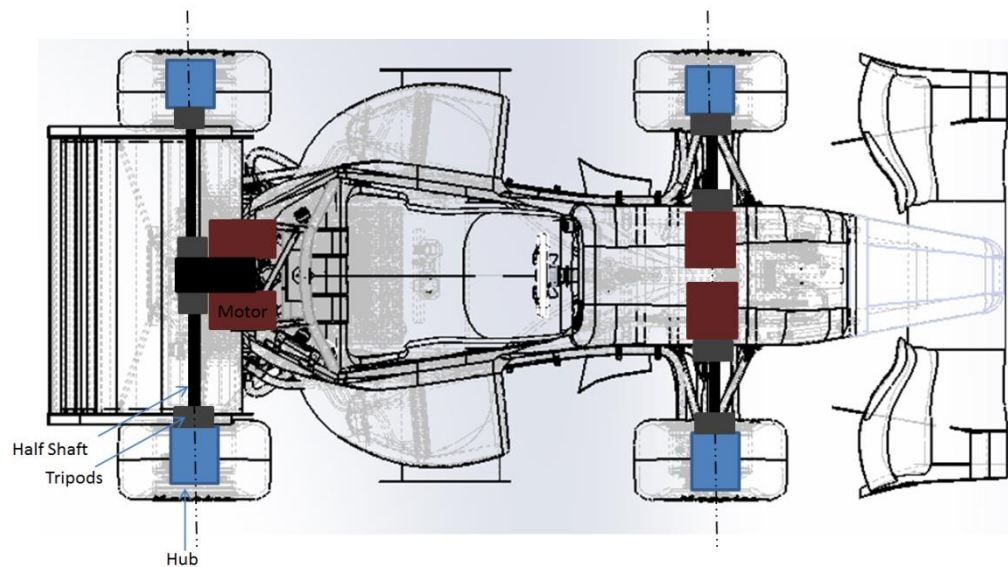
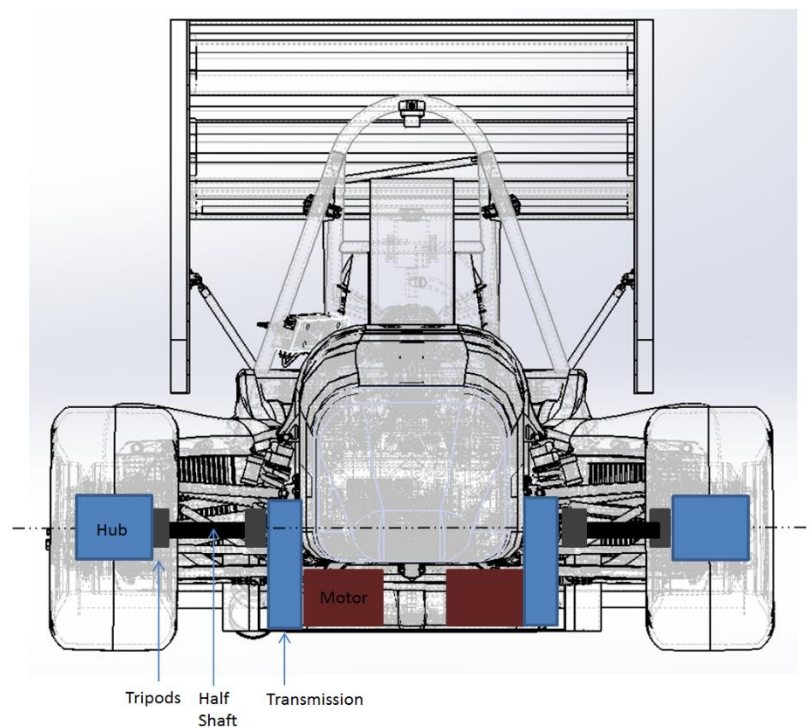


Figure 1: Four Inboard Motors Top View

This configuration optimizes the power split between the front and rear wheels during acceleration to maximize the traction limit. The architecture also keeps the mass inboard which improves vehicle dynamics in comparison to adding outboard mass.

The downfall of the system is the limited geometric constraints under the monocoque causing an alteration in chassis design to fit the motor under the driver's feet.



Configuration Two

The second configuration investigates the opposite approach and packages all four Plettenberg Nova 15 motors outboard. This approach would minimize mass of the vehicle while also decreasing the necessary design and analysis work by approximately ½ due to using the same In-hub motor design for each corner.

This system dramatically decreases cost due to the elimination of the gearbox housing, CV joints, ½ shafts and material necessary. The reduction of components will also increase the efficiency of the system. However due to the size of the motors, the Nova 30s would not package within the wheel and therefore the system peak power decreases from 90 kW to 60 kW.

The mounting position of the front motors is now higher, which increases the CG. This configuration also results in decreased power and added unsprung mass which all degrade the vehicle dynamics of the car.

Overall this configuration allows for a more unified manufacturing approach but degrades multiple performance metrics.

Figure 2: Four Inboard Motors Front View

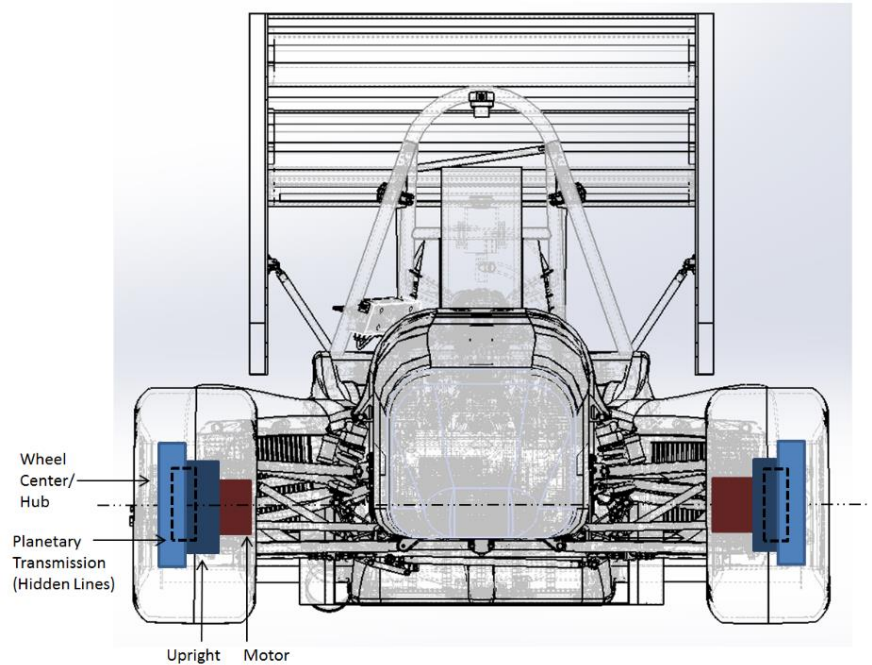


Figure 3: Four Outboard Motors Front View

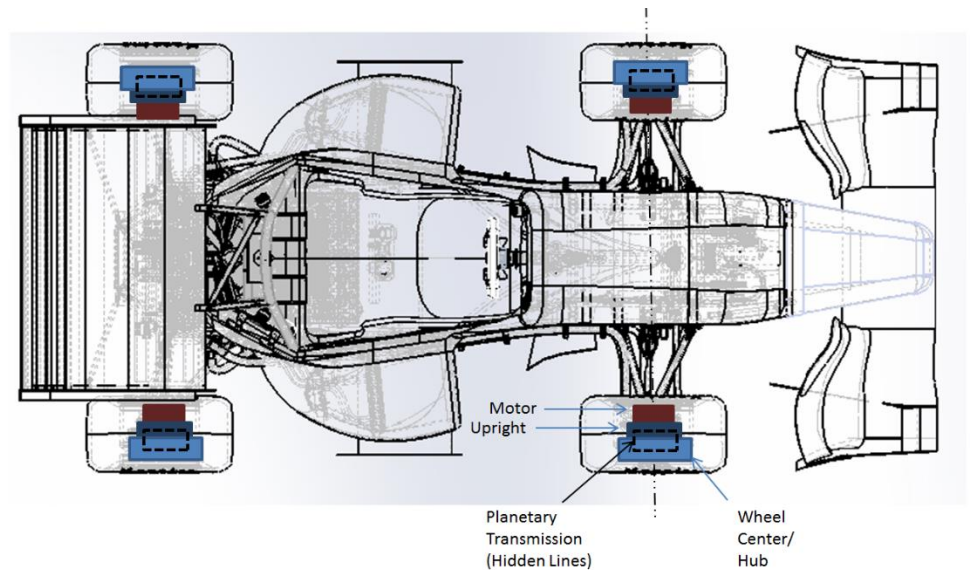


Figure 4: Four Outboard Motors Top View

Configuration Three

Configuration three takes advantage of the benefits of both systems while minimizing the drawbacks of each.

The front in-hub motor design allows for the implementation of the Plettenberg Nova 15 motors into the front wheels eliminating the CV joints, gearbox, tripods and half shafts, which increases the efficiency.

While the CG of the front corners and the yaw inertia both increase, the slightly higher CG is a design tradeoff that is worth the increase in acceleration capability. The controls strategy for torque vectoring can adequately overcome the increased yaw inertia.

The rear of the vehicle incorporates the Plettenberg Nova 30 motors with a symmetric two stage single speed reduction parallel axis gearbox. The gearbox outputs the torque through two CV joints. Torque then travels through half-shafts to the wheels. This configuration accommodates the larger motors, which achieve the desired 75% power to the rear wheels while keeping the mass sprung and decreasing the number of complex components to be manufactured.

The inertia of the system is also kept to a minimum with the mass located low in the vehicle and along the centerline.

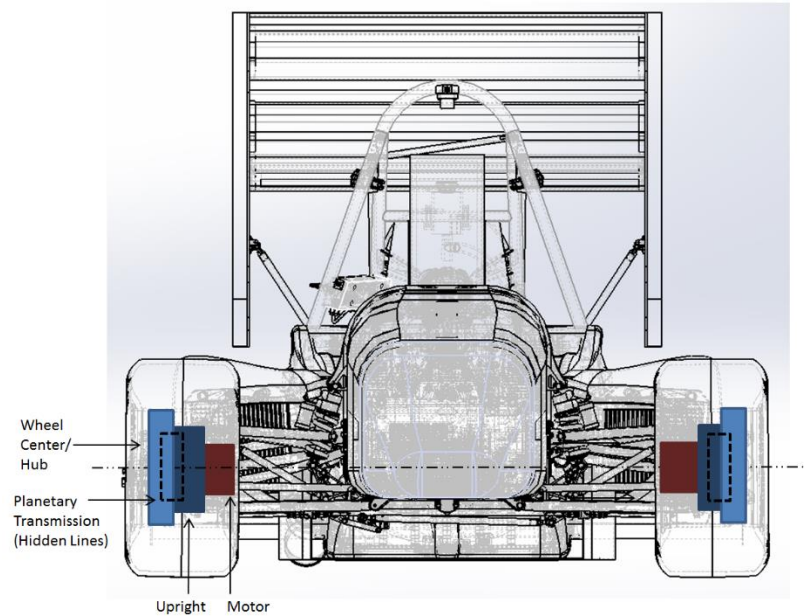


Figure 5: Inboard Front, Outboard Rear Front view

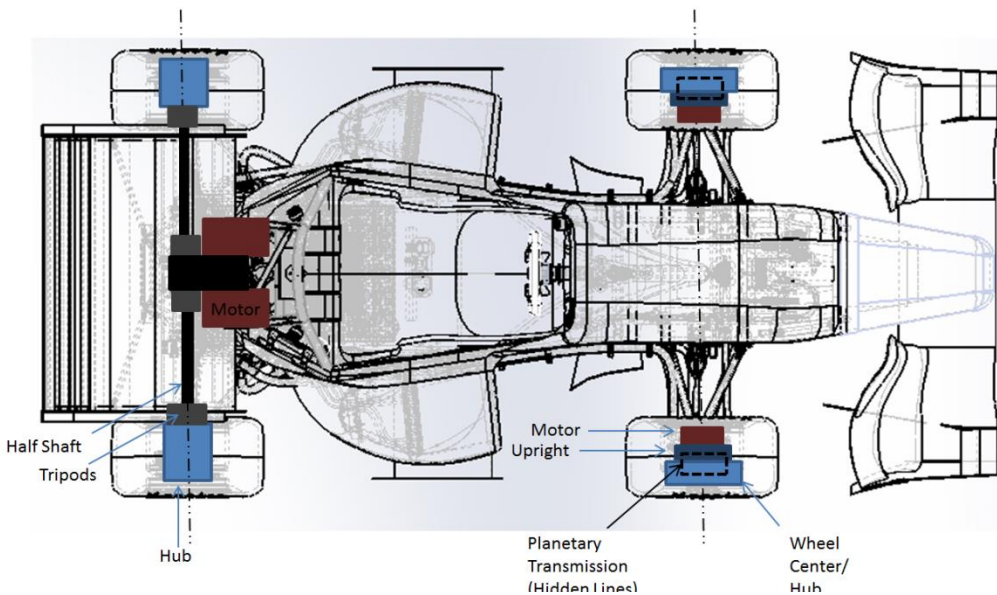


Figure 6: Inboard Front, Outboard Rear Top view



Drivetrain Selection

The three drivetrain concepts are evaluated based on their compliance to the FSAE rules, performance and feasibility of implementation and likelihood of gaining design points at competition. The QFD matrix allows for the quantitative and qualitative analysis of the systems to determine the optimal solution to the design challenge.

The matrix gives a one for red, two for yellow and three for green. Each of the three designs is shown to be fairly equivalent with configuration three rated at a slightly higher score. This is not surprising as each of these three design configuration is utilized in the Formula Student competition and each configuration has shown to develop a vehicle capable of placing in the top three in both design and overall.

The WR-217e will move forward with configuration three for its score in the study as well as its overall feasibility and likelihood to succeed. The independent front and rear transmission designs allow an added safety factor to the vehicle as failure to one system does not render the car un-drivable. This configuration also allows for a larger design challenge.

Table2: Quality Function Deployment for Drivetrain Selection

Drivetrain QFD			
	Configuration One	Configuration Two	Configuration Three
Rules Compliance	Green	Green	Green
Weight	Red	Green	Yellow
Cost	Red	Yellow	Yellow
Performance	Green	Red	Green
Efficiency	Red	Green	Yellow
Reliability	Yellow	Yellow	Yellow
Overall Concept Feasibility	Green	Yellow	Yellow
Desireable Power Split Front to Rear	Green	Red	Yellow
Manufacturability	Yellow	Red	Yellow
Innovation	Red	Yellow	Green
Total	20	20	23

Planetary Design

The planetary design is constrained by both the operating speed of the Plettenberg Nova 15, desired torque, and the geometric design space allotted for the transmission. This allocated area is located between the front face of the motor and the back face of the caliper housing. All of the components of the sub-system must lie within this space. The components are the planetary gears, upright mounting surface, transmission enclosure plate, fasteners, and seals, mounting features and retaining features.

Design Space

The design space for the planetary is indicated below in figure 7. The bold red lines highlight the areas the system must stay within, while the shaded red region highlights the packaged system.

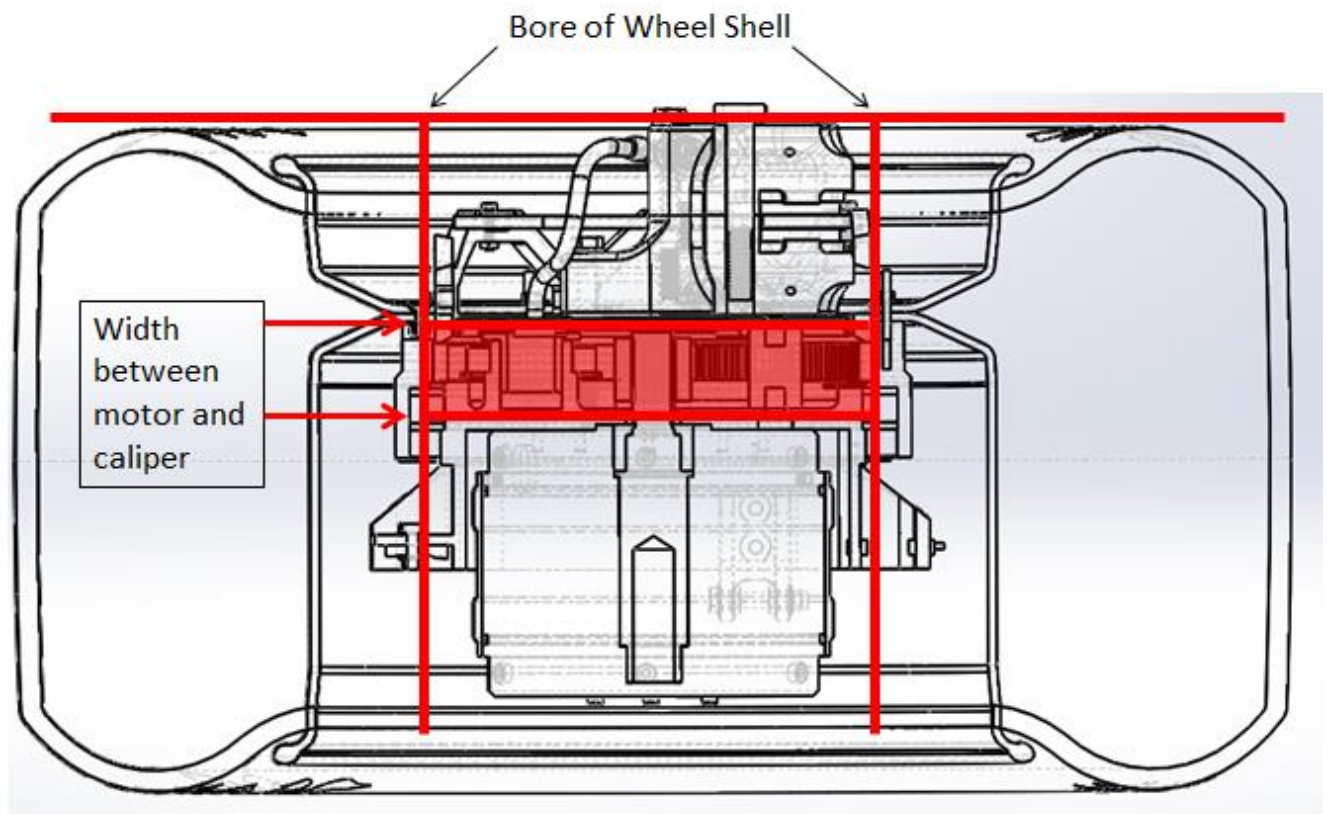


Figure 7: Front In-Hub Motor Transmission Packaging Design Space

Gear parameters

Table 3: Planetary Gear Parameters

Parameter	Value	Unit
Diametral Pitch	24	[teeth/inch]
Pressure Angle	20	[degrees]
Number of Teeth (sun/planet/ring)	24 / 60 / 144	[teeth]
Pitch Diameter (sun/planet/ring)	1 / 2.5 / 6	[inch]
Face Width (sun/planet/ring)	0.9 / 0.5 / 0.5625	[inch]
Addendum	0.04167	[inch]
Dedendum	0.05208	[inch]
Clearance	0.01042	[inch]
Whole Depth	0.09375	[inch]
Train Ratio	6	[-]

We began with a vehicle top speed goal of 70 mph. With the Nova motor's peak speed of 10,000rpm, this required a planetary train ratio of approximately 7.5 to accomplish. To fit within the space constraints of the wheel shell, we aimed for a maximum ring gear pitch diameter of 6". Since our sun gear needed to be mounted to the motor shaft, it needed to have a pitch diameter of at least 0.9" to fit the interior spline while still maintaining strength. To avoid the complications of uneven planet spacing, a particular equation needed to be met regarding the number of teeth in each planetary member: $N_r = 2*N_p + N_s$.

Many different geometries were considered, but in the end a diametral pitch of 24 provided the best balance of train ratio and sun/ring gear size. Once this was set, the other requirements fixed the basic parameters shown in the table above. Unfortunately our train ratio was lower than what we specified, but in the end the geometric constraints were far more important because we simply could not make the motor spline smaller or the wheel shell larger without extensive development and testing.



Material Selection

The material selection of the planetary gears was conducted with an industry partner, Edgerton Gear. Edgerton gear is a well-established gear manufacturing company that has provided the UW-Madison SAE Chapter with gear manufacturing support for multiple years. Edgerton Gear has provided their support through manufacturing tours, design support and rapid manufacturing when needed.

Due to the high loading and tight geometric packaging the gears needed to be optimized to minimize their spatial footprint within the assembly. The manufacturing quality, tolerances, material and polishing were important parameters that all affect the strength of the gear.

With Edgerton's professional experience 4140 was the material selected for the high strength and hardness. The material is supplied pre-hardened to 35 Rockwell C and nitrided post-machining to achieve a surface hardness of Rockwell C 52-55 and depth of 0.015 inches.

The gear is polished to a mirror finish using an isotropic acid drip and tumbling process to achieve a mirror finish quality 12 gear.

Lubrication

The lubrication for the planetary transmission is to be accomplished through a grease as opposed to an oil. Due to the packaging of the planetary assembly sealing is a major design challenge. The transmission will be shielded to exterior through the use of an X-type O-ring operating in a rotary seal fashion while the second side of the transmission is separated from the environment with two angular contact bearings. Testing of multiple lubrications will be conducted both off and on the vehicle.

Manufacturing considerations

Gears have a wide variety of parameters to specify the profile of the gear teeth. A standard gear drawing and gear drawing table were created through the use of the 24th Edition of the Machinery's Handbook. The drawings for the sun, planet and ring gears are provided in the drawings section of this report.

The driving factor in the gear manufacturing was to obtain the highest quality, minimal backlash for proper assembly and hardest surface with as smooth of a surface profile as possible.

Spreadsheet Analysis of Gear Tooth Bending and Wear

During their operation, gear teeth are constantly under bending and contact stresses, too much of which can cause the tooth to wear excessively, deform, or even break off entirely. To ensure that the gear teeth wouldn't fail over their intended lifetime, we calculated the contact and bending stresses they would be under and the strength they'd have against these stresses.

To do these calculations, we used equations from Chapter 14 of Shigley's Mechanical Engineering Design, 10th Edition. These equations were formatted for use between two external spur gears, so the calculations were restricted to the sun and planet gears. Because the sun gear is the smallest and weakest gear, we're confident that despite the fact the ring gear was not analyzed here, we are still covering the worst-case scenario in terms of gear-tooth stresses.

The process of equations that we used is shown below:

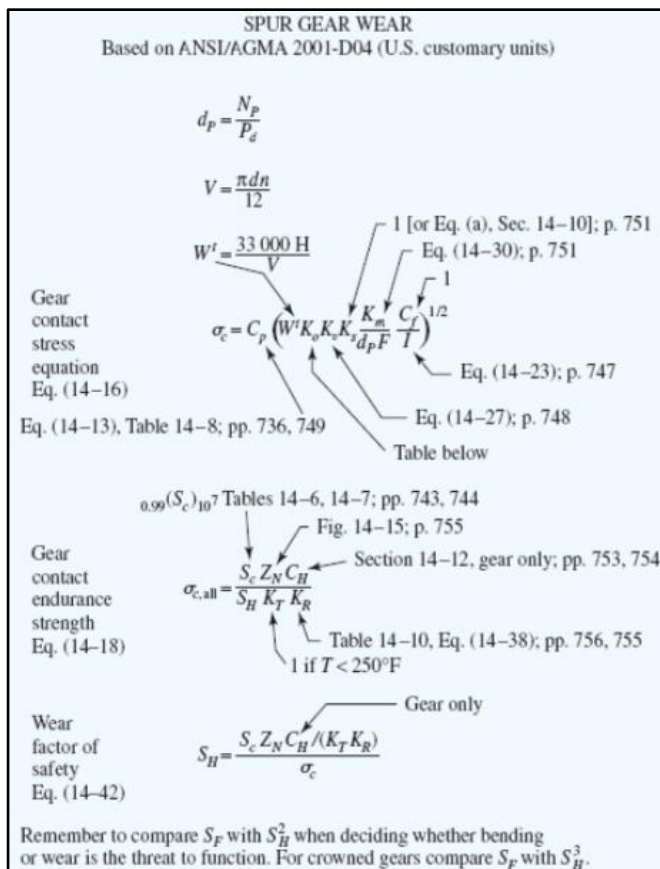
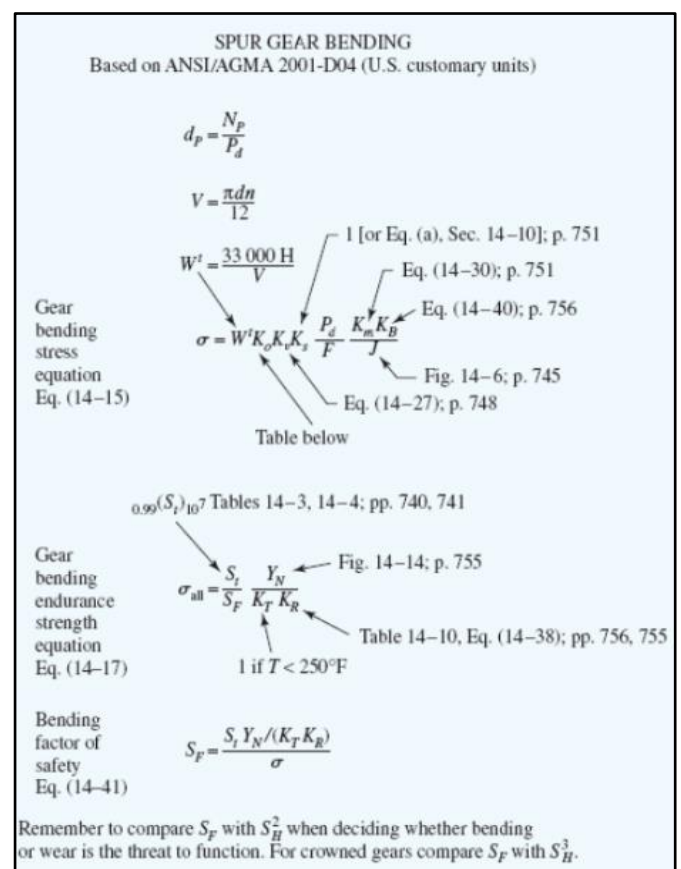


Table 8a: Spur Gear Wear



b: Spur Gear Bending



Due to the iterative nature of the calculation, we created a spreadsheet to calculate all of the factors and variables necessary to determine our safety factors. As shown in the diagram, all of these calculations are in English units.

We began by specifying the following:

Table 4: Spreadsheet Inputs

Diametral Pitch
Number of Teeth (Pinion / Gear)
Pitch Diameter (Pinion / Gear)
Angular Velocity (Pinion / Gear)

Note: we used the values of our maximum angular velocity here. Because we won't be running at top speed for the entire specified lifetime of the system, this will net us an extra safety factor.

Table 5: Spreadsheet Inputs

Face Width (Pinion / Gear)
Tangential Velocity
Input Power
Tangential Load

Next we calculated all of the following factors:

The Overload Factor (K_o) is intended to make allowance for all externally applied loads in excess of the nominal tangential load. Examples include variations in torque from the mean value due to the firing of pistons, or in our case the torque under numerous sudden acceleration and braking events. This factor is usually established after considerable field experience, but we estimated a value for our system using the table given below:

One habit we practiced throughout all of our analyses (and already seen in our specification of the angular velocities) was when we were unsure of what value to specify, we would always choose based on what we'd consider the worst case scenario. This entire analysis already assumes our gears will be running at maximum power (and maximum torque) throughout

their lifetime, a scenario far worse than what our actual system will see. In keeping with this habit, we specified an unlikely overload factor of 2 on top of the worst case assumption already in place to ensure we have as big a buffer as possible from failure.

Table of Overload Factors, K_o			
Driven Machine			
Power source	Uniform	Moderate shock	Heavy shock
Uniform	1.00	1.25	1.75
Light shock	1.25	1.50	2.00
Medium shock	1.50	1.75	2.25

Figure 9: Overload Factors (K_o)

The Dynamic Factor (K_v) is used to account for inaccuracies in the manufacturing and meshing of gear teeth in action, including transmission error. Transmission error is defined as the departure from uniform angular velocity of the gear pair, and can be caused by vibration of the tooth during meshing, wear of the contacting portions of the teeth, tooth friction, and other factors. AGMA defines a set of quality numbers Q which define the tolerances for gears of various sizes manufactured to a specified accuracy in an attempt to account for these effects. Quality numbers from 8 to 12 are of precision quality. Because our gears were being custom-made, we defined our gears to be of quality 12 (the highest quality the equation allows). With the quality number set, the dynamic factor is calculated with the following equation.

$$K_v = \left(\frac{A + \sqrt{V}}{A} \right)^B \quad V \text{ in ft/min}$$

where

$$A = 50 + 56(1 - B)$$

$$B = 0.25(12 - Q_v)^{2/3}$$

Figure 10: Dynamic Factor Equations

The Size Factors (K_{s_p} / K_{s_g}) reflect the nonuniformity of material properties due to size. They can be calculated using Lewis Form Factor values (Y_p, Y_g) that vary based on the number of teeth. We obtained these values from the table 4 shown below, which is defined for a normal pressure angle of 20° and full-depth teeth:

Table 4: Lewis factor values

Number of Teeth	Y	Number of Teeth	Y
12	0.245	28	0.353
13	0.261	30	0.359
14	0.277	34	0.371
15	0.290	38	0.384
16	0.296	43	0.397
17	0.303	50	0.409
18	0.309	60	0.422
19	0.314	75	0.435
20	0.322	100	0.447
21	0.328	150	0.460
22	0.331	300	0.472
24	0.337	400	0.480
26	0.346	Rack	0.485

Once these values were obtained, the Size Factors were calculated from the following equation:

$$K_s = 1.192 \left(\frac{F\sqrt{Y}}{P} \right)^{0.0535}$$

Figure 11: Size Factor Equation

The Load Distribution factor (K_m) modifies the calculated stress equations to reflect the non-uniform distribution of the load across the line of contact. Ideally, the gears in a system will be centered between two bearings, located at the zero slope place when the load is applied. Although the factor is difficult to apply to our planetary and we certainly could have just set it to 1, we felt that calculating a value larger than unity couldn't hurt if we felt we had the capability to do so. This factor is a combination of the following smaller factors:

- Lead Correction Factor (C_{mc}) - this factor varies based on whether there is any crowning in the tooth profile, with a value of 1 for uncrowned teeth and 0.8 for crowned teeth. Because we did not specify crowning in our gears, we set this value to 1.
- Pinion Proportion Factor (C_{pf}) - this factor varies based on the face width and pitch diameter of the pinion, with different equations based on different ranges of face width shown below:

$$C_{pf} = \begin{cases} \frac{F}{10d_p} - 0.025 & F \leq 1 \text{ in} \\ \frac{F}{10d_p} - 0.0375 + 0.0125F & 1 < F \leq 17 \text{ in} \\ \frac{F}{10d_p} - 0.1109 + 0.0207F - 0.000228F^2 & 17 < F \leq 40 \text{ in} \end{cases}$$

Figure 12: Overload Factors (Ko)

- Pinion Proportion Modifier (C_{pm}) - this factor compensates for any uncentered placement of the pinion between its bearings.
- Mesh Alignment Factor (C_{ma}) - this factor accounts for the how well the gears align and mesh based on the condition and types of gears used. Because a larger face width brings on a larger area for misalignment, the value of this factor is based on a quadratic function based on the face width as follows:

Table 5: Mesh alignment Factor equation values based on system conditions

$C_{ma} = A + BF + CF^2$			
Condition	A	B	C
Open gearing	0.247	0.0167	$-0.765(10^{-4})$
Commercial, enclosed units	0.127	0.0158	$-0.930(10^{-4})$
Precision, enclosed units	0.0675	0.0128	$-0.926(10^{-4})$
Extraprecision enclosed gear units	0.00360	0.0102	$-0.822(10^{-4})$

Because our gears will be enclosed and are being custom-made, we specified the condition of extra precision enclosed gear units when calculating our mesh alignment factor.

- Mesh Alignment Correction Factor (C_e) - this factor is used to account for any adjustments made to the gearing at assembly to reduce the problems the load distribution factor accounts for. Therefore, if the gearing is not adjusted at assembly, the value of this factor should be specified as unity. Otherwise, a value of 0.8 is recommended. Because we would have full access to the system at its assembly to spot errors and adjust, we set this value to 0.9.

With all of these smaller factors specified, the Load Distribution Factor was calculated using the following equation:

$$K_m = 1 + C_{mc}(C_{pf}C_{pm} + C_{ma}C_e)$$

Figure 13: Equation for Load distribution factor

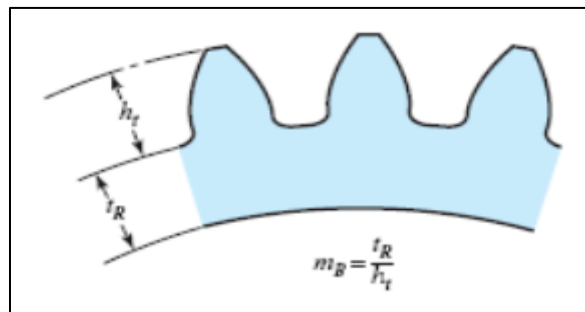


Figure 14: Rim Thickness compared to whole depth

The Rim Thickness Factor (K_b) is used when the rim thickness is not sufficient to provide full support for the tooth root, which raises concerns that bending fatigue failure may occur in the rim rather than at the tooth fillet. The factor is a function of the backup ratio m_b , intuitively shown in the diagram on the right

If the backup ratio is greater than or equal to 1.2, the rim-thickness factor can be set to 1 because the rim thickness is deemed sufficient enough to support the tooth root. Because our backup ratio meets this criteria, we set our rim thickness factor to unity.

The Bending Stress Cycle Factor (Y_{n_p} / Y_{n_g}) is used to modify the gear strength for lives other than 10^7 cycles (where Y_n is given a value of unity). Because our gears are spinning at different speeds, they will have a different number lifetime cycles, so this factor must be calculated for both the pinion and gear. Because different materials and treatments can vary lifetime reliability, different equations for the bending stress cycle factor are required for each type. We used the following graph to determine the right equation for our system:

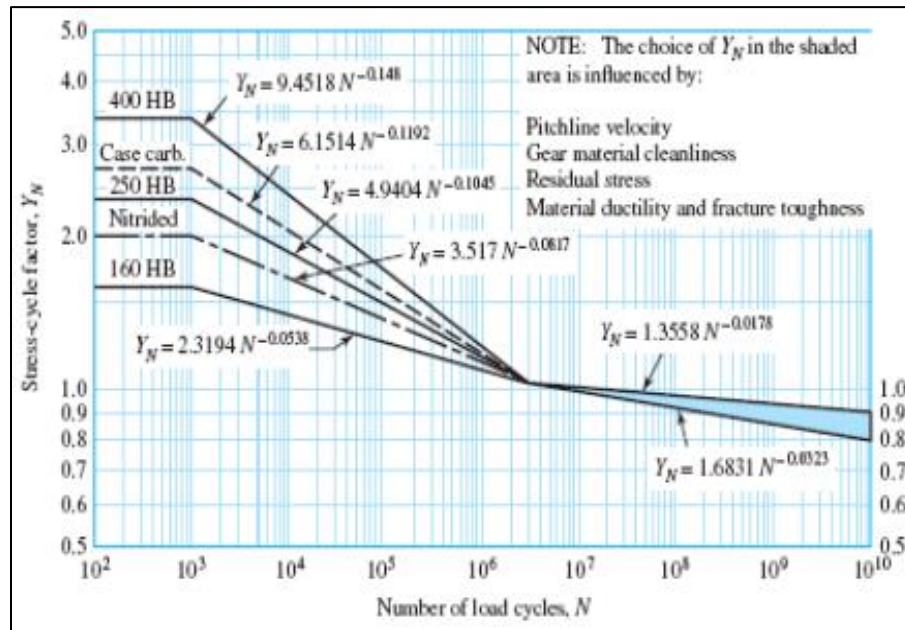


Figure 15: Bending Stress Cycle Factor equations

At first we were confused that both surface finish and Brinell hardness were used in this graph, and we were unsure which parameter to use. We spoke to one of the professors at the university, who explained that while our nitrided surface was beneficial because it increased our surface hardness, this extra hardness could have a detrimental effect on the amount of wear on the surface and increase stress seen in the material. Therefore, we chose the equation line based on a nitrided treatment.

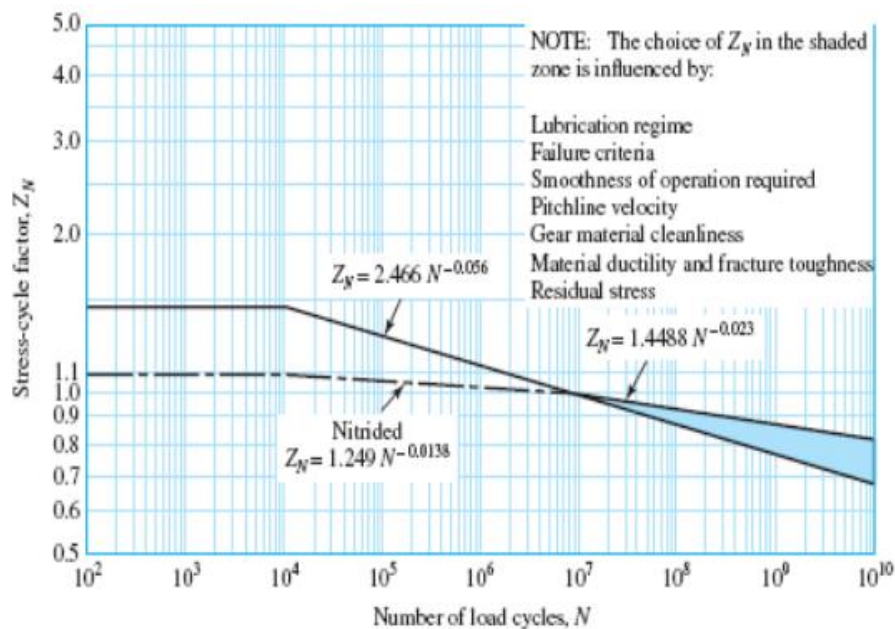


Figure 16: Stress-cycle Factor Equations



The pitting stress cycle factor (Z_n_p/Z_n_g) works using the same premise as the bending stress cycle factor, but for contact stress instead. In a similar process as followed above, the graph on the right is used to determine the right equation. Just as before, we chose to use the nitrided line for our calculation

Table: 6 Reliability Factor values for different reliability percentages

Reliability	$K_R (Y_2)$
0.9999	1.50
0.999	1.25
0.99	1.00
0.90	0.85
0.50	0.70

The Reliability Factor (K_r) is used to account for any specified reliability other than 99%. It's used as an additional safety factor to ensure that you are completely safe using your system for its intended purpose. We specified a reliability factor of 1.25 with the main goal of improving our on-paper reliability from 99% to 99.9%, and as an added cushion to our calculations to ensure we don't fall to any errors.

The Temperature Factor (K_t) is given a value greater than 1 when the system is operated in temperatures greater than 250°F. Because our planetary is not expected to see any temperatures that high, we set this factor to 1.

The Surface Condition Factor (C_f) depends on the surface finish, residual stress, and other related properties of the material used. Standard surface conditions for gear teeth haven't yet been established, but if the surface condition is known to be poor, AGMA recommends a value greater than 1. Because our gears are being custom-made, our manufacturers will provide a proper surface finish, so we set this value to unity. If we were to be mistaken in this, we're confident that our overestimation of other factors will be more than enough to compensate.

The Load Sharing Ratio (m_n) is equal to the face width divided by the total length of the lines in contact. Lucky for us, for spur gears the load sharing ratio is equal to unity, so we don't need to go into specifics on how this is found.

The Pitting Resistance Geometry Factor (I) is a rather self-explanatory factor that specifies both gears resistance to pitting based on the pressure angle, load sharing ratio, and speed ratio of the gears using the following equation.

$$I = \frac{\cos \phi_t \sin \phi_t}{2m_n} \frac{m_G}{m_G + 1}$$

M_g is the speed ratio of the gears, simply defined as $m_g = (N_g / N_p)$. It should be noted that this equation is intended for use in external gears only

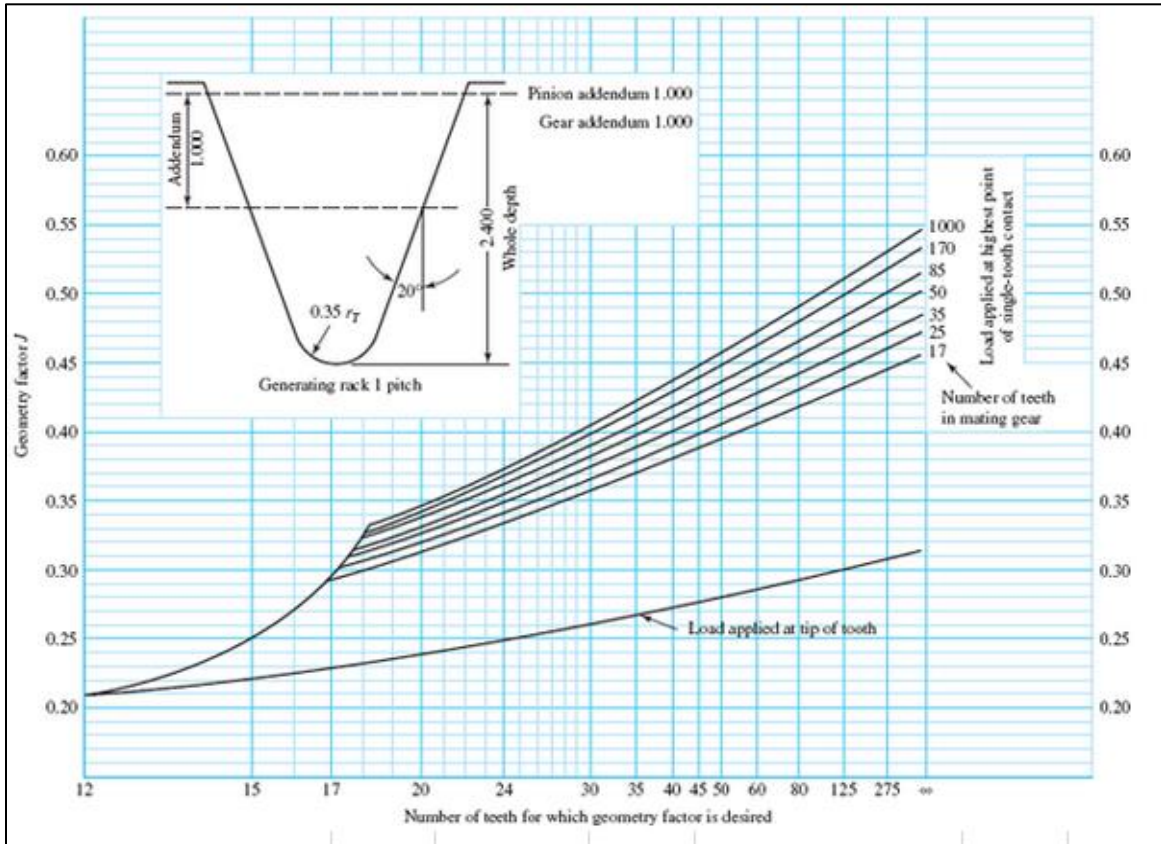


Figure 17: Geometry Factor values based on number of teeth in analyzed gear and mating gear

The Bending Resistance Geometry Factors (J_p, J_g) function similarly to the pitting resistance factor, but for use in the analysis of bending stress rather than contact stress. These factors depend on the ratio of the numbers of teeth between the meshing gears, shown in the graph below:

To use the graph, first find the number of teeth on the gear you want to find the factor for on the x-axis. Then trace your way vertically to the black line that represents the number of teeth of the mating gear. Simply trace horizontally left from the point of intersection to determine the geometry factor for that gear. Then do the same for the other gear in the pair.

The Elastic Coefficient (C_p) is used in the equation for contact stress, and is based on the ductility of the materials used in the pinion and gear. More specifically, it depends on their elastic moduli and poisson's ratios as follows:

$$C_p = \left[\frac{1}{\pi \left(\frac{1 - \nu_p^2}{E_p} + \frac{1 - \nu_g^2}{E_g} \right)} \right]^{1/2}$$

Figure 18: Equation for Elastic Coefficient

The Allowable Bending Stresses (St_p/St_g) dictates how much bending stress our gear teeth can handle, and is to what we will compare our calculated stresses in order to determine whether the teeth will fail in bending. To put it another way, this is our tooth bending “strength”, and it depends on the metallurgical quality and Brinell hardness of the material used in our gears as shown in the graph below:

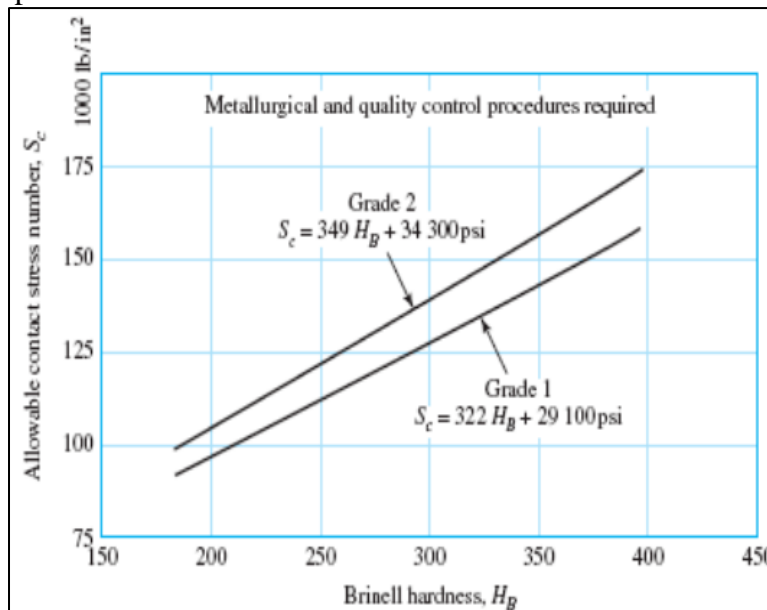


Figure 19: Allowable bending stress equations based on metallurgical quality and Brinell hardness

The Allowable Contact Stress (S_{c_p}/S_{c_g}) dictates how much contact stress our gear teeth can handle, and is what we'll compare our calculated stresses to to determine whether the teeth will fail in wear. To put it another way, this is our tooth contact “strength” and it depends on the same properties as the allowable bending stress, as shown below:

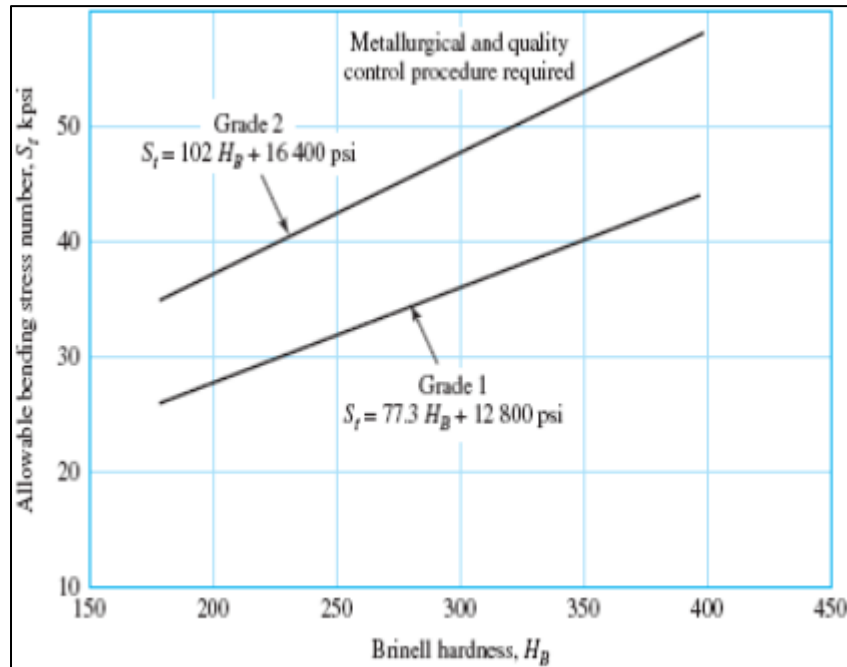


Figure 20: Allowable contact stress equations based on metallurgical quality and Brinell hardness

The Hardness Ratio Factor (Ch) is used only for the gear in the pair, or in our case for the planet. Because the pinion has a smaller number of teeth than the gear, it's subjected to more cycles of contact stress over time. By making the pinion harder than the gear, a uniform surface strength can be achieved. This factor is meant to account for this difference in hardness when calculating the contact stresses on the gear. In our case we did not specify different hardnesses for the sun or planet gears (i.e. our hardness ratio = 1), so $Ch = 1$ for both our pinion and our gear.

With all of these properties and factors determined, we were able to calculate bending/contact stresses, bending/contact strength, and bending/wear safety factors for our sun and planet gears. Despite specifying all of our factors for the worst case and adding extra safety factors whenever possible, our lowest safety factor was 1.43 for pinion tooth wear.

Shrink Fit Analysis

To prevent slip between the ring gear and the bearing into which it is shrink-fit, the frictional force between the two surfaces needs to be able to counteract the largest torque seen at the interface between them. The calculations below determine if the friction from the press fit is large enough to prevent slip:

Table 7: Calculations to determine whether the shrink fit will slip under maximum load torque

Definition	Variable	Equation	Result	Comments
Force due to Torque	F _T	T / r_{out_ring}	504.3367	
Force due to Friction	F _f	$\mu * N$	592.3837	
Torque at interface	T	(known)	1593.1260	
Outer radius of Ring gear	r _{out_ring}	$D_{out_ring} / 2$	3.1589	
Coefficient of Friction	μ	(estimated)	0.1000	Friction coefficient between two metals, worst case, assumed to be .1 (from Alex Gehrke)
Normal Force between Ring and Bearing	N	$\sigma * A$	5923.8368	
Pressure between Ring and Bearing	σ	(known)	530.6047	Assuming the loosest shrink fit
Contact Area between Ring and Bearing	A	$2 * \pi * r_{out_ring} * FW$	11.1643	The surface area over which the pressure acts -- the outer surface area of the ring gear
Face Width of Ring Gear	FW	(known)	0.5625	

Based on the results of the above table, the loosest Class FN3 fit will not fail under the maximum possible torque the ring gear can experience. Defining the safety factor as the $F_{actual} / F_{allowable}$, this shrink has a safety factor of 1.175.

The temperature of the outer member in a shrinkage fit (in our case, the wheel center) depends on total expansion required and coefficient alpha of linear expansion of the metal. The total expansion required consists of the total allowance for shrinkage with an added amount for clearance. The below calculations look at the worst case scenario for parts we need to shrink fit together -- the smallest bore of the wheel center (+0 thou_{in}) with the largest ring gear to fit into it (+7 thou_{in}). The first possibility is to just heat the wheel center, and keep the ring gear at room temperature, shown in Table 8 below:

Table 8: Calculations to determine heating required to shrink fit by heating only

Heating the Wheel Center		
Coefficient of Thermal Expansion - Wheel Center	0.0000131	in/F
Total Interference	0.007	in
Clearance	0.002	in
Total Expansion Required	0.009	in
Temperature Required (above room temp)	687.02	F



The second possibility is to just cool the ring gear, and keep the wheel center at room temperature, shown in Table 9 below:

Table 9: Calculations to determine cooling required shrinking fit by cooling only.

Cooling the Ring Gear		
Coefficient of Thermal Expansion - Ring Gear	0.00000678	in/F
Total Interference	0.007	in
Clearance	0.002	in
Total Contraction Required	0.009	in
Temperature Required (below room temp)	1327.433628	F

Because the coefficient of thermal expansion is larger for the wheel center than it is for ring gear, it will be much easier for us to expand the wheel center than it will be to shrink the ring gear. Also problematic -- we can't really cool the ring gear to -500K, despite how awesome that would be. We're more limited by how much we can cool than by how much we can heat. Liquid Nitrogen can reach roughly -320F, so let's assume that we use it to cool our gear down to -300F (to compensate for thermal losses). Knowing the contraction of the gear at this temperature, we can calculate the (reduced) temperature of the wheel center required to expand it the rest of the required allowance, shown in Table 10 below:

Table 10: Calculations to determine heating required on wheel center to shrink fit with -300F ring gear

Cooling of Ring Gear			Heating of Wheel Center		
Temperature below RT	-300	F	Expansion required	0.0069	in
Contraction	0.0020	in	Temperature above RT	531.75	F

Shaft Analysis

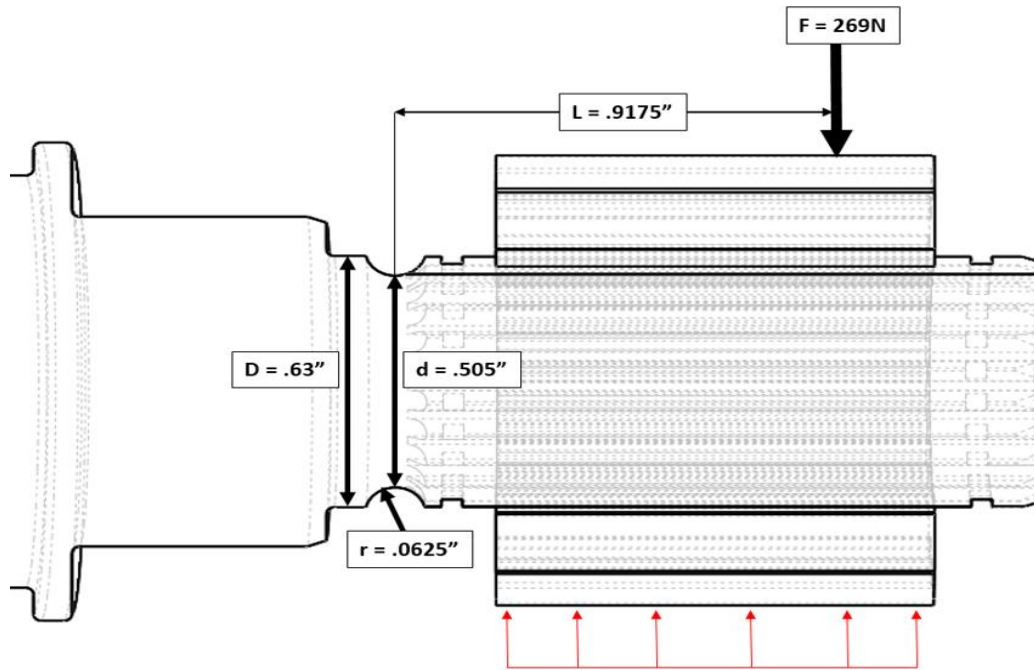


Figure 21: A really badass drawing of our shaft and sun gear

We evaluated our motor shaft using the stress-life method to determine whether the shaft would fail in fatigue.

Table 11: Important material properties and geometric dimensions for shaft strength analysis.

Material Properties (AISI 4140 Steel)	Value	Geometric Dimensions	Value
Ultimate Strength (S_{ut})	670 MPa	Major Diameter (D)	.63 in
Yield Strength (S_y)	435 MPa	Minor Diameter (d)	.505 in
Elastic Modulus (E)	205 GPa	Fillet Radius (r)	.0625 in
Modulus of Rigidity (G)	79.3 GPa	Minimum Area (A)	.200 in ²
Number of Cycles (N)	2.5e6	Moment Arm (L)	.9175 in



The analysis began with finding the endurance strength of the shaft, S_e , determined by the equation below:

$$S_e = k_a k_b k_c k_d k_e k_f S'_e$$

Figure 22: Equation for S_e

An explanation of the chosen values for each factor in this equation is as follows:

$$S'_e = \begin{cases} 0.5S_{ut} & S_{ut} \leq 200 \text{ kpsi (1400 MPa)} \\ 100 \text{ kpsi} & S_{ut} > \text{kpsi} \\ 700 \text{ MPa} & S_{ut} > 1400 \text{ MPa} \end{cases}$$

Figure 23: Equation for S'_e

The Endurance Limit (S'_e) is the endurance strength of a similar specimen under completely-reversed loading, and was defined by equation shown on the right. Because $S_{ut} < 1400 \text{ MPa}$, $S'_e = .5 * S_{ut}$.

$$k_a = a S_{ut}^b$$

Figure 24: Equation for k_a

Table 12: Values for a and b depending on surface finish

Surface Finish	Factor a		Exponent
	S_{ub} kpsi	S_{ub} MPa	b
Ground	1.34	1.58	-0.085
Machined or cold-drawn	2.70	4.51	-0.265
Hot-rolled	14.4	57.7	-0.718
As-forged	39.9	272.	-0.995

The Surface Factor (K_a) is based on the quality of the surface finish and ultimate tensile strength of the material. Using the equation and table on the right, we assumed a machined surface finish in our calculations.

$$k_b = \begin{cases} (d/0.3)^{-0.107} = 0.879d^{-0.107} & 0.11 \leq d \leq 2 \text{ in} \\ 0.91d^{-0.157} & 2 < d \leq 10 \text{ in} \\ (d/7.62)^{-0.107} = 1.24d^{-0.107} & 2.79 \leq d \leq 51 \text{ mm} \\ 1.51d^{-0.157} & 51 < d \leq 254 \text{ mm} \end{cases}$$

Figure 25: Equation for k_b



The Size Factor (Kb) was determined by the minimum diameter of the shaft being analyzed using the equations in the graphic on the right.

The Loading Factor (Kc) depends on the loading scenario of the specimen being analyzed (axial, bending, torsion). Because we analyzed the shaft under a combined loading scenario (torque and bending), this factor was given a value of 1.

The Temperature Factor (Kd) factors in an increased endurance for temperature rises up to 500F, where the endurance begins to decrease. For our analysis we're assuming that the shaft will be operating in room-temperature environments, where this factor is prescribed a value of 1.

Table 13. Reliability factor for different specified reliability percentages.

Reliability, %	Transformation Variate z_s	Reliability Factor k_e
50	0	1.000
90	1.288	0.897
95	1.645	0.868
99	2.326	0.814
99.9	3.091	0.753
99.99	3.719	0.702
99.999	4.265	0.659
99.9999	4.753	0.620

The Reliability Factor (Ke) accounts for the scatter of experimental data during fatigue sample testing. A reliability of 99.9% was chosen and a Ke value of .753 was set based on the table on the right.

With our Se calculated, we then calculated the fatigue strength Sf using the equations below. f is found using the graph shown on the right:

$$S_f = a N^b$$

$$a = \frac{(f S_{ut})^2}{S_e}$$

$$b = -\frac{1}{3} \log \left(\frac{f S_{ut}}{S_e} \right)$$

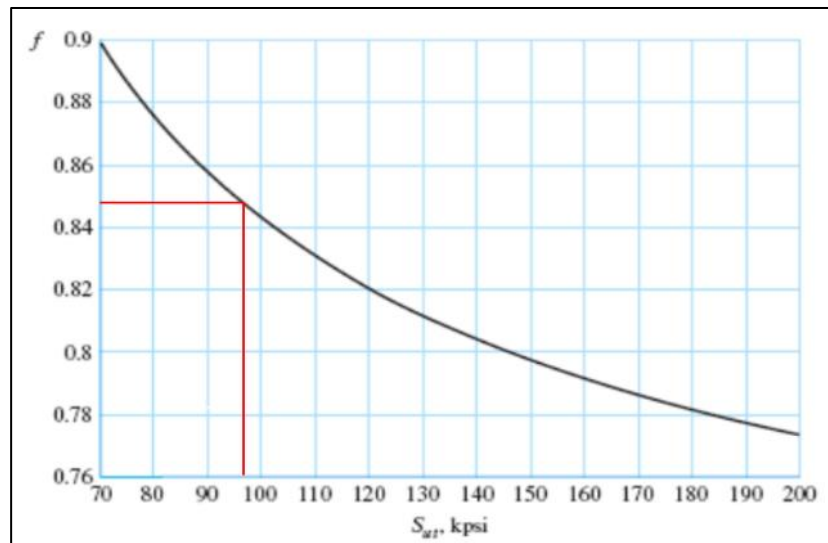


Figure 28: Fatigue strength factors depending on the ultimate tensile strength

To calculate the mean and alternating stresses, the fatigue stress concentration factors (k_f and k_{fs}) must be found using the stress concentration factors (k_t and k_{ts}) and the notch sensitivity (q):

$$K_f = 1 + q(K_t - 1) \quad \text{or} \quad K_{fs} = 1 + q_{\text{shear}}(K_{ts} - 1)$$

The Notch Sensitivity (q) defines how sensitive the specimen is to notches in fatigue loading. It was determined using the graph on the right using the notch radius and ultimate tensile strength.

The Stress Concentration Factors (K_t , K_{ts}) were found based on tabulated graphical values for a grooved round bar under bending (K_t) and torsional loading (K_{ts}).

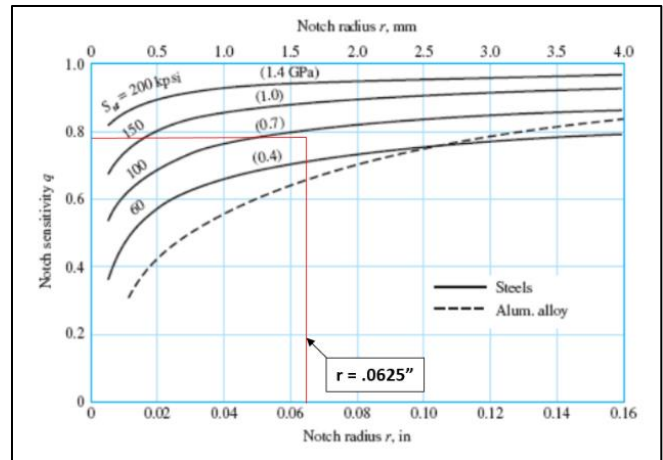


Figure: 29: Notch sensitivity q based on notch radius and ultimate tensile strength

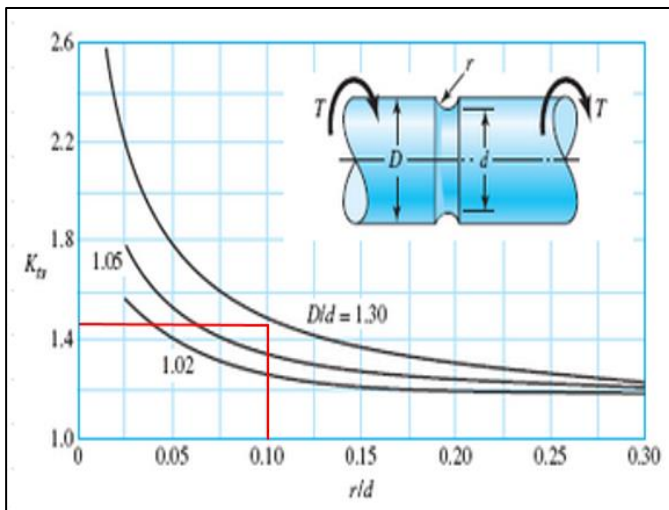


Figure 30: Stress concentration factors for a grooved round bar under torsion

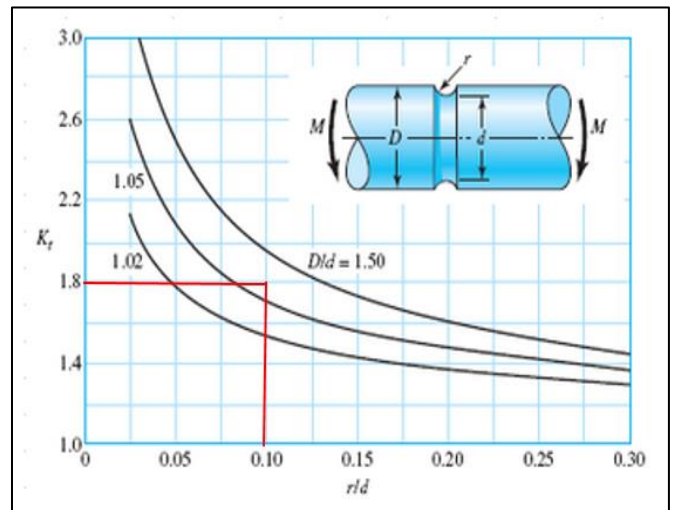


Figure: 31: Stress Concentration factors for a grooved round bar under bending.



Once the strength of the shaft was known, we calculated the Von Mises mean and alternating stresses based on the equations below:

The mean stress is only from the shear stress on the shaft due to the motor torque T

$$\sigma'_m = \{ [(K_f)_{\text{bending}}(\sigma_m)_{\text{bending}} + (K_f)_{\text{axial}}(\sigma_m)_{\text{axial}}]^2 + 3[(K_{fs})_{\text{torsion}}(\tau_m)_{\text{torsion}}]^2 \}^{1/2}$$

The alternating stress is only from the bending stress on the shaft due to the distributed radial load, approximated as a point force F.

$$\sigma'_a = \left\{ \left[(K_f)_{\text{bending}}(\sigma_a)_{\text{bending}} + (K_f)_{\text{axial}} \frac{(\sigma_a)_{\text{axial}}}{0.85} \right]^2 + 3[(K_{fs})_{\text{torsion}}(\tau_a)_{\text{torsion}}]^2 \right\}^{1/2}$$

A factor of safety (n) of 1.57 was determined using the Modified-Goodman equation shown below.

$$\text{mod-Goodman} \quad \frac{\sigma_a}{S_e} + \frac{\sigma_m}{S_{ut}} = \frac{1}{n}$$

In-Hub Architecture

The architecture for this system was selected to minimize mass, maximize the transmission ratio, achieve a safety factor of 1.5, achieve a minimum operating life of 69 hours and be as reliable as high as possible. The assembly is shown below highlighting each component in an exploded view.

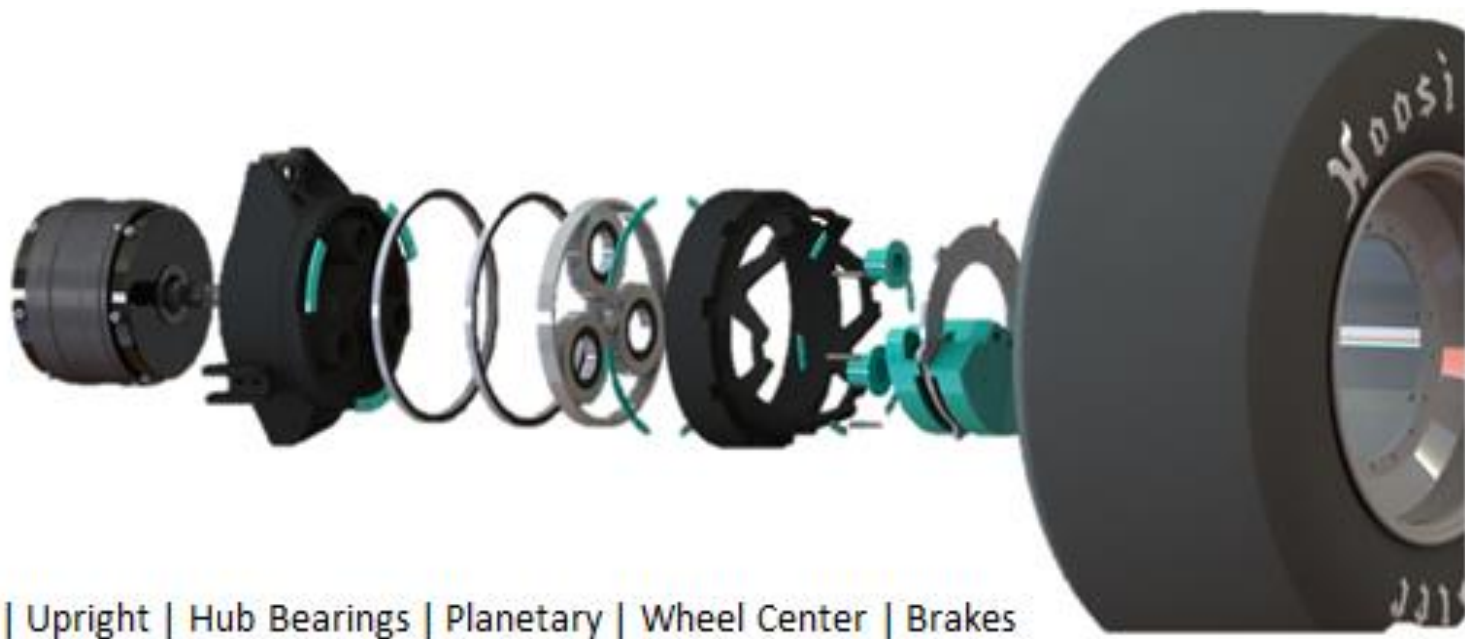


Figure 32: Exploded and labeled view of assembly

The motor is face mounted via 12 M5 bolts to the back side of the upright, and the front side of the upright mates to the transmission system, wheel center, transmission plate and brake system. Each component in the system is fully analyzed using hand calculation, solidworks simulations and where necessary the use of more in-depth software such as thermal desktop and KISSsoft.

The load cases for each component are driven from vehicle dynamics simulations. The simulations calculate the traction limit of the tires based on the mass, weight distribution and kinematics of the vehicle. The simulation forces are always verified by simplified calculation for conservative load cases. These estimated forces are always conservative to ensure an added safety factor for forces that are unaccounted for or misunderstood.

Upright Design

System Requirements

The upright of the WR-217e upright combines the conventional requirements of multiple components into one novel architecture. Firstly the upright satisfies reacting the loads of the A-arms, steering tie rod as well as the pull rod for the front suspension system. Secondly the upright satisfies offsetting the rotation of the wheel from the vehicle through the use of two large thin section bearings. Finally the upright acts as the inner half of the transmission enclosure and locates the motor and planet gears through three 120 degree separated bearing mounts. The combination of the upright, hub and transmission housing are an efficient and lightweight way of packaging the In-hub drivetrain entirely within the tire of the vehicle.

This system must pass all FSAE 2017-2018 rules, reduce the speed of the electric motor and increase the torque to provide the desired acceleration and regen targets and support all operating loads.

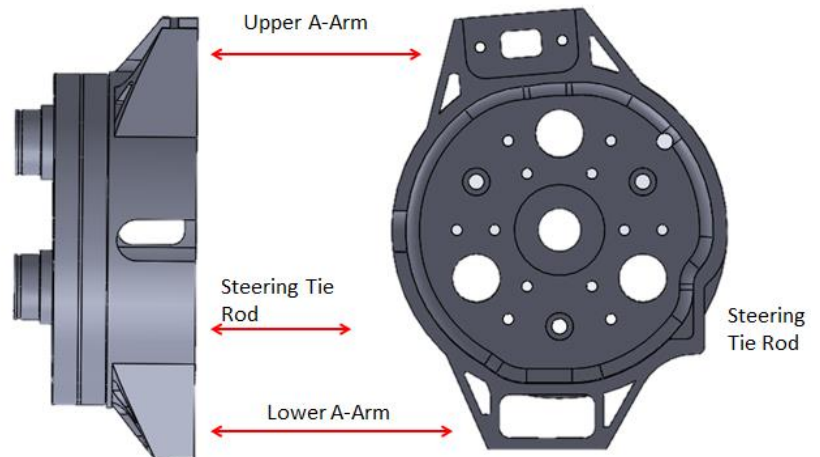


Figure 33: Upright Suspension Mount points

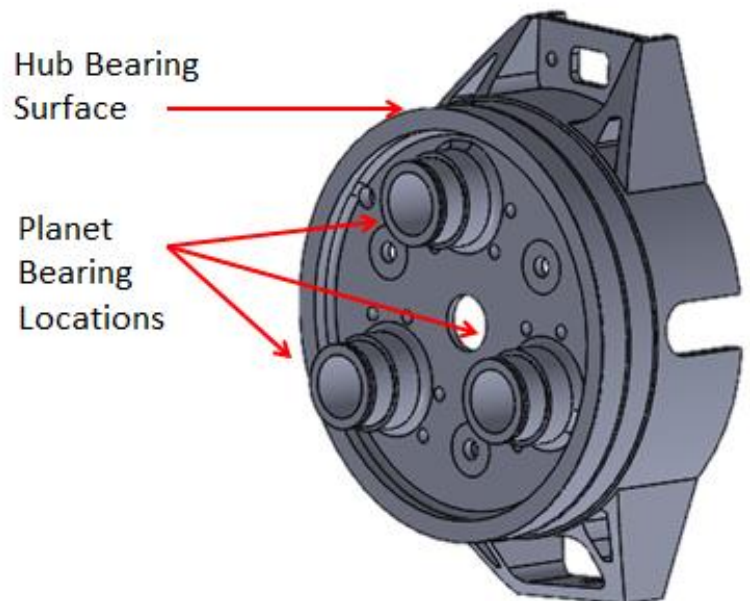


Figure 34: Upright Bearing Mount points

Transmission Interface

The transmission system for the front corners of the vehicle is tightly constrained within the width axis of the vehicle. To accommodate a reduction of 6.0 -7.5 a planetary transmission either single or dual stage was necessary.

The planetary transmission system rides on three NSK deep groove ball bearings in a sun drive, fixed planet and ring driven configuration. While a fixed ring and planet drive would increase the gear ratio by 1.0, the width of such a system pushed the package out of the axial constraint region and into the front pull rod.

With the ring drive planetary transmission the implementation of large ID bearings was necessary. In order to minimize mass and cross sectional area occupied by the large bearings, research brought thin section bearings to light.

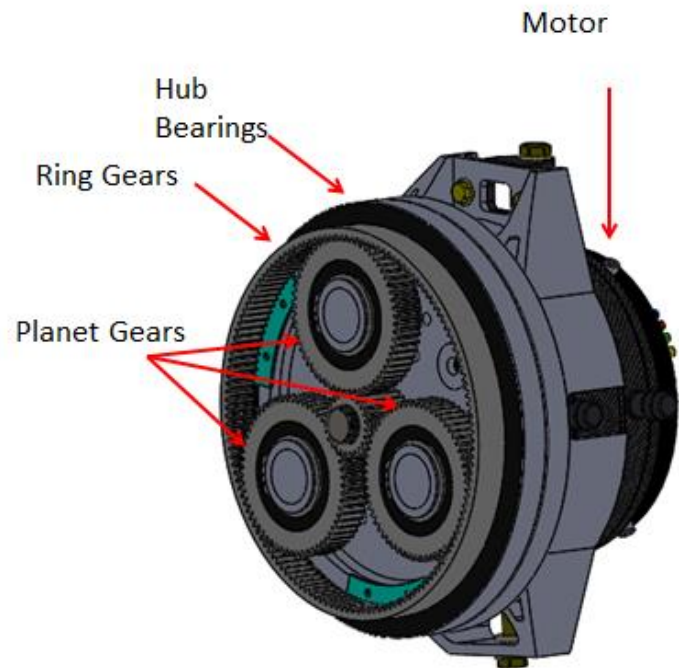


Figure 35: Planetary, hub bearing and motor mounting

The thin section bearings, while extremely costly, allow the designer to react the required forces and moments through extremely small cross sections. Multiple companies such as NSK, Kaydon, Timken, SKF and SilverThin supply this style of bearings in multiple configurations.

Due to budget considerations each company was contacted and SilverThin agreed to support the project through a ~50% reduction in cost. The life and load ratings of each company's bearings were determined to be of a negligible delta.

Bearing Selection

Due to the unique architecture of the in-hub motor design, the utilization of SilverThin thin section angular contact bearings was necessary to achieve the packaging of the assembly. The angular contact bearings are precision ground as a pair and mounted back to back with a predefined preload imparted through the tightening of the inner and outer bearing race retainers.

Load Case

Silverthin's engineering staff supported the project through a bearing selection study. Both four point contact and angular contact bearings of various sizes were investigated. It was determined that due to the loading of the bearing, shown below, a 1/2 inch by 1/2 inch cross section would provide the desired life to the system.

Table 15: Load cases

Bearing Load Case Study
RPM Range: 0-1300 RPM
Max Thrust Load: 780 lbs
Max Radial Load: 390 lbs
Max Moment Load: 7020 lbs-in

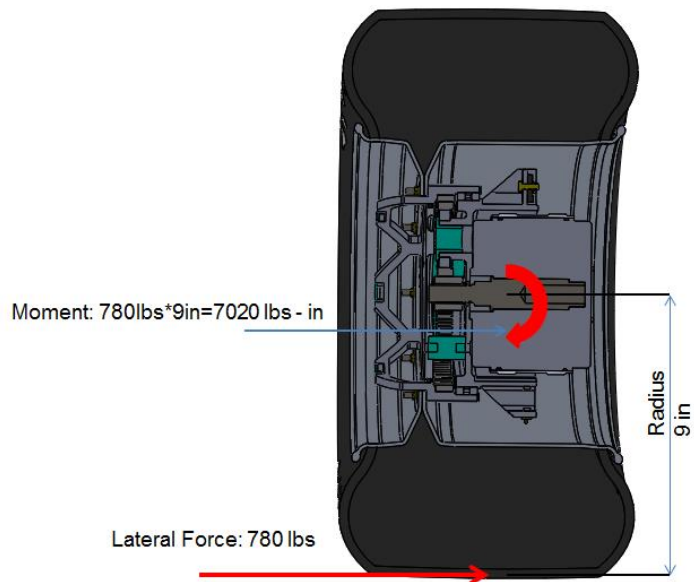


Figure 36: Hub bearing loading diagram

Through the collaboration with Silverthin it was determined that the expected minimum life of the bearing, based on a worst case analysis, would be between 69.2871 and 122.745 hours. The two studies shown below investigated were the 3/8 x 3/8 and 1/2 x 1/2 angular contact bearings. As shown there is a very large delta between the life of the smaller and larger cross sections. There are numerous parameters that affect the life of the bearing including, environmental, loading, thermal, friction, lubrication, preload, axial and radial clearance, and many more.

Bearing Life

This study, however, only investigated two of those parameters which were the load case, axial clearance and bearing size. Since the bearings are of the same type and would operate under the same conditions it was determined to simplify the analysis by dropping the other parameter.

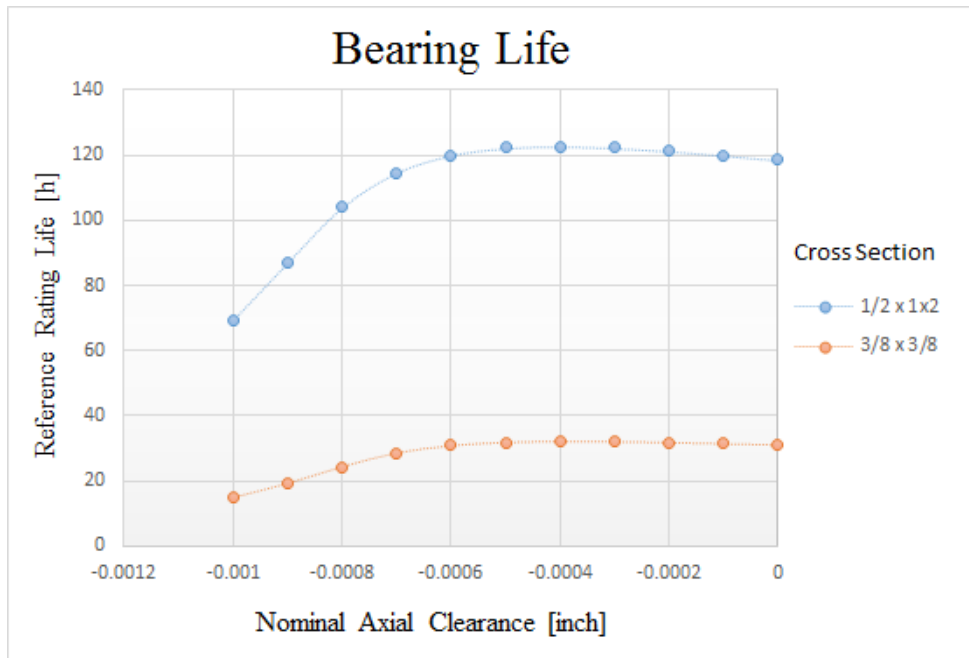


Figure 37: Bearing life graph showing pre-load vs. life rating for two bearing cross sections

The axial preload is achieved through a clamp force a bearing race features machined into the wheel center and upright along with two sets of pressure tabs. The schematic to the right highlights the various components holding the bearing in place.

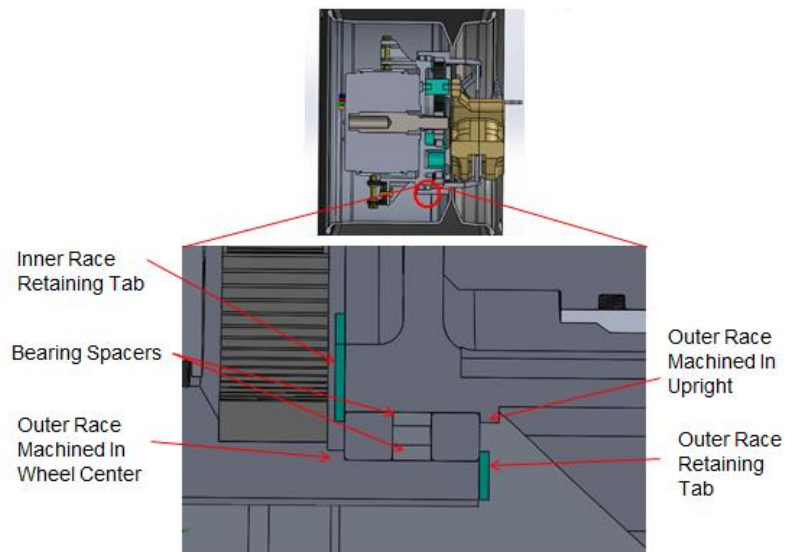


Figure 38: Bearing retainer method schematic

Simulation

This life study ran by SilverThin looked into the load distribution within the bearing and the resulting maximum contact stress within the bearing. The contact stress of a bearing is similar to a Hertzian contact stress between a ball and a cylinder or a ball in a cup. Multiple Hertzian contact stress analysis can be easily performed using Roark's Handbook or an online Hertzian contact stress calculator such as that of amesweb.info. A few of the loading scenarios are shown below.

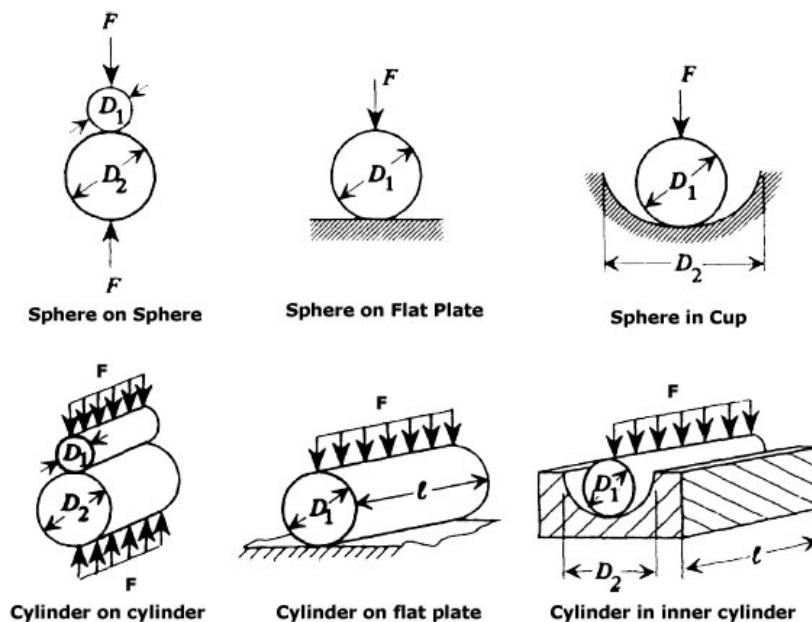


Figure 39: Hertzian contact stress force diagrams for multiple loading scenarios

The life rating provided is statistical. The number provided signifies the life that ninety percent of bearings manufactured with exactly the same construct and subjected to the same conditions would survive before the first signs of fatigue failure arise. This is a study investigated for one million revolutions of the bearing.

The fatigue calculations are simulating a rolling element over the same location repeatedly. This simulation creates a stress before the note prior to the "ball" rolling over and a stress in the opposite direction as it passes the node. The manifestation of the failure occurs through a crack in the subsurface that propagates to the race surface and results in a fatigue failure called 'spall'.

A mentioned previously this analysis did not factor in things such as excessive heat, contamination, vibrations, lubrication, etc.

Proper Assembly

Due to the failure mode of the front in-hub motor system, the lower level details of bearing selection, mounting, internal clearances, and lubrication were also investigated to mitigate the potential of unforeseen issues. The specific fillet radius for each bearing in the upright assembly was selected according the bearing manufacturer's data as shown below from the NSK Roller Ball Bearing Catalog.

The next parameter investigated for the bearings was the calculation of the nominal internal clearance of the bearings within the assembly. Each bearing is manufactured with a specified internal clearance between the roller elements and the raceways. This clearance is decreased by multiple parameters of the system. These include the press fit between the outer race and the housing bore, the press fit between the inner race and the shaft, the operating temperature and thin film layer if lubricated.

The lubrication layer film layer becomes increasingly important with the choice of a grease over an oil is selected. The grease occupies a larger volume and generates more friction, which results in decreased efficiency and higher operating temperatures.

These temperatures then create a larger thermal expansion of the various components and further decreases the internal clearances within the bearing.

Table 11.2 Recommended Minimum Shoulder Heights for Use with Metric Series Radial Bearings
Units : mm

Nominal Chamfer Dimensions r (min.) or r_1 (min.)	Shaft or Housing		
	Fillet Radius r_a (max.)	Minimum Shoulder Heights h (min.)	
		Deep Groove Ball Bearings, Self-Aligning Ball Bearings, Cylindrical Roller Bearings, Solid Needle Roller Bearings	Angular Contact Ball Bearings, Tapered Roller Bearings, Spherical Roller Bearings
0.05	0.05	0.2	—
0.08	0.08	0.3	—
0.1	0.1	0.4	—
0.15	0.15	0.6	—
0.2	0.2	0.8	—
0.3	0.3	1	1.25
0.6	0.6	2	2.5
1	1	2.5	3
1.1	1	3.25	3.5
1.5	1.5	4	4.5
2	2	4.5	5
2.1	2	5.5	6
2.5	2	—	6
3	2.5	6.5	7
4	3	8	9
5	4	10	11
6	5	13	14
7.5	6	16	18
9.5	8	20	22
12	10	24	27
15	12	29	32
19	15	38	42

- Remarks**
1. When heavy axial loads are applied, the shoulder height must be sufficiently higher than the values listed.
 2. The fillet radius of the corner is also applicable to thrust bearings.
 3. The shoulder diameter is listed instead of shoulder height in the bearing tables.

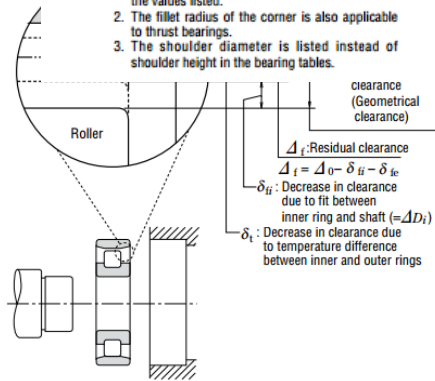


Fig. 9.2 Changes in Radial Internal Clearance of Bearings

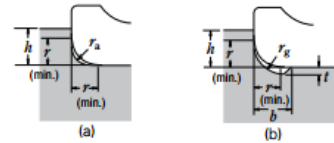


Fig. 11.2 Chamfer Dimensions, Fillet Radius, and Shoulder Height

Table 11.3 Shaft Undercut
Units : mm

Chamfer Dimensions of Inner and Outer Rings r (min.) or r_1 (min.)	Undercut Dimensions		
	t	r_g	b
1	0.2	1.3	2
1.1	0.3	1.5	2.4
1.5	0.4	2	3.2
2	0.5	2.5	4
2.1	0.5	2.5	4
2.5	0.5	2.5	4
3	0.5	3	4.7
4	0.5	4	5.9
5	0.6	5	7.4
6	0.6	6	8.6
7.5	0.6	7	10

..... (9.6)
clearance due to
between inner and

- α : Coefficient of linear expansion of bearing steel $\approx 12.5 \times 10^{-6}$ (1/°C)
- Δt : Temperature difference between inner and outer rings (°C)
- D_e : Outer ring raceway diameter (mm)

For ball bearings

$$D_e \approx \frac{1}{5} (4D + d) \dots \dots \dots (9.7)$$

For roller bearings

$$D_e \approx \frac{1}{A} (3D + d) \dots \dots \dots (9.8)$$

Figure 40: Bearing Clearance diagram and equations

Planet Bearings

The bearings utilized for the planets of the transmission were selected based on the normal load transmitted from the gears. The force diagram for a planetary transmission is shown to the right. The force imparted upon the tooth creates a transverse force used to drive the gears and a normal force acting to separate the bears. The planet bearings were selected with a high safety factor to minimize the possible deflection in the system as the gears must be properly mounted to avoid improper mating of the gears.

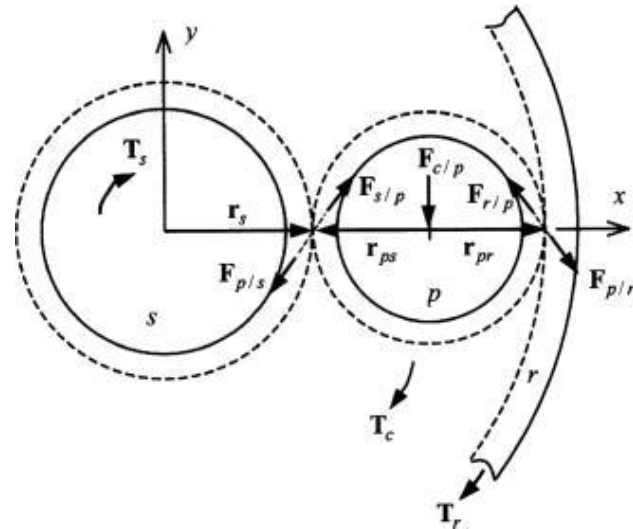


Figure 41: Planetary force diagram

The major operating parameter of interest for the system is the internal clearance of the bearing created during press fit of the bearing into the gear and onto the shaft. Since axial translation of the planet gear is unlikely the inner press fit is loose to minimize the reduction in clearance. Thermal expansion of each element, bearings, gears and housing are all critical as the expansion of each element creates smaller internal clearances. The aforementioned technique was utilized to calculate the estimated clearance of the bearings during installation and operation.

The selected bearings are the NSK 6809 VV 30 mm ID and 47 mm OD with a Cr rating of 7250.

Table 16: Bearing size table

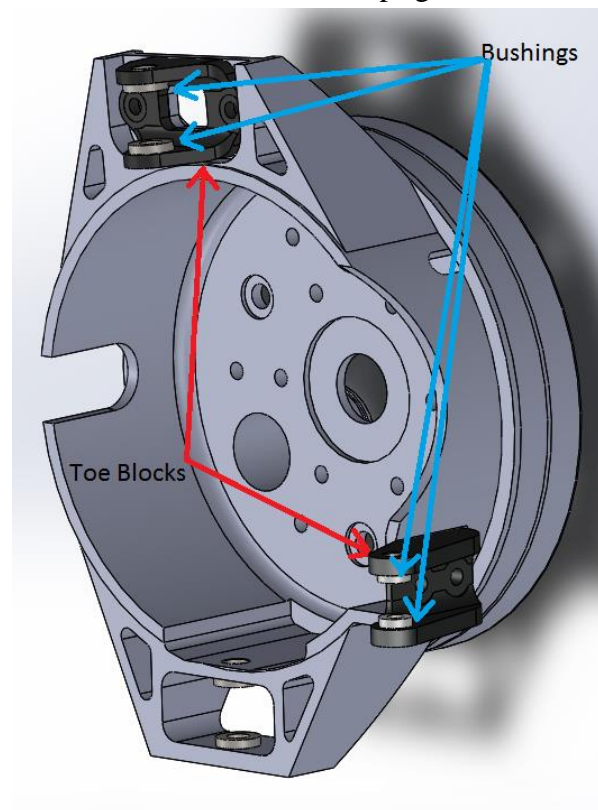
Boundary Dimensions (mm)				Basic Load Ratings				Factor	Limiting Speeds (min ⁻¹)			Bearing Numbers			
<i>d</i>	<i>D</i>	<i>B</i>	<i>r</i> min.	<i>C_r</i>	<i>C_{0r}</i>	<i>C_r</i>	<i>C_{0r}</i>		Grease		Oil	Open	Shielded	Sealed	
				(N)		{kgf}		<i>f₀</i>	Open Z · ZZ V · VV	DU DDU	Open Z				
25	37	7	0.3	4 500	3 150	455	320	16.1	18 000	10 000	22 000	6805	ZZ	VV	DD
	42	9	0.3	7 050	4 550	715	460	15.4	16 000	10 000	19 000	6905	ZZ	VV	DDU
	47	8	0.3	8 850	5 600	905	570	15.1	15 000	—	18 000	16005	—	—	—
	47	12	0.6	10 100	5 850	1 030	595	14.5	15 000	9 500	18 000	6005	ZZ	VV	DDU
	52	15	1	14 000	7 850	1 430	800	13.9	13 000	9 000	15 000	6205	ZZ	VV	DDU
	62	17	1.1	20 600	11 200	2 100	1 150	13.2	11 000	8 000	13 000	6305	ZZ	VV	DDU
28	52	12	0.6	12 500	7 400	1 270	755	14.5	14 000	8 500	16 000	60/28	ZZ	VV	DDU
	58	16	1	16 600	9 500	1 700	970	13.9	12 000	8 000	14 000	62/28	ZZ	VV	DDU
	68	18	1.1	26 700	14 000	2 730	1 430	12.4	10 000	7 500	13 000	63/28	ZZ	VV	DDU
30	42	7	0.3	4 700	3 650	480	370	16.4	15 000	9 000	18 000	6806	ZZ	VV	DD
	47	9	0.3	7 250	5 000	740	510	15.8	14 000	8 500	17 000	6906	ZZ	VV	DDU

SolidWorks Finite Element Analysis

SolidWorks simulation was used to identify high and low stress zones of the upright in different situations, so material can be added or removed accordingly. The goal was to achieve an even stress distribution throughout the part. An even stress distribution means weight and strength of the part has been optimized, because there is no material where it's not needed and there is enough material in places that experience higher forces.

Simulations

The four load cases used are peak lateral acceleration during a left turn, right turn, and copies of the first two with braking included. These simulations were ran after each change to a geometry in the part, to see if a certain change brings significant benefits for strength or weight. The geometries considered for optimization included thicknesses, radii, cut depth, hole size, and all fillets of features on the upright.



Since the upright is connected to the vehicle by A-arms and they are secured to the upright by toe blocks, these simulations were done in an assembly with the upright, toe blocks, and toe block steel bushings mated together. The bushings are where the A-arm bolts would be inserted. Therefore, their inner cylindrical surfaces were set as fixtures. For the turning cases, a remote load was set at the contact patch of the tire, acting on the surface which the 6" bore bearings fit over. This force has a component in the lateral direction as well as the travel direction of the tire. To model braking, torque is applied to the 3 holes and surrounding surfaces where the brake assembly is mounted on.

Figure 42: Assembly used for FEA

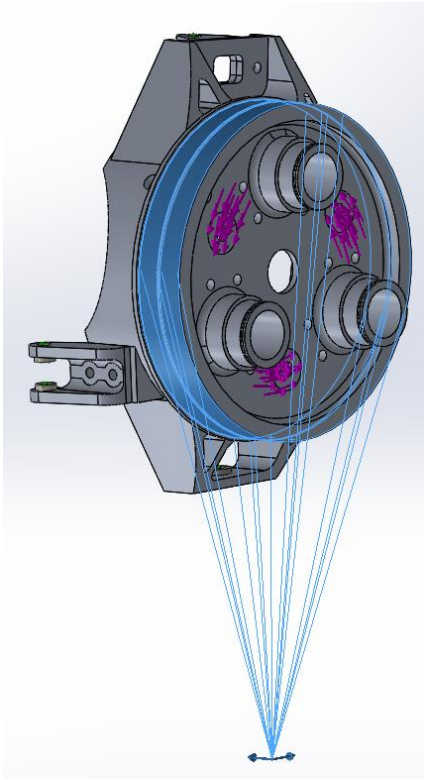


Figure 43: Load case with braking and turning forces applied

Results

Stress results of FEA studies are shown here. The point of maximum Von Mises stress is indicated by the red arrow in each result. Notice that the max stress point is in one of the bushings for all load cases.

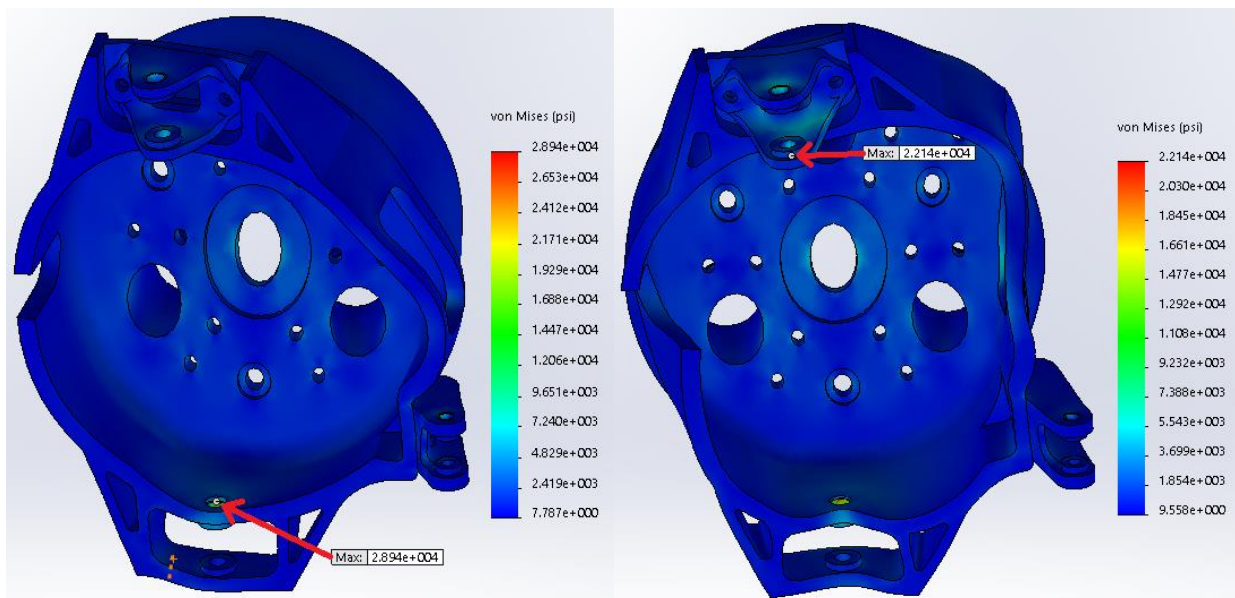


Figure 44: Left Turn Max $\sigma = 28.94$ ksi

Right Turn Max $\sigma = 22.14$ ksi

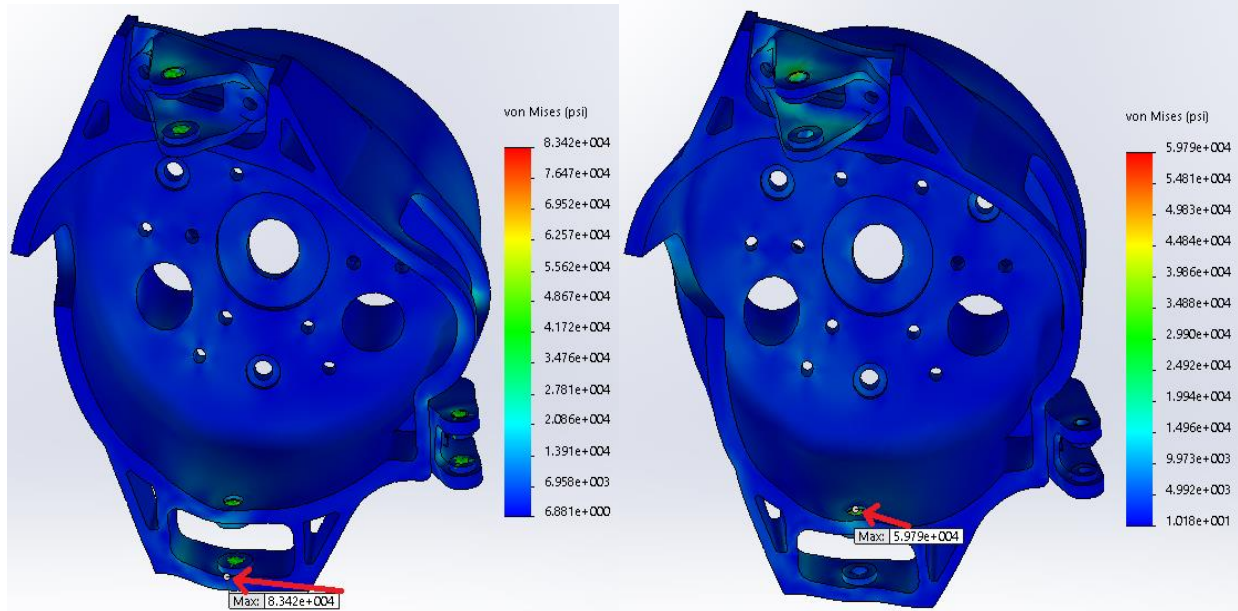


Figure 45: Left Turn + Brake $\text{Max } \sigma = 83.42 \text{ ksi}$ Right Turn + Brake $\text{Max } \sigma = 59.79 \text{ ksi}$

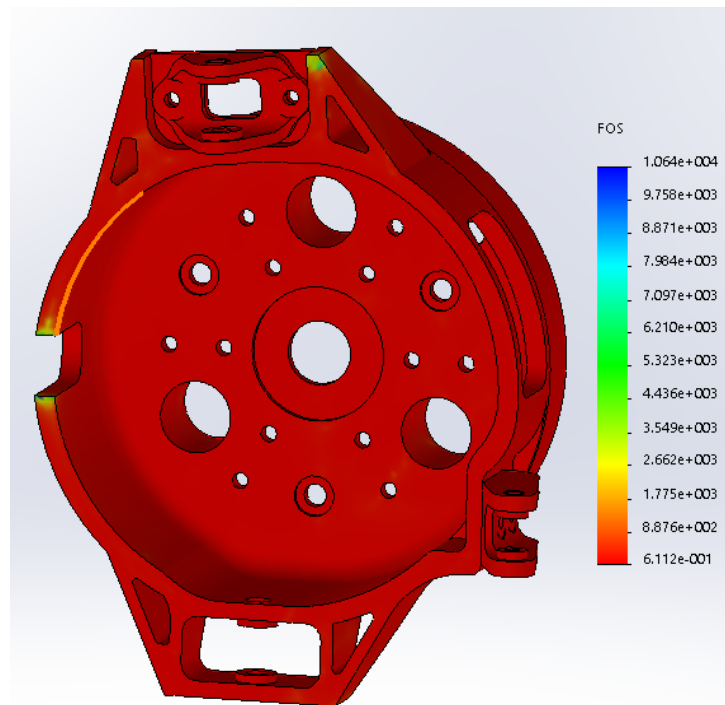


Figure 46: The left turn with simultaneous braking case shows the highest stress for the left upright. Although, safety factor across the assembly is consistent



Design Study

Optimizing a part's features with the method outlined above can be a very iterative. To change a dimension, run the FEA, compare results, then repeat is a tedious process. Even though it only takes a few seconds to run the FEA for a part such as this, it can add up. SolidWorks has a function that will somewhat reduce the workload of the designer. In the Design Study feature, dimensions that are to be optimized can be designated, then it will run a previously built load case multiple times with set goals in mind (max strength, lowest weight, etc.), and it will provide the best combination of dimensions. Design Study was used to find the optimum shape of the side cutout and inner radius of the main bore. Below is the Design Study report generated by SolidWorks.

Design Study Setup

Design Variables

Name	Type	Value	Units
Main bore end radius	Range with Step	Min:0.16667 Max:0.38 Step:0.01	in
depth of inner pockets	Range with Step	Min:0.035 Max:0.105 Step:0.01	in

Constraints

Sensor name	Condition	Bounds	Units	Study name
Stress1	is less than	Max:70000	psi	left brake
Stress2	is less than	Max:70000	psi	right brake

Goals

Name	Goal	Properties	Weight	Study name
Mass1	Minimize	Mass	10	-

Study Results

10 of 10 scenarios ran successfully.

Component name	Units	Current	Initial	Optimal	Scenario1	Scenario 2
depth of inner pockets	in	0.105	.035	0.105	0.035	0.045
Stress1	psi	62325	62681	62325	62681	62611
Stress2	psi	50324	51520	50324	51520	53558
Mass1	lb	2.10577	2.24309	2.10577	2.24309	2.22351

Component name	Units	Scenario3	Scenario4	Scenario5	Scenario6	Scenario7
depth of inner pockets	in	0.055	0.065	0.075	0.085	0.095
Stress1	psi	61981	64929	61559	64176	63742
Stress2	psi	50032	52068	50568	53714	53334
Mass1	lb	2.20391	2.18431	2.16469	2.14506	2.12542
Component name	Units	Scenario8				
depth of inner pockets	in	0.105				
Stress1	psi	62329				
Stress2	psi	49899				
Mass1	lb	2.10577				



Wheel Center Design

System Requirements

The wheel center connects the transmission output to the wheel. The planetary gear reduction ring gear drives the wheel center, and it in turn drives the wheel shells. The wheel center also holds the brake rotor. Since the ring gear is press fitted into the wheel center, the press fit needs to be able to withstand the max torque output from the motor as well as max torque from braking. We would also like to absolutely minimize the amount of deflection in the planetary gears; therefore the wheel center is also supported by two 6" bore bearings. This is done to prevent gears from seizing at high speeds, which would be catastrophic. Massive amounts of thermal energy are created as the vehicle undergoes braking. Even though contact area between the rotor and the wheel center is very small, it's possible for a considerable amount of heat to transfer to the wheel center. Therefore, the wheel center has to be designed to be strong enough to retain a safety factor under high heat scenarios.

Wheel Center Architecture

Originally, the wheel center and brake hat were two individual parts, simply because this is the convention in vehicle design. We then realized that we did not need to have two separate parts. Combining them allows for a lighter overall weight and less complexity, due to not having to worry about fasteners to secure the parts together.

When the motor engages and the ring gear spins, torque is transmitted through the press fitted ring gear to the wheel center, then to the wheel shell. The two large bearings are also press fitted into the inner surface of the wheel center, although in a section with a larger diameter. The torque goes through a thick cylindrical part of the wheel center and into the wheel shell through the wheel shell mounting face.

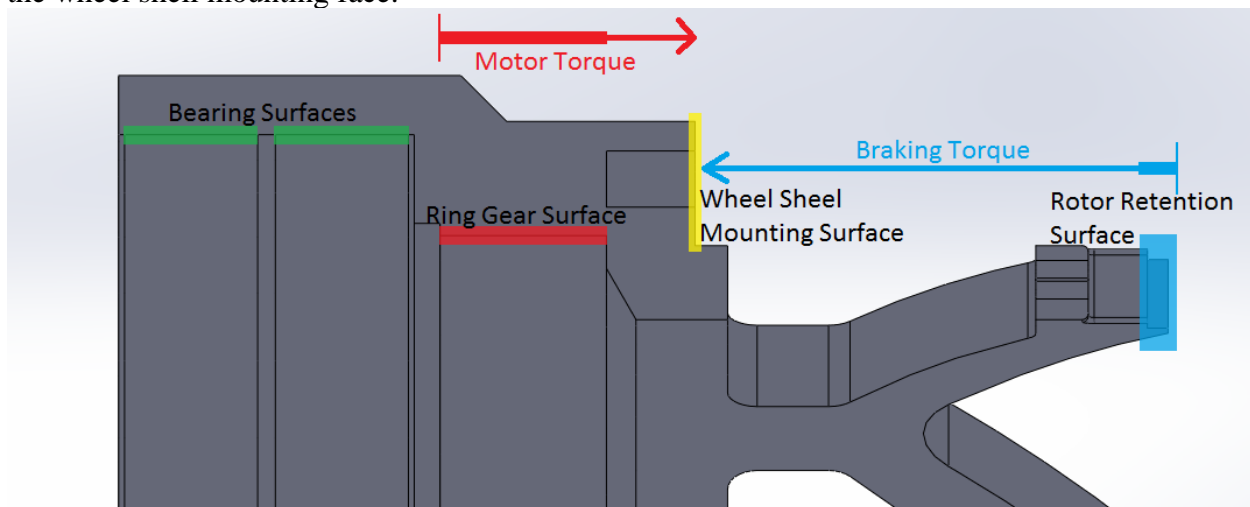
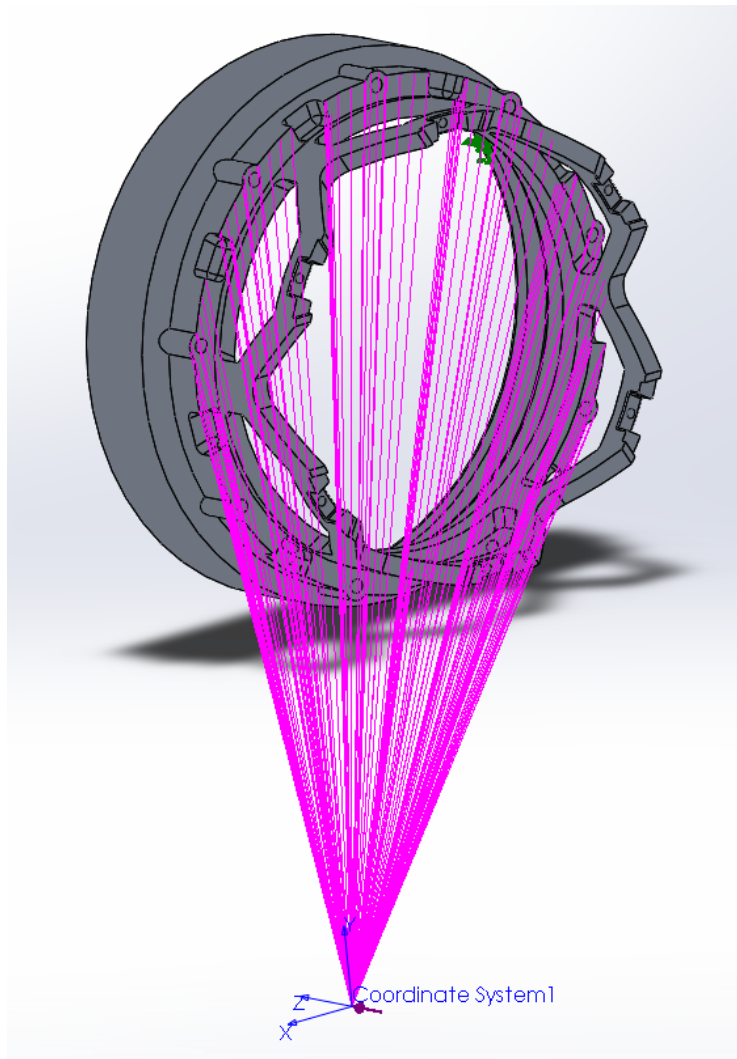


Figure 47: The section view of the wheel center illustrates load-bearing surfaces and paths of torques traveling through the part

Under braking, braking force is transmitted from the brake rotor tabs to the retainer recesses on the outer end of the wheel hat. The path in which torque transmits again terminates at the mounting face for the wheel shells, but now it begins on the outer end where the rotor is mounted.

When the vehicle turns, a lateral load is applied to the corner assembly from the contact patch of the tire. To prevent the bearings from being pulled out of the wheel center by this force, which can be as high as 1500 N, there needs to be some way to retain the bearings. We've decided to bolt semicircular tabs on the inner end of the upright. These tabs will be contacting the outer race of a bearing and keeping everything on the corner assembly that is external of the upright (bearings, wheel center, wheel shells, brake system) from sliding off the car under lateral loads.

SolidWorks Finite Element Analysis



The use of SolidWorks simulation to model forces loading the wheel center was essential in its design. Forces and torques to be expected on the wheel center were calculated using EES, then entered into solidworks.

Turning Case

When the vehicle turns, lateral force at the contact patch of the tire will cause the wheel shells to push into the bottom half of their contact surface with the wheel center, and pull on the top half of the contact surface; or vice versa, depending on the direction of the turn. Therefore, this case is modeled as a remote load in SolidWorks. The force acts at the contact patch of the tire, and the wheel shell mounting surface is affected. The part is fixed at the bearing contact surfaces, as the bearings will be providing the support to react to this load.

Figure 48: FEA showing how the tire lateral force affects the wheel center

Braking Case

Under braking, the floating brake rotor will rotate to contact a surface in the rotor retaining recesses on the outer end of the wheel center. Since the rotor is rotating as the car slows down, this contact force is modeled as a torque with the axis being the centerline of the wheel. This force is reacted at the holes where the wheel shells are bolted into the wheel center, so the bolt holes are fixed for this simulation.

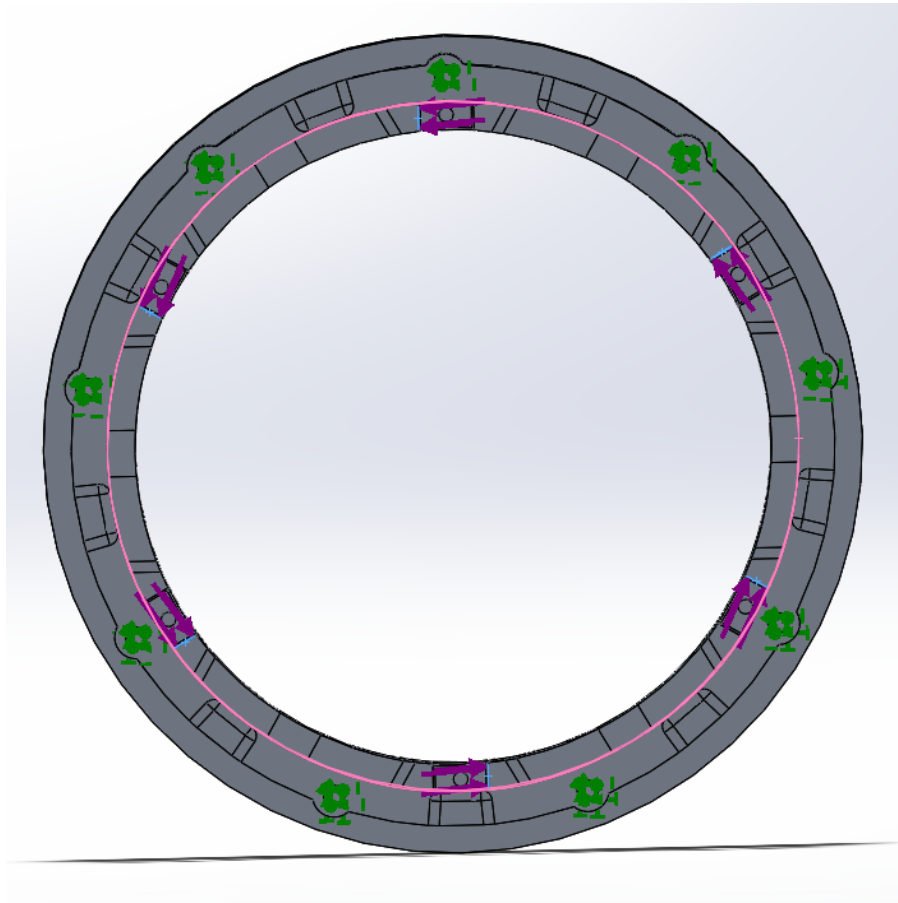


Figure 49: FEA showing how braking torque affects the wheel center

Aside from the two individual load cases, a combined case where both braking and turning happen at the same time is tested. It is interesting to note that the part actually sees 15.2% less maximum stress in the combined load case than the braking load case.

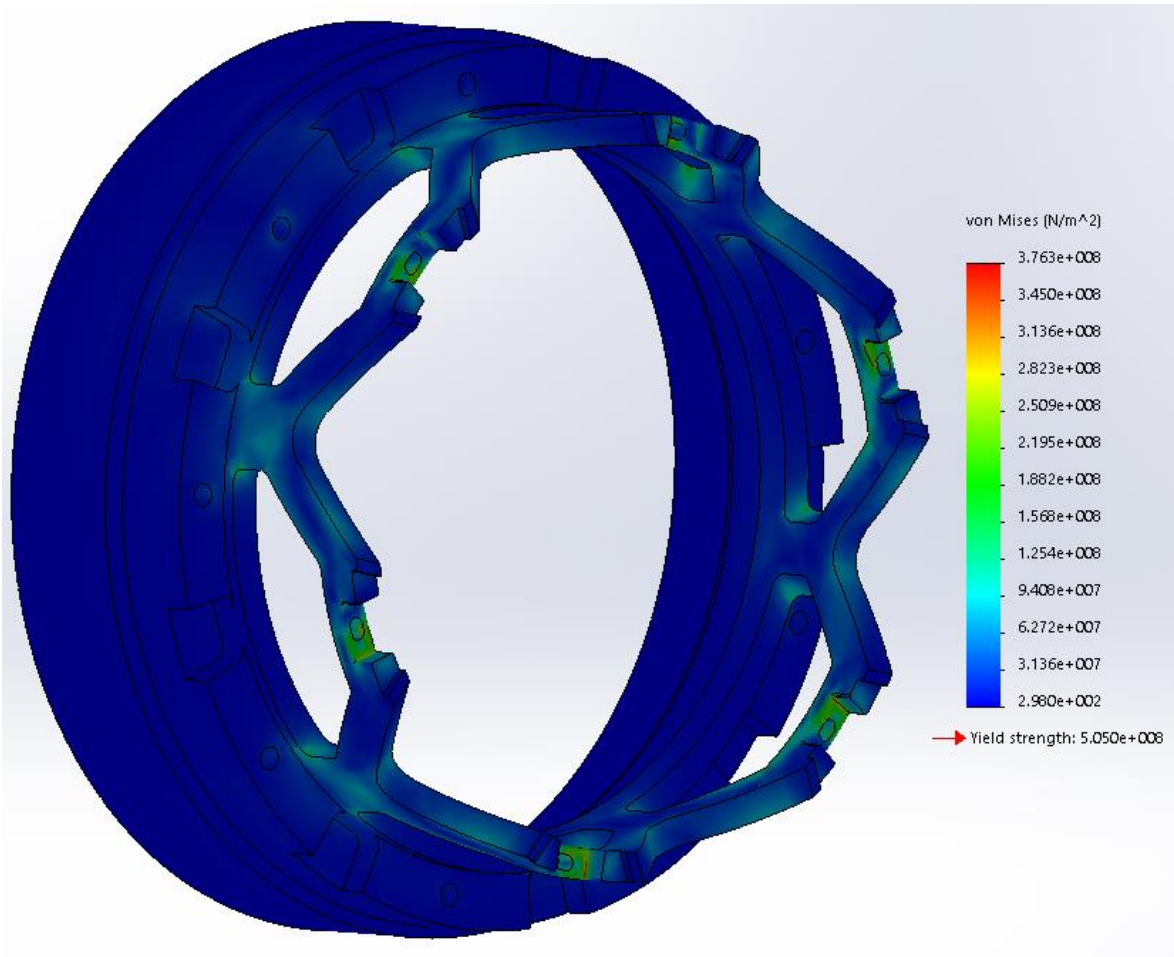


Figure 50: The result of combined load simulation

Table 17: FEA load cases and results

	Force [N]	Torque [Nm]	Von Mises Stress [kN/m ²]	Safety Factor
Turning	500	N/A	5.75e3	87.82!!
Braking	N/A	700	3.92e5	1.29
Combined Load	500	700	3.70e5	1.36

The safety factor for the braking load case might seem small, but when the part does fail from a higher braking torque, the simulation shows that the failure mode will be the rotor slightly digging into its retention surface. This happens without the rest of the part reaching its tensile yield stress. Theoretically, if a very high braking torque is applied, the next thing to fail would be the structure which the rotor rests on; and that won't happen until the braking torque reaches 3000 Nm or so, which is unattainable with our brake system.

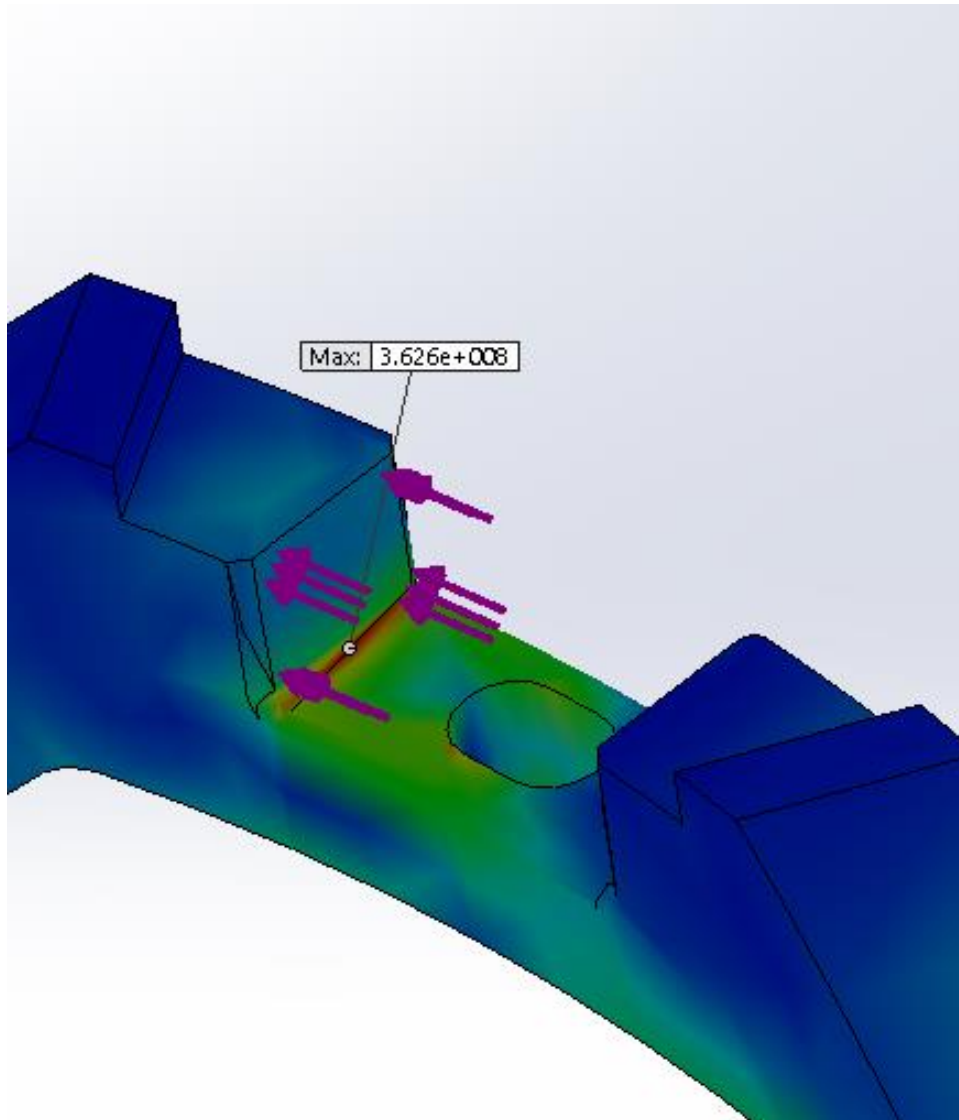


Figure 51: Initial failure of brake hat on the rotor retention surface. The purple arrows indicate torque from the rotor. Max stress value in Nm and location are also shown



Brake Caliper Design

System Requirements

The brake system for the Wisconsin Racing WR-217e is being designed with safety as the highest priority. As will be discussed, the front brakes will utilize a custom built, student designed inverted brake caliper. The caliper must comply with all FSAE rules. This means that the brake system must be capable of locking up all 4 tires at the end of an acceleration event without the use of the regenerative braking system. Additionally, all system components must be capable of withstanding a 2000N input on the brake pedal.

The Wisconsin Racing team has also set additional requirements for the system. First, in order to accomplish the all-wheel drive system that is being implemented, the rotor and caliper must package inside of a 10inch FSAE tire. This requirement is discussed further in the Inverted Orientation section that follows. The brake system must also be capable of providing 1.8g of deceleration. This value was selected because that is typically the peak that previous vehicles have been able to achieve. This consistency will help our drivers quickly acclimate to the system. Additionally, the system should provide this deceleration with 150 lbf input to the brake pedal.

Inverted Orientation

The front brake system for this vehicle requires an unconventional layout. Per the FSAE rules, no part of the vehicle can extend beyond the outer surface of the wheel. Because this vehicle utilizes an all-wheel drive system with an outboard electric motor in each of the front wheels, the only packaging option for the front brake system is within the 10 inch wheel shell. However, during testing and competition, it is not uncommon for the wheels to be removed several times throughout the course of the day. Thus, in order to remove the tire from the vehicle without removing the entire brake system, the entire system must be compressed further to package inside a 6.25 inch diameter space in the rim. This can be seen in the Figure at right.

The graphic at right shows a cross section of the front drive train inside of the wheel. The section that is highlighted in red shows the motor and driveline assembly. The solid red line on the left side of the tire shows the edge of the allowable design space per the FSAE Rules. The current brake system aligns with the edge of the allowable space. An alternative solution was presented to extend the motor shaft in towards the monocoque of the car and place a larger rotor in this location. Doing so would remove the rotor size restriction caused by removing the tire. However, to implement this brake system, we would have to drill a hole in the motor assembly and extend the shaft. This was not a possible shaft option from the motor supplier and would risk damaging the motor. In addition, the suspension geometry would need to be redesigned to accommodate a larger rotor. Thus, this option was not pursued.

The figure at right shows the available design space highlighted in red. This space represents the area between the edge of the tire and the brake hat. The diameter is constrained to allow the tire to be removed without removing the brake system. With such a constrained space requirement, using a conventional caliper mounted on the outside of the rotor would result in the rotor diameter being significantly limited. This means that the rotor would be smaller than the 6-8" minimum rotor diameter that



Figure 52: Maximum Diameter of Caliper Assembly as Determined by 10" FSAE Tire

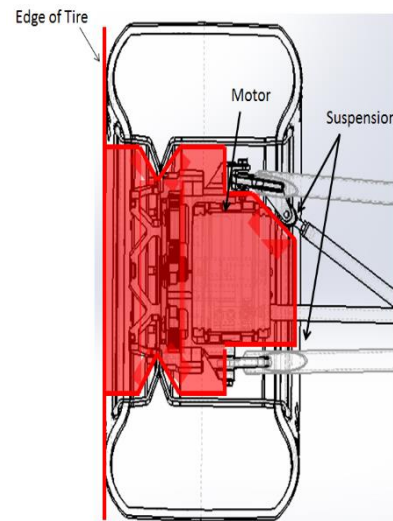


Figure 53: Section View Front Drivetrain and Design Space for Extended Motor Shaft

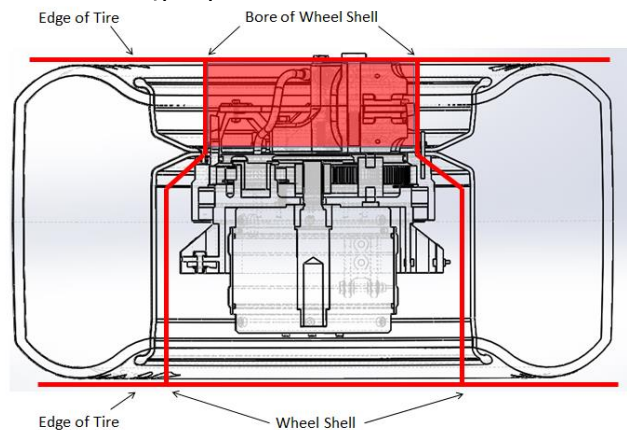


Figure 54: Section View of Design Space of Front Brake Assembly

is specified by calipers that are traditionally used by FSAE teams. Even if the calipers were modified to allow for such small rotors, overcoming the reduction in torque capability caused by the downsizing would require unachievable operating pressures. This leads to the need for a custom inverted caliper.

The brake system team has decided to pursue a custom designed inverted caliper that mounts to the planetary gear assembly. The system is very similar to the one that is used as a front caliper on Eric Buel Racing's EBR 1190RX sport bike. The inverted geometry allows the rotor to be extended to the maximum possible diameter, and therefore provide the maximum possible brake torque for a given line pressure and piston diameter.

This inverted brake system has also been implemented in FSAE Electric competition. TU Delft, a team based in the Netherlands, has developed a custom inverted caliper based on an ISR 2-Piston caliper. The team built a system that is very similar to what the Wisconsin Racing Team is designing, however the TU-Delft design is based on a 13 inch wheel. The reduction in braking torque capacity caused by moving to a 10 inch wheel makes this caliper insufficient for Wisconsin Racing's needs.



Figure 55: EBR 1190 front caliper features an inverted geometry similar to what Wisconsin Racing is attempting



Figure 56 : TU Delft custom inverted caliper



Brake Calculations

To appropriately size the custom caliper, a student programmed Engineering Equation Solver (EES) Code was used to predict brake system performance. This code, originally designed by Formula SAE team member and UW-Madison Grad student Dan Janecek, takes inputs of vehicle parameters and outputs information such as caliper torque output, rotor temperature increase for a given stop, torque capacity of the tire, and hydraulic line pressures. The EES code includes tire data, effects of the aerodynamics package, and vehicle dynamics calculations to accurately predict the longitudinal grip of the vehicle at a given speed. With this, we are able to determine the required caliper torque output in order to overcome the vehicle grip during the brake test. This EES code was updated with the parameters of the electric vehicle and modified to include the rotor expansion calculations. Additionally, the rotating mass from the motor, planetary gear set, brake rotor and tire were also included into the torque requirement for the caliper.

Table 18: Thermal Expansion Outputs From Student Built EES Code

Therm Expansion Coefficient	Air Temperature	Rotor Temperature	Radial Expansion	Thickness Expansion
micron/m-C	C [F]	C [F]	mm [in]	mm [in]
11	37.78 [100]	485 [905]	0.3186 [0.0125]	0.025 [0.0010]

Collaboration with Hayes Performance Systems

To facilitate the design of a custom brake caliper, Wisconsin Racing partnered with Hayes Performance Systems. Hayes is a supplier of brake systems for nearly every application. Their vast experience with vehicles of our size and with racing applications proved vital to the success of our caliper design.

Throughout the course of the semester, members of the Wisconsin Racing team visited the Hayes facility twice to complete design reviews. From these meetings, we were able to refine our brake system design to a point in which we are confident in our brake system success.

One of the major improvements that was suggested by Hayes brakes was utilizing sintered metal pads. These pads are made by heating and compressing metallic powder on a copper backing plate (EBC Brakes). These pads are commonly used in racing applications and provide a high coefficient of friction regardless of system temperature. While the metal to metal contact between brake pad and rotor provides consistent braking, the process is very aggressive and can lead to rotor wear if the wrong material is used. Because of this, custom 410 Stainless Steel rotors have been sourced for this race car.



Figure 57: Sintered metal pad that was donated by Hayes performance systems

The combustion car currently utilizes custom organic pads made by Carbotech. Previous testing has shown that these pads vary greatly with temperature as can be seen at right. This is a concern because the brake test, in which the vehicle must lock up all four tires, will be at a cold system condition.

One important consideration when using sintered pads is the break in period. In order to effectively produce the high friction coefficient associated with sintered pads, the pad and rotor combination will need to be burnished. This process essentially involves several iterations of gentle braking. By doing this, the pads will leave a small amount of material on the rotor surface. If this is done properly, the sintered pad compound that will be used will provide a friction coefficient of at least 0.6 throughout the entire temperature range. These pads will be donated at no cost by Hayes Performance Systems.

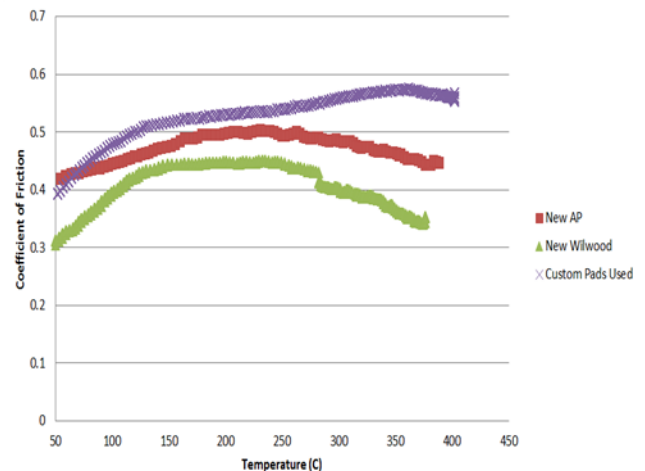


Figure 58: Brake compound testing data compiled from brake dynamometer testing

As was previously mentioned, the use of sintered metal pads requires a rotor material with a high hardness throughout the entirety of the rotor operating temperature. The collaborating engineers from Hayes Performance systems recommended 410 stainless steel for this application. This alloy is commonly used by the company for the rotors of racing motorcycles and other high performance applications. It offers high strength and hardness up to

temperatures of around 1200F, well below the predicted temperature of the rotor (“410 Stainless Steel”). Rotor material for this vehicle has been generously donated by Apache Stainless Equipment.

With the material selected, the rotor has been designed to maximize the effective radius while still allowing the wheel to be removed. This has resulted in a rotor outer diameter of 5.7 inches. By matching the rotor thickness to the pad area, the inner diameter was selected to be 3.15 inches. The blank disks that are being supplied by Apache Stainless Equipment will be sent to Midwest Grinding to be blanchard ground to a final thickness of 0.18 inches thick with a flatness specification of ± 0.01 ". This flatness measurement should be taken using 6 approximately evenly spaced points throughout the rotor. This thickness tolerance was advised by Hayes as this is what is used on motorcycle racing applications. Midwest Grinding Inc. has donated this service to the team. The front and rear rotors were designed to have a common thickness, thus allowing the same rotor blanks to be used for either system as needed. Once the blanks have been ground to their final thickness, the final profiles will be cut using the waterjet at the university’s student shop.

Due to the high clamping forces that the front rotor will see, the rotor was designed without the use of cross drilling. Cross drilling is a common practice for rotors to allow for enhanced cooling and to allow gases to escape during braking. However, on this vehicle, the small size of the rotor means that small holes will need to be used, and thus, large stress concentrations would be added to the rotor. Additionally, by utilizing sintered metal pads, gas formation from organic pad decay is no longer an issue.

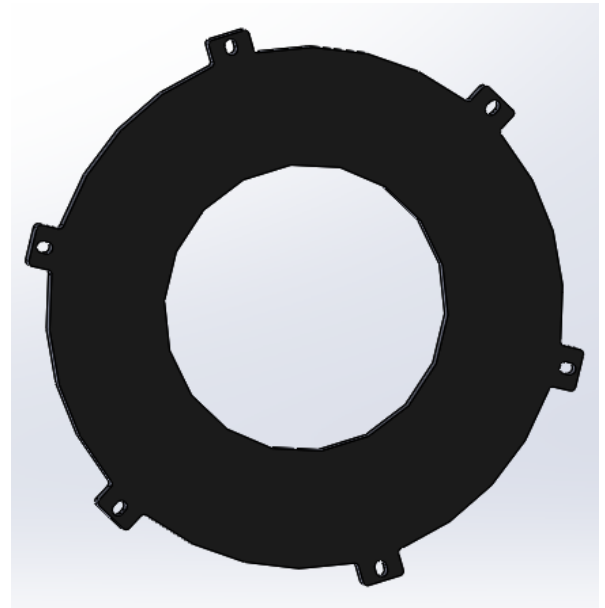


Figure 59: Solidworks model of proposed rotor design

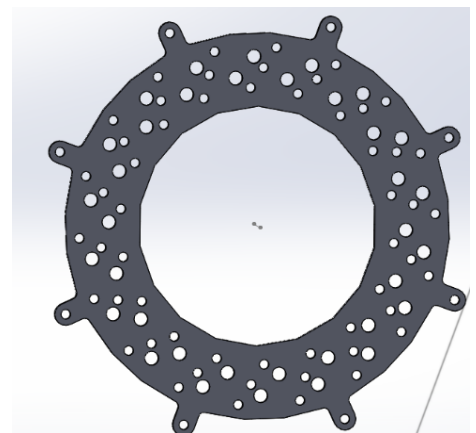


Figure 60: Solidworks model of cross-drilled rotor from WR216 combustion car

The front rotors will mount to the wheel center using floating rotor mounts. These mounts utilize slots to allow the rotor to expand and contract as the system heat cycles. The rotor mounts connect the rotor to the brake hat which transmits the braking torque to the wheel and stops the vehicle.

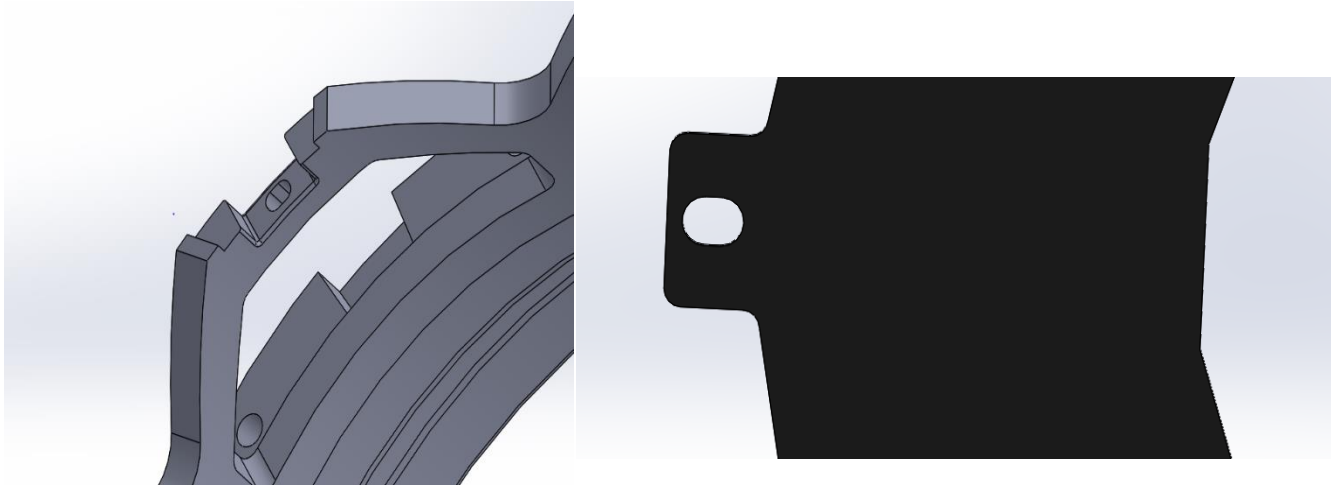


Figure 61: Solidworks model of floating rotor mounts. The groove in the brake hat (left) is positioned transmit braking torque to the chassis even during thermal expansion. The slot in the brake hat ensures the brake hat takes the torque load rather than shearing the bolt. The slot in the brake rotor (right) allows for thermal expansion of the part.

The high clamp load that will be output during the FSAE Rules specified 2000N pedal input provides extreme design challenges for the caliper body design. During these high loads, the caliper body will tend to want to separate the two halves, similar to a clamshell opening. The consulting engineers at Hayes Performance Systems advised us to utilize 2 smaller pistons instead of the original large single bored piston. Additionally, they advised that these be oriented as far apart radially as possible in order to increase the moment of inertia of the caliper. To further resist the bending tendency, the two halves of the caliper will be secured together using 3 grade 10.9 bolts. These bolts will be mounted with washers to decrease the stress concentration caused by the bolt head.

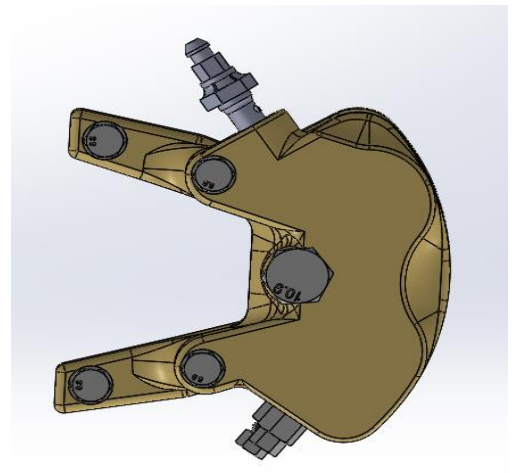


Figure 62: Solidworks model of brake caliper mounting bolts.

The fluid routing to the two halves of the caliper also provided a unique design challenge. The caliper geometry and tight packaging restrictions provided a difficult shape to allow for an internal cross caliper fluid path. The engineers at Hayes asked us to use an external fluid routing system to minimize the complexity of the build. Therefore, a small hole was bored in each half of the caliper. This hole connects the two pistons on each half to a common fluid path. The top of each hole is counterbored to allow a brake line fitting to be attached. These fluid paths can be seen in the figures at right.

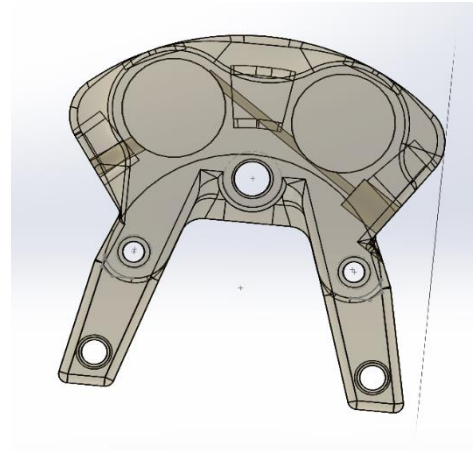


Figure 63: Solidworks model of internal fluid passages

To connect the two sides, a hard line fitting was added to the bottom of each half of the caliper. At the top of each caliper, a bleeder valve is connected to allow the system to be bled. The side on the outside of the vehicle also contains a banjo fitting for the brake fluid inlet. The exterior fluid routing can be seen at right. Routing the brake lines this way allow us to connect both halves while still maintaining clearance around the rotor and other spinning components.

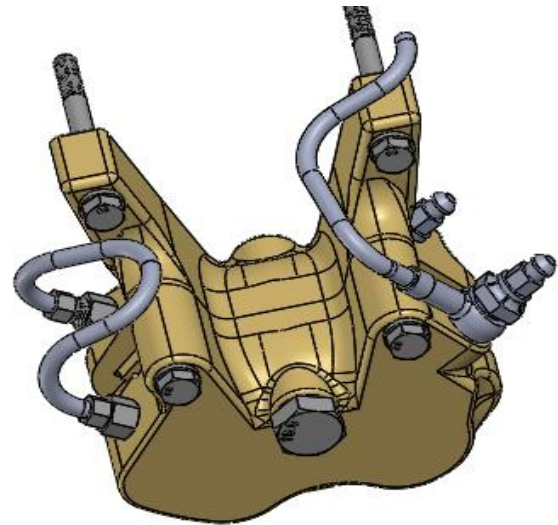


Figure 65: Solidworks model of external fluid passages

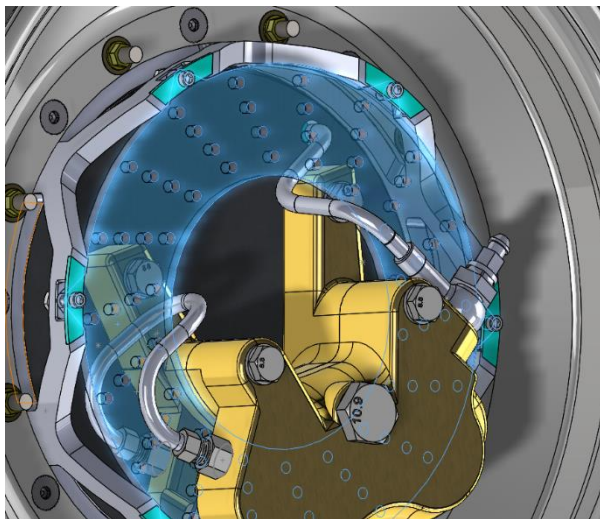


Figure64: Solidworks model of front brake assembly. This model shows the reason for the external brake line geometry

Thermal Desktop Model

A thermal model of the rotor temperatures was created by student contractor Will Sixel in order to predict the temperature of the front rotors. The model utilizes Thermal Desktop software. To create this model, velocity and rotor temperature data from a test day with the WR-216, the Wisconsin Racing combustion car for the 2016 season, was used. A heat generation model was created by analyzing 155 seconds of driving. The kinetic energy of the vehicle was calculated at every point in time giving q_{total} . Any decrease in kinetic energy was assumed to be due to brake activation. The temperature input to the rotor was calculated using 80% of the kinetic energy difference, an assumption that was recommended by Hayes consulting engineers. The model utilizes a left to right split of 50% and a front to rear split of 65%.

Convective cooling of the rotor to the surrounding air was modeled as flow over a flat plate. Using the built in convection correlations from Engineering Equation Solver, a convection coefficient was calculated based on free stream velocity. Since the rotor rotates at some fraction of the vehicle speed due to geometry and has some flow over it (particularly in cornering situations) from the vehicle free stream, the initial velocity of air across the rotor was set as the vehicle velocity. Radiation was modeled to the ambient environment with an emissivity of 0.7. Convection and radiation were modeled to ambient temperatures from all faces of the rotor. The ambient temperature was set to 30°C

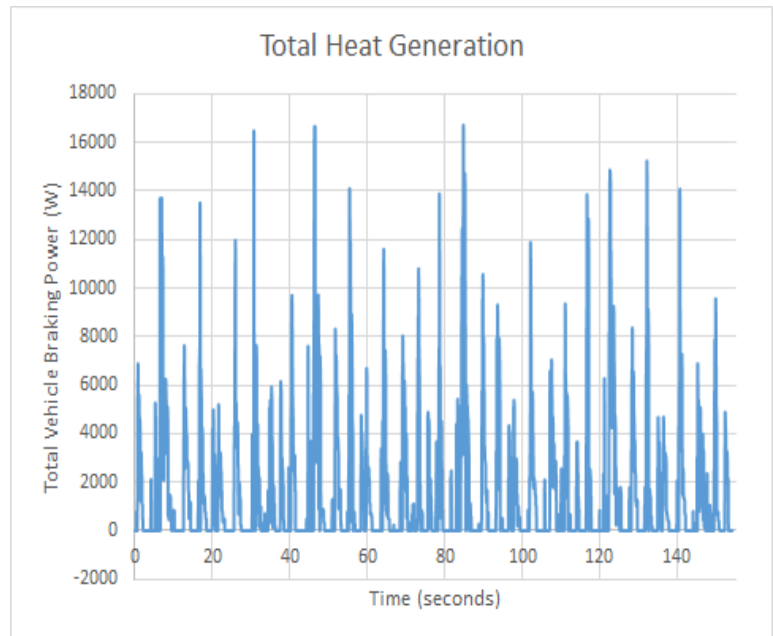


Figure 66: Heat generation model of front brake rotor per given timestep during a test day with WR216

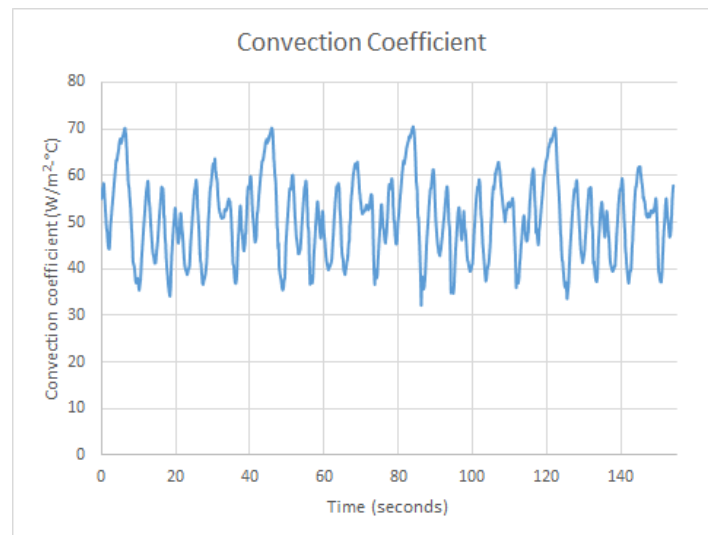


Figure 67: Convective heat transfer coefficient (H) per given timestep during a test day with WR216

The heating and cooling models were then correlated to the measured brake rotor temperatures from the test data. To improve the accuracy of the model, the velocity of the airflow over the plate was modified to be 1.25 times the vehicle velocity. The resulting correlation can be seen at right.

To apply this thermal model to the WR-217e configuration, the material was updated from cast iron to 410 stainless steel and the geometry was updated to match the current rotor configuration. The heat generation model was updated to include the updated vehicle mass and the acceleration was assumed to be consistent with the WR-216. The rotor heat flux was applied over both surfaces of the rotor. The resulting heat input to

the rotor is thus given by:

$$\dot{q}_{rotor} = \dot{q}_{total} * \frac{m_{217e}}{m_{216}} * PC_{left-right} * PC_{front-rear} * PC_{rotor-pad}$$

Note: In this equation, PC stands for “Percentage” and is in decimal form

The steady state temperature of the rotor was then found by running the updated thermal desktop model. The original 155 seconds of data did not supply a stable steady state temperature so the data was repeated for four periods. The resulting 620 of run time provided a steady state temperature of approximately 480C. While this temperature is well within the operating range of the rotor and pad material, the conduction to other components needs to be investigated to ensure system strength at elevated temperatures.

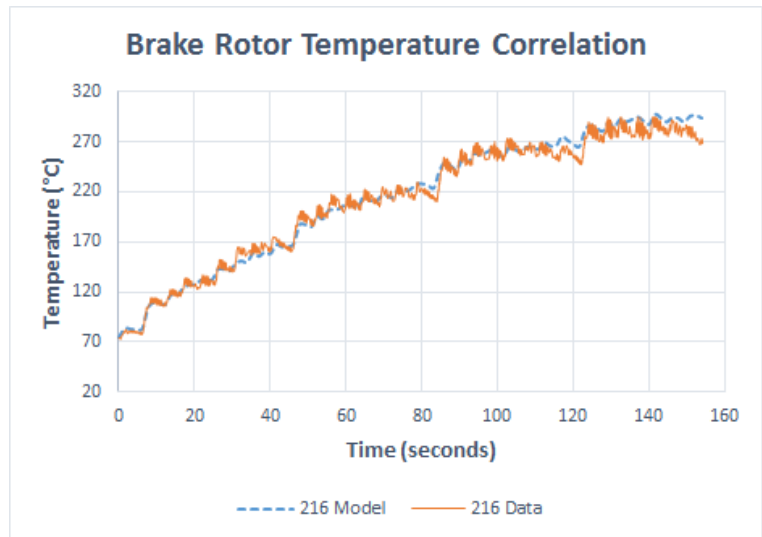


Figure 68: Brake rotor temperature model correlation to WR216 test data

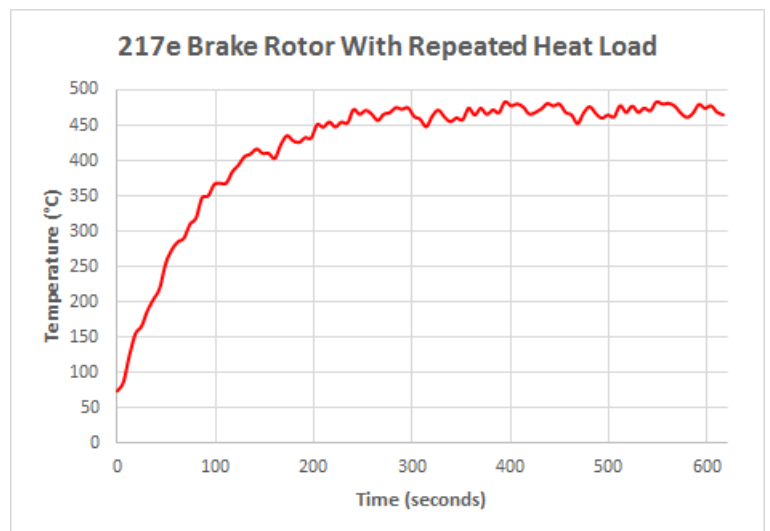


Figure 69: Brake rotor steady state temperature prediction. Model utilizes wr217e vehicle parameters and a 620 second velocity trace from WR216 testing

Solidworks Thermal Analysis

In order to determine the structural properties during operation of the vehicle a thermal analysis of the brake caliper housing was necessary. Due to material property degradation at elevated temperatures it is critical to have an understanding of the material temperature when the loads are applied during a braking event.

Due to the complexity of the caliper housing, Solidworks Thermal Analysis was utilized instead of Thermal Desktop. While thermal desktop provides a much more accurate model of the heat transfer building a representative caliper geometry within the software was out of the scope of our current skill set and time constraints.

The initial study of the caliper was conducted with 7075-T6 aluminum due to its superior mechanical properties to other aluminum alloys. However after running the initial calculations on the caliper and determining a steady state operating temperature of 270 degrees C the material was changed to 2024-T6.

The 7075-T6 would lose 87% of its yield strength at the operating temperature while 2024 would decrease by 66%. Therefore in order to achieve the necessary strength at operating temperature the 2024-T6 was selected.

The heat load is applied to the surface area of the pads and is modeled at various loads. These loads are based on 20% of the energy being transferred to the pad and 80% of the energy to the rotor. This correlation was given to the team by Hayes and validated through the thermal model of the rotor in thermal desktop.

The back of caliper is modeled as a conductive surface to the transmission plate, which will be achieved through the use of thermal paste. The transmission plate also conducts to the upright through the mounts and is modeled as a temperature boundary at 40 degrees Celsius.

All surfaces of the caliper housing except for the face mounting to the transmission plate are modeled as convective surfaces with a heat rejection of $25\text{W}/\text{m}^2$. This heat transfer coefficient was determined from the use of a model based on real world data and is shown to the right.

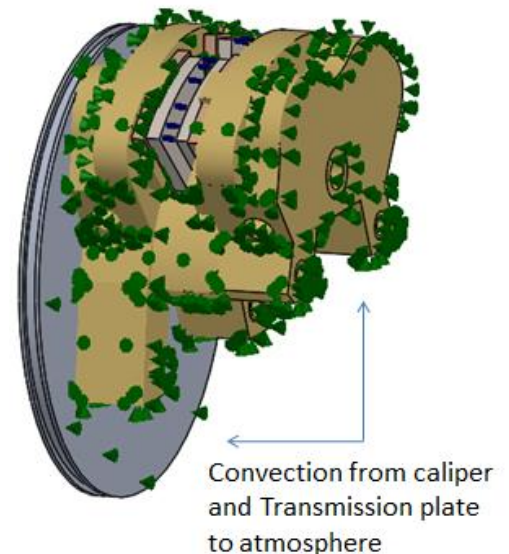
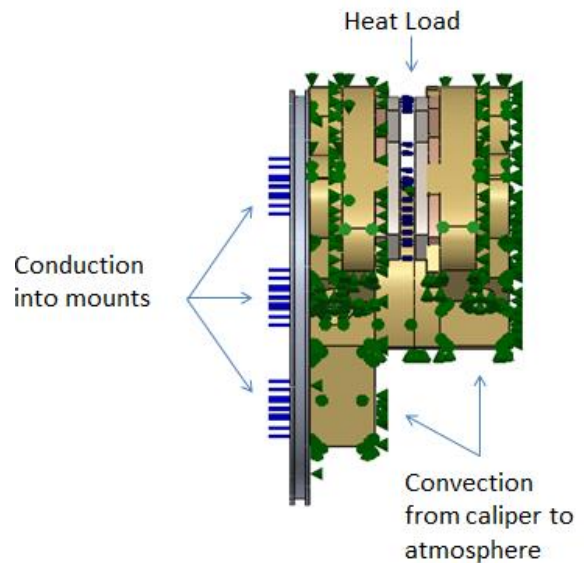


Figure 70: Brake Caliper Conduction Model

The model was extended to include the thermal mass of the upright and more accurately reflect the modes of heat transfer. The constant temperature boundary was defined as the area in contact with the motor face as the motor is held at a steady state temperature of 60 degrees Celsius with the vehicles liquid water cooling system. The convection boundaries remained the same.

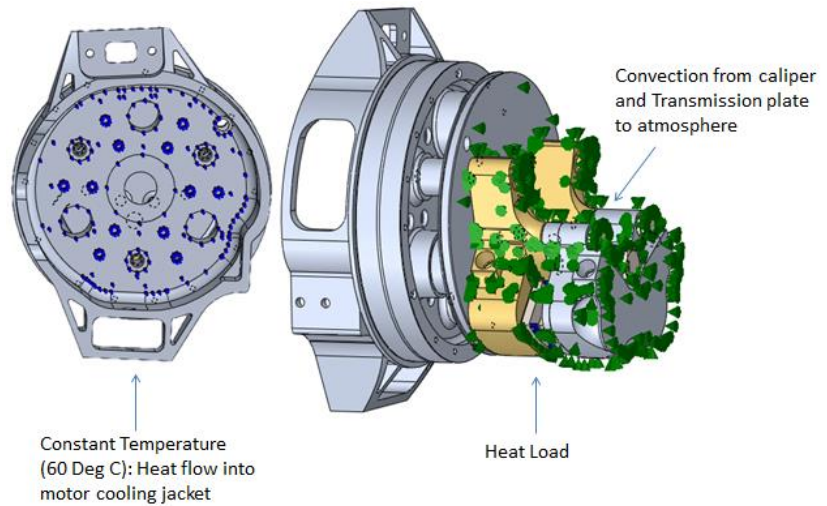


Figure 70b: Brake Caliper Conduction Model

The low heat transfer coefficient was selected as a conservative approximation due to the inside half of the caliper being in a low air flow region. In real world operation the rotation of the wheel center should generate higher velocity airflow and increase the heat transfer coefficient, therefore rejection more heat and keeping the caliper at a lower temperature

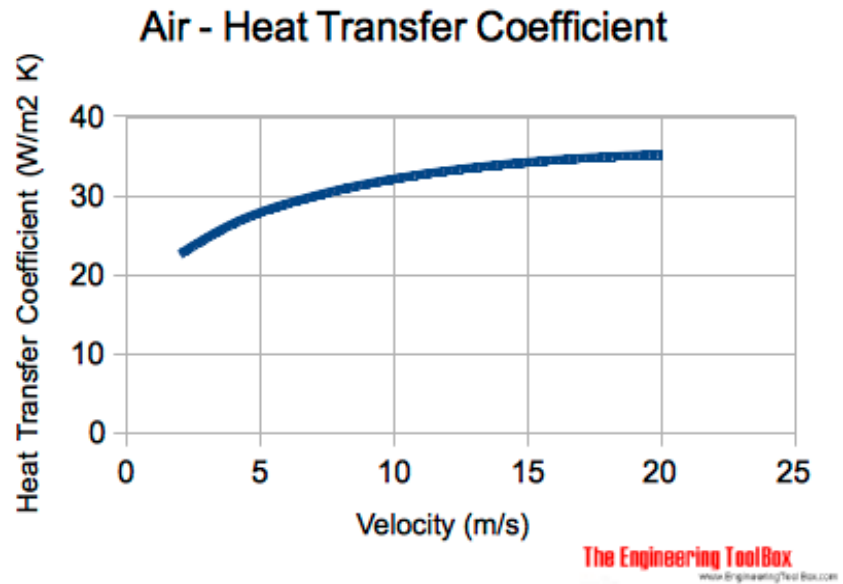


Figure 71: Convective heat transfer coefficient for a given air speed over a flat plate

Solidworks Finite Element Analysis

Solidworks Finite Element Analysis (FEA) was utilized to analyze the design of the custom caliper. This software was used to analyze the normal driving load cases the caliper would see, as well as the peak forces that would be experienced under the panic braking case. The load cases that were modeled can be seen below. The FEA model utilizes a piston force along the center axis of each piston bore. Each piston bore is modeled as having $\frac{1}{4}$ of the total force shown in the table below. The torque on the caliper was modeled using the torque capacity of the tire rather than the torque capacity of the caliper. During a braking event, the vehicle will eventually become traction limited, as it is in both of the cases modeled below. Thus, the highest torque the caliper could see is actually the peak grip of the vehicle. This torque value was applied to the pad supports, tangential to the radius of the rotor.

Pedal Input	Pedal Ratio	Torque Capacity of Tire	Torque Capacity of Caliper	Piston Force
lbf (N)	-	ft-lbf (N-m)	ft-lbf (N-m)	lbf (N)
150 (667)	4.5	419.4 (586.6)	483.9 (656)	2624 (11674)
450 (2000)	5	419.4 (586.6)	1612 (2185)	8741 (38880)

Initial FEA results showed a few stress concentrations throughout the caliper, especially the area where the caliper connected to the mounts. To remedy this, the fillet radius was increased to resemble what is shown at right. Once this was fixed, the caliper was well below the yield strength of the 7075-T6 aluminum that was to be used. However, the thermal model showed substantial increase in temperature, which will result in thermal degradation of the material strength. The caliper housing is now being modified to be made out of 2024-T851 Aluminum. This alloy has a lower yield strength, but a higher resistance to temperature increases. This material change requires several caliper design modifications to ensure reliable performance.

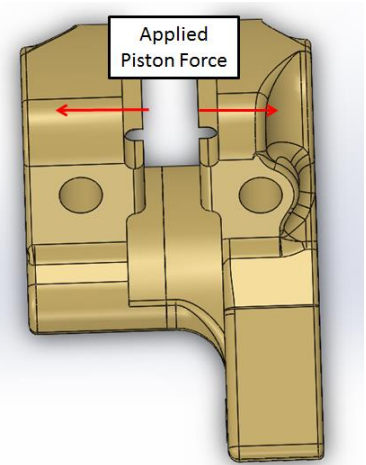


Figure 72: Applied piston force direction used during FEA

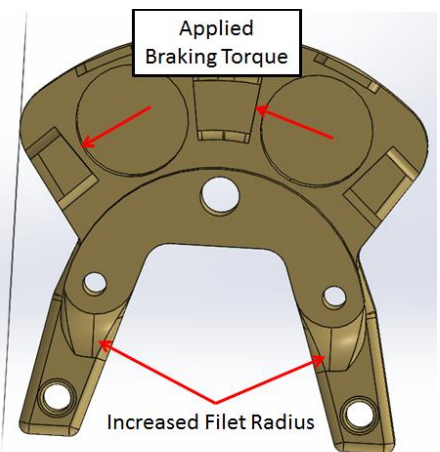


Figure 73: Applied braking torque direction used during FEA. Shows area with largest stress concentration prior to modification

Prototype

The brake calipers will be prototyped in two architectures, a billet machined 2024 caliper with external fluid routing and a direct metal laser sintered titanium caliper with internal fluid routing. The first method is more cost effective and similar to manufacture while the second allows for more optimized fluid routing, higher temperature operating ranges and smaller deflections of the caliper at high pressures.

The brake pads are water jet from proprietary Hayes Performance System pads. The rotor is also a water jet profile out of a Blanchard ground 410 stainless disk. Below a computer generated image shows the Hayes Performance pads with the water jet profiles while the photograph to the right shows the pads post water jet. This water jetting technique allows for a cheap and accurate pad manufacturing process with great flexibility in design for quick changes during testing.

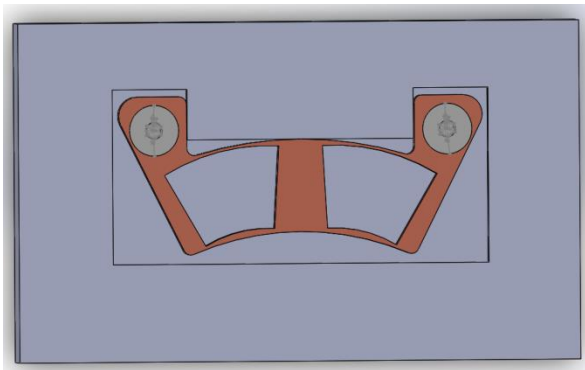
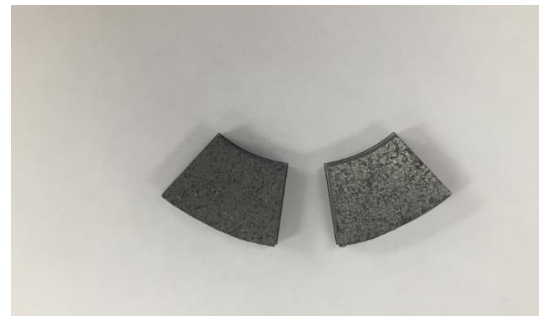


Figure A: CAD Rendering of initial pad geometry



B: Custom water jet

The billet machined 2024 calipers were manufactured first as the machining could be completed in house on the team HAAS VF3 3-axis vertical milling machine. Each caliper half is a two setup part with post machining to be completed by Hayes machinists. The post machining processes are to bore the piston holes, machine the piston seal grooves, cross drill the fluid channel and drill the fitting holes. These processes were either proprietary to Hayes or out of the capability of the HAAS VF3. The initial prototype is shown below.



Figure A: Assembled Caliper



B: Pad placement

Testing Plan

Once the custom caliper has been built, the Wisconsin Racing team will work with the engineers at Hayes Performance Systems to thoroughly test the caliper. Hayes has the capabilities to pressure cycle the caliper, both at room temperature and at elevated temperatures. This capability will allow us to validate our FEA analysis of the caliper during normal conditions, as well as test the caliper to failure if we see fit. Additionally, we are able to test the caliper and rotor together using a brake dynamometer. Hayes has offered to let us use their brake dyno as long as there is room in their testing schedule. Otherwise, one can be constructed using the electric motor of the lathe in the automotive shop. Testing with the brake dyno allows for high temperature cycling of both the rotor and caliper as well as a way of measuring the brake pad coefficient.

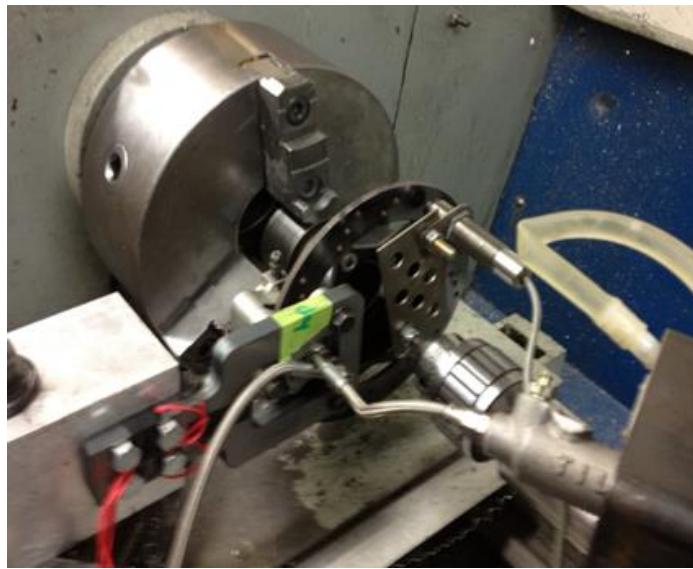


Figure 74: Student built brake dynamometer which utilizes the electric motor from a lathe



Finalization of In-Hub Motor Design

In order to close out the in-hub motor design each system must undergo a final Critical Design Review by the team and automotive advisor Dr. Glenn Bower. This design review will go through the structural, vibration and thermal analysis conducted on each component in the system. Secondly, manufacturing and component sponsors will each conduct a final manufacturing meeting to determine the manufacturing process for the upright, wheel center, transmission enclosure and brake caliper.

Upon completion of the design review and possible design changes to improve manufacturability, the components will be machined in house or by Formula Electric Team Sponsors. Once manufacturing is complete, the assembly process will begin and the components will be tested both on and off the vehicle. The testing of this system will first be component based and off the vehicle. Upon proving nominal system performance, this preliminary testing will lead to full system testing on the vehicle at track days. Detailed test plans and procedures will be created using the Wisconsin Racing template and documented accordingly.

Table 19: Corporate Sponsors for each component are located below.

Component	Sponsor	Partnership
Brushless Surface Permanent Magnet 15 kW Motor	Plettenberg	Design Support
Motor Controller	Plettenberg	Design Support
Motor Shaft	Edgerton Gear	Design Support
Upright	Revolutionary Machine & Design LLC	Machining
Wheel Center	Revolutionary Machine & Design LLC	Machining
Transmission Enclosure	Cate Machining and Welding	Machining
Custom Caliper	Hayes Performance	Design Support, Machining, Testing and Component donation
Thin Section Angular Contact Hub Bearings	SilverThing	50% Discount
Deep Groove Ball Bearings	NSK	100% Discount
Bearing Retainers	EMP	Laser Cutting and Material Supplier
Rotor Material	Apache Stainless Equipment	Full Donation
Rotor Blanchard Grinding	Midwest Grinding Inc.	Full Donation



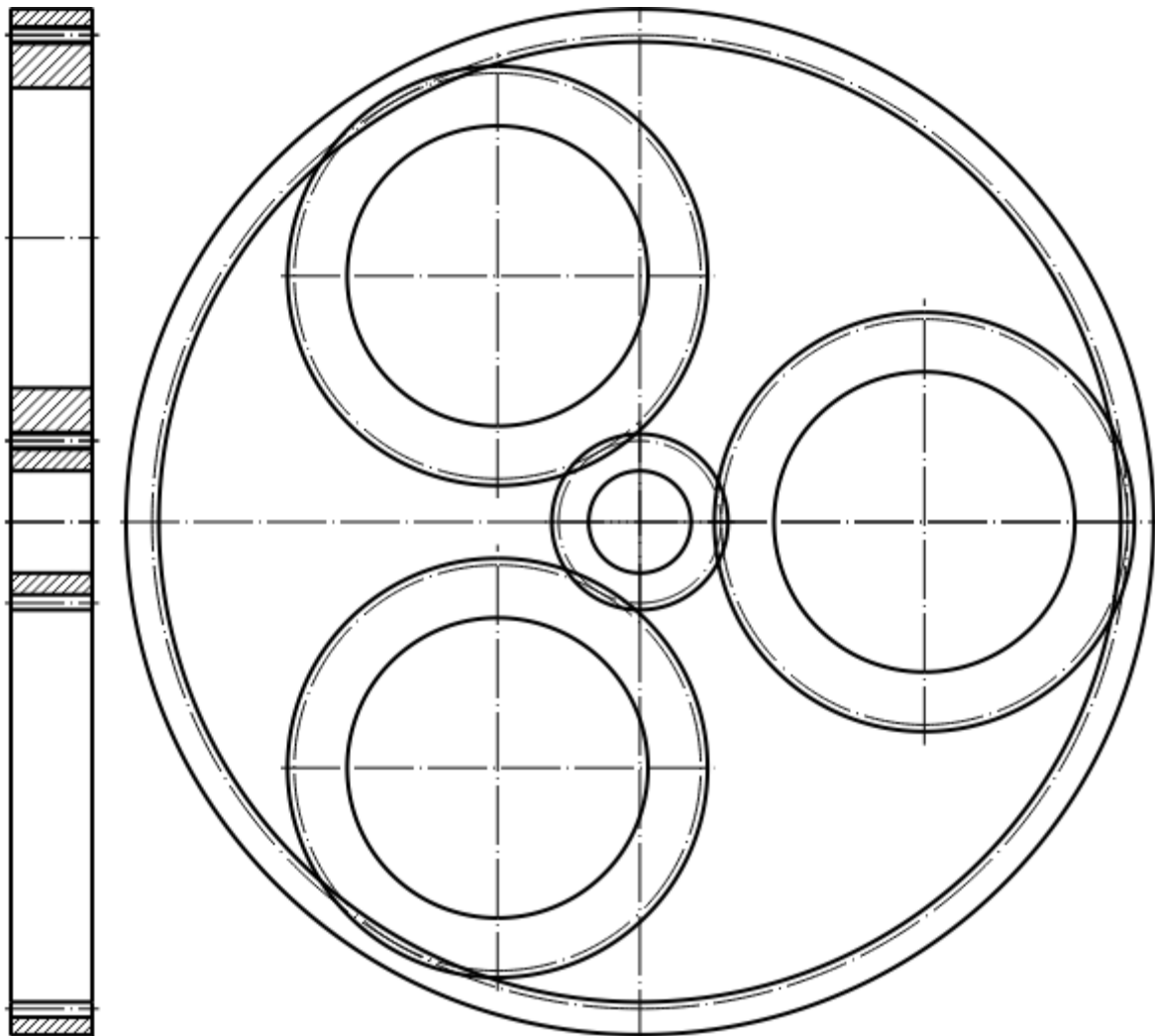
Spring Semester Manufacturing, Assembly and Testing Plan

Table 20: Spring semester plan

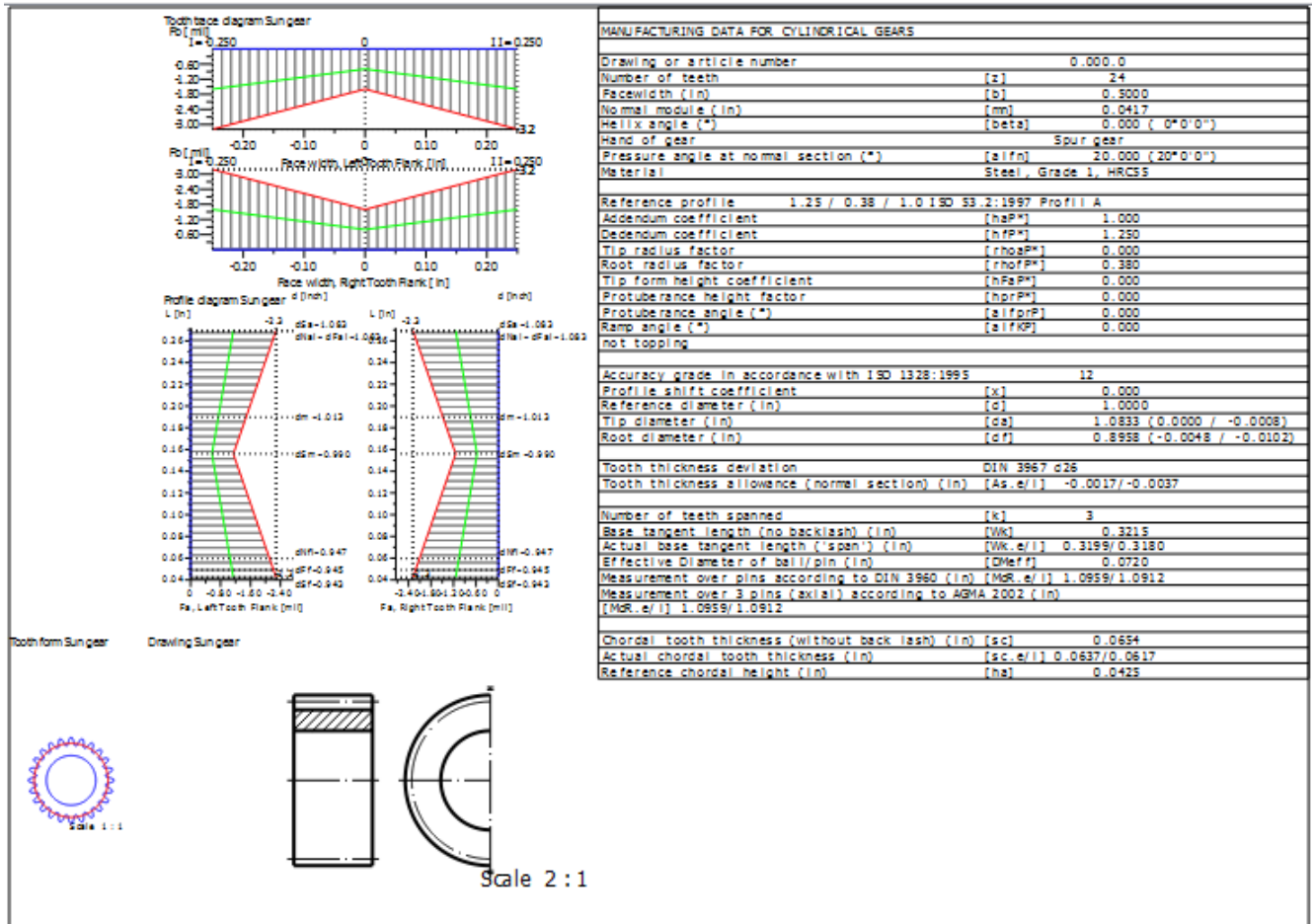
	<u>Jan</u>	<u>Feb</u>	<u>March</u>	<u>April</u>	<u>May</u>	<u>June</u>
Upright Manf Wheel Center Manf. Gear Manf. Trans Enc Manf. Retainer Manf. Pillow Block Manf.						
Bearing Orders						
In-Hub Assembly						
Motor Delivery						
Motor Dyno Testing						
Motor Marriage to Upright						
Caliper Testing						
Planetary Gear Testing to Failure						
Shaft Testing to Failure						
System Marriage to Vehicle						
Vehicle Testing						
System Inspection						
Competition						

Manufacturing Design

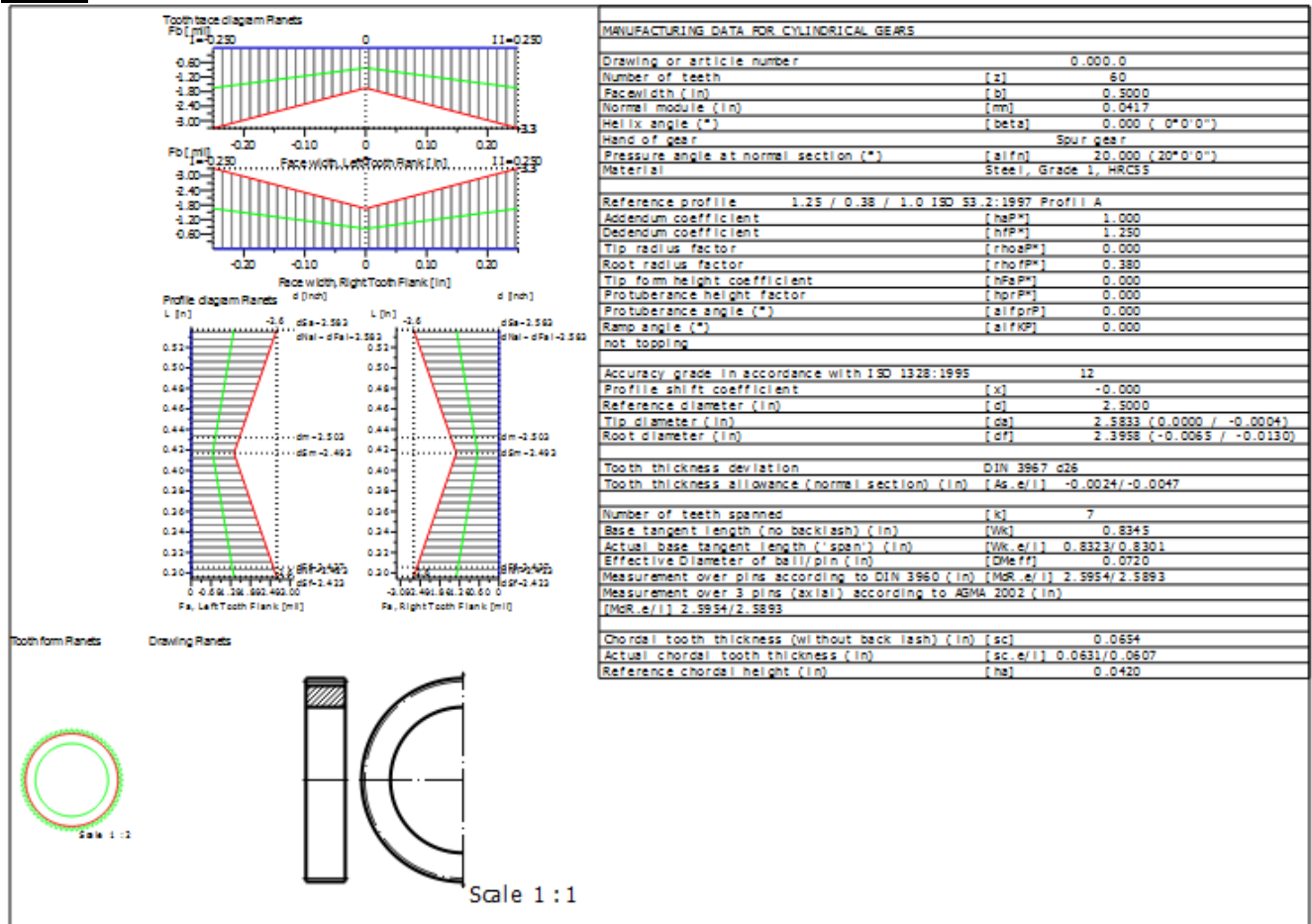
KISSsoft manufacturing Data



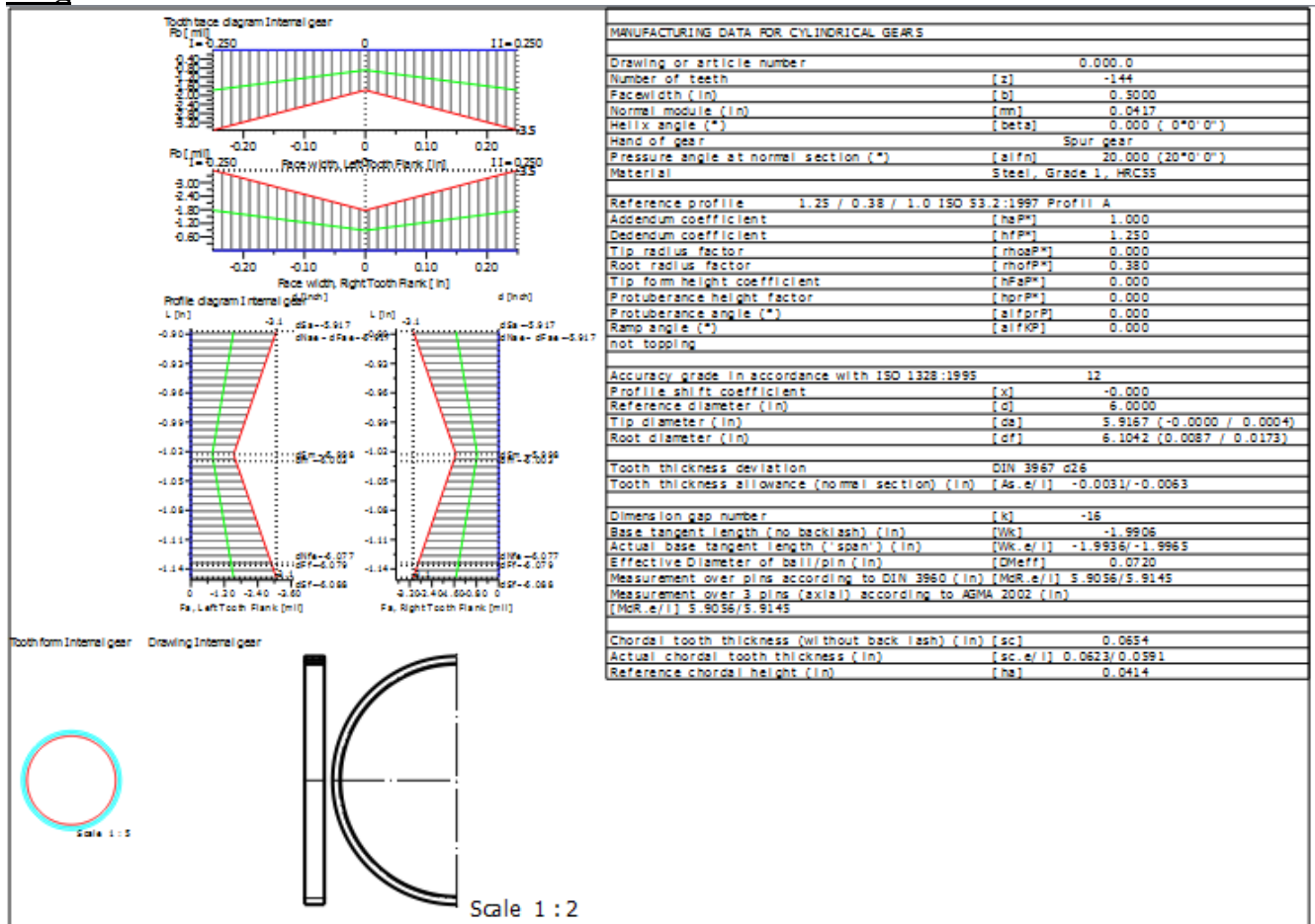
Sun



Planet

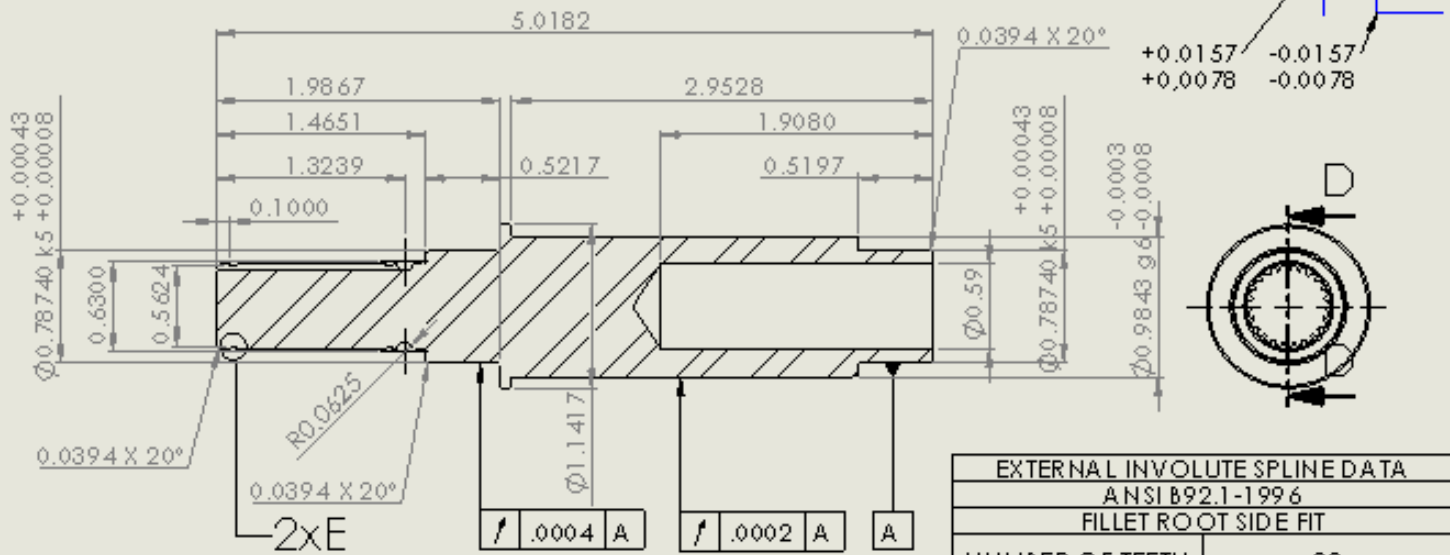


Ring



Drawings

1. MATERIAL: 4140 28-32 ROCKWELL PRE-HARD
2. HARDEN SLINE UP TO BEARING SEAT 50-55 ROCKWELL



SECTION D-D
SCALE 1 : 1

DETAIL 2xE
SCALE 4 : 1

EXTERNAL INVOLUTE SPLINE DATA	
ANSI B92.1-1996	
FILLET ROOT SIDE FIT	
NUMBER OF TEETH	23
SPLINE PITCH	40/80
PRESSURE ANGLE	30°
BASE DIAMETER	.497965 REF
PITCH DIAMETER	.575 REF
MAJOR DIAMETER	0.600/0.597
FORM DIAMETER	0.546
MINOR DIAMETER	0.513 MIN
CIRCULAR SPACE WIDTH	
MAX EFFECTIVE	0.0393
MIN ACTUAL	0.0366

NOTES:

IF NOT SPECIFIED +/- .004 INCH
EXTERNAL FILLETS: R 0.0157 INCH
INTERNAL FILLETS: R 0.0157 INCH

SCALE: 1:1

MATERIAL
4140 PRE-HARD

TITLE:

SIZE UW-MADISON PART NUMBER
A 217e-330-03

WEIGHT: LBS

SHEET 1 OF 1



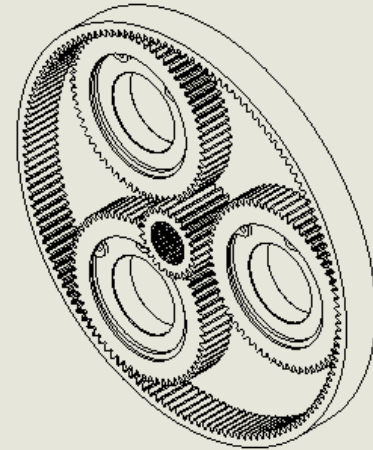
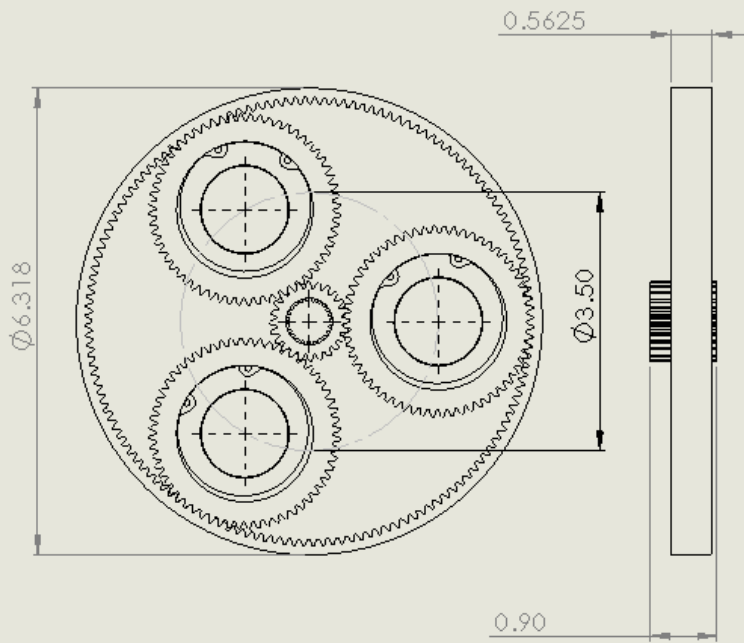
5

4

3

2

1



NOTES:

SCALE: 1:2

TITLE:

MATERIAL

SIZE

A

UW -MADISON PART NUMBER

217e-320-00-24

WEIGHT: LBS

SHEET 1 OF 1

5

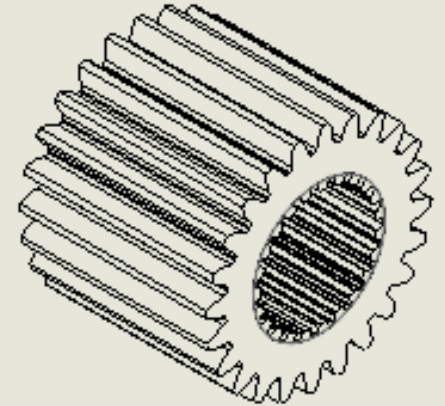
4

3

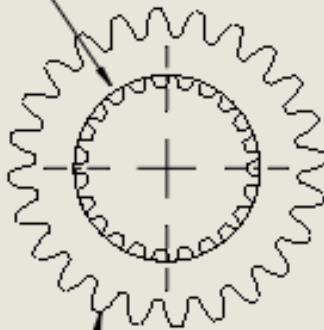
2

1

1. MATERIAL: 4140 28-32 ROCKWELL PRE-HARD
2. GAS NITRIDE SURFACE 50-55 ROCKWELL. DEPTH .015 INCH
3. POLISH TO MIRROR FINISH RA: 4-8 (PENDING CAPABILITY)



INTERNAL
INVOLUTE SPLINE
(TABLE 1)



INVOLUTE SPUR GEAR
24/48 DIA METRAL PITCH
20 DEG PRESSURE ANGLE
24 TOOTH, QUALITY 12

0.900 ±0.005



TABLE 1

INTERNAL INVOLUTE SPLINE DATA	
ANSI B92.1-1996	
FILLET ROOT SIDE FIT	
NUMBER OF TEETH	23
SPLINE PITCH	40/80
PRESSURE ANGLE	30°
BASE DIA METER	.497965 REF
PITCH DIA METER	.575 REF
MAJOR DIA METER	.632 MAX
FORM DIA METER	.604
MINOR DIA METER	.533/.550
CIRCULAR SPACE WIDTH	
MAX EFFECTIVE	0.0419
MIN ACTUAL	0.0366

NOTES: QTY: 3
GEAR AND SPLINE PARAMETERS CAN
BE ALTERED PENDING CAPABILITIES.
CONTACT BILLY KUCINSKI (715) 307-
3266

SCALE: 2:1

MATERIAL 4140

TITLE: SUN GEAR

SIZE A BY WABOND PART NUMBER
217e-320-01-24

WEIGHT: LBS

SHEET 1 OF 2



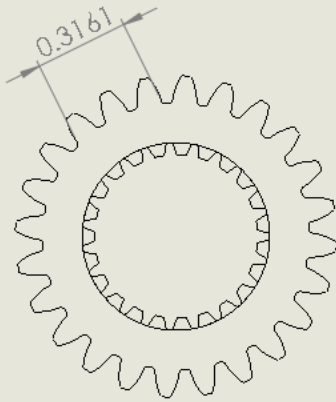
5

4

3

2

1



DATA FOR SPUR GEAR (SUN)		
TYPE OF DATA	VALUE	DATA
BASIC SPECIFICATIONS	24	NUMBER OF TEETH
	24	DIAMETRAL PITCH
	20°	PRESSURE ANGLE
	2.50	STANDARD PITCH DIAMETER
	STANDARD	TOOTH FORM
	.12083	MAX. CALC. CIRCULAR THICKNESS ON STD. PITCH CIRCLE
MANUFACTURING AND INSPECTION	12	A.G.M.A. QUALITY CLASS
	E	BACKLASH DESIGNATION
	ZERO	ALLOWANCE, PER GEAR, INCH
	0 TO .001	TOLERANCE, PER GEAR, INCH
	0.0003	MAX. TOOTH-TO-TOOTH COMPOSITE ERROR
	0.0005	MAX. TOTAL COMPOSITE ERROR
	1.0833	OUTSIDE DIAMETER (SHOWN ON DRAWING)
		MIN MEAS. OVER TWO .XXXX DIA. PINS
	26.3997	MAX MEAS. OVER TWO .XXXX DIA. PINS
ENGINEERING REFERENCE	60	NUMBER OF TEETH IN MATING GEAR

NOTES:

SCALE: 2:1

TITLE:



MATERIAL

SIZE

UW-MADISON PART NUMBER

A

217e-320-01-24

WEIGHT: LBS

SHEET 2 OF 2

5

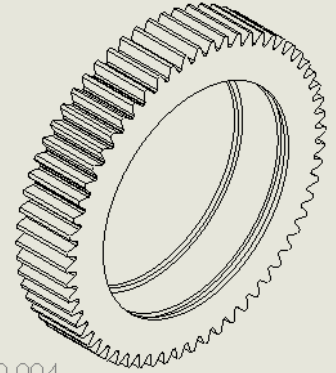
4

3

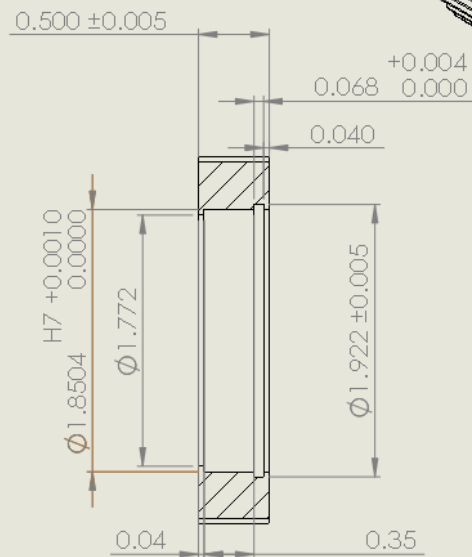
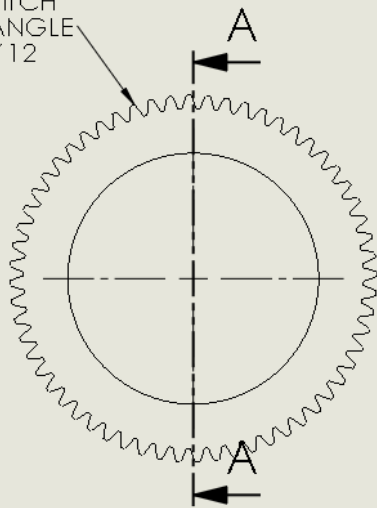
2

1

1. MATERIAL: 4140 28-32 ROCKWELL PRE-HARD
2. GAS NITRIDE SURFACE 50-55 ROCKWELL. DEPTH .015 INCH
3. POLISH TO MIRROR FINISH RA: 4-8 (PENDING CAPABILITY)



INVOLUTE SPUR GEAR
 24/48 DIAMETRAL PITCH
 20 DEG PRESSURE ANGLE
 60 TOOTH, QUALITY 12



SECTION A-A



NOTES: QTY: 9
 IF NOT OTHERWISE SPECIFIED
 0.000 +/- 0.005
 0.00 +/- 0.01

SCALE: 1:1
 MATERIAL 4140

TITLE: PLANET GEAR

SIZE UW-MADISON PART NUMBER
A 217e-320-02-24

WEIGHT: LBS SHEET 1 OF 2

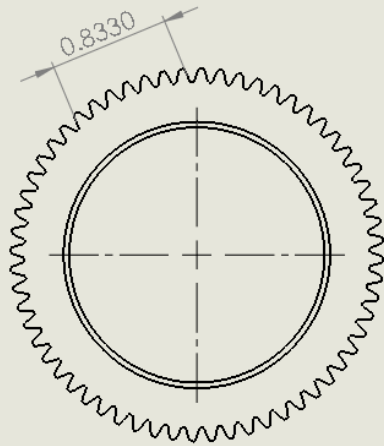
5

4

3

2

1



DATA FOR SPUR GEAR (PLANET)		
TYPE OF DATA		DATA
BASIC SPECIFICATIONS	60	NUMBER OF TEETH
	24	DIAMETRAL PITCH
	20°	PRESSURE ANGLE
	2.50	STANDARD PITCH DIAMETER
	STANDARD	TOOTH FORM
	.12083	MAX. CALC. CIRCULAR THICKNESS ON STD. PITCH CIRCLE
MANUFACTURING AND INSPECTION	12	A.G.M.A. QUALITY CLASS
	B	BACKLASH DESIGNATION
	.002	ALLOWANCE, PER GEAR, INCH
	0 TO .001	TOLERANCE, PER GEAR, INCH
	0.0003	MAX. TOOTH-TO-TOOTH COMPOSITE ERROR
	0.0006	MAX. TOTAL COMPOSITE ERROR
	2.5833	OUTSIDE DIAMETER (SHOWN ON DRAWING)
	62.424	MIN MEAS. OVER TWO .XXXX DIA. PINS
62.4292	MAX MEAS. OVER TWO .XXXX DIA. PINS	
ENGINEERING REFERENCE	144	NUMBER OF TEETH IN MATING GEAR

NOTES:

SCALE: 1:1

TITLE:

MATERIAL

SIZE

UW-MADISON PART NUMBER

A

217e-320-02-24

WEIGHT: LBS

SHEET 2 OF 2



5

4

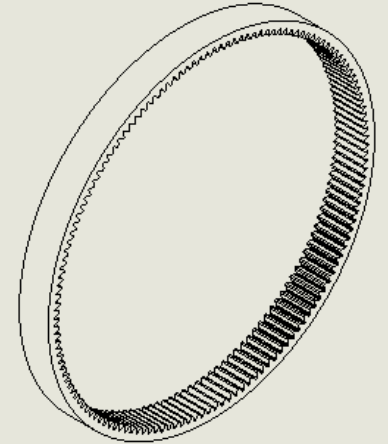
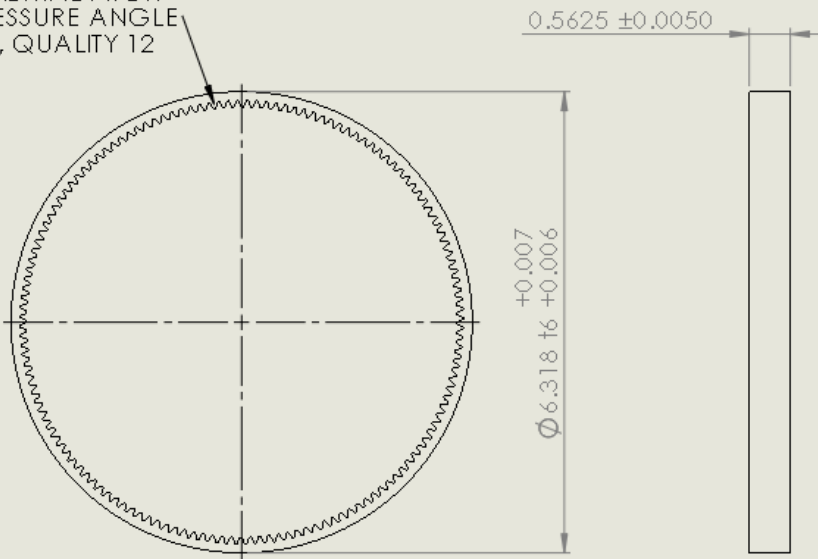
3

2

1

1. MATERIAL: 4140 28-32 ROCKWELL PRE-HARD
2. GAS NITRIDE SURFACE 50-55 ROCKWELL. DEPTH .015 INCH
3. POLISH TO MIRROR FINISH RA: 4-8 (PENDING CAPABILITY)

INTERNAL INVOLUTE SPUR GEAR
 24/48 DIAMETRAL PITCH
 20 DEG PRESSURE ANGLE
 144 TOOTH, QUALITY 12



NOTES: QTY; 3

SCALE: 1:2

TITLE: RING GEAR

MATERIAL 4140

SIZE UW-MADISON PART NUMBER

A 217e-320-06

WEIGHT: LBS

SHEET 1 OF 2

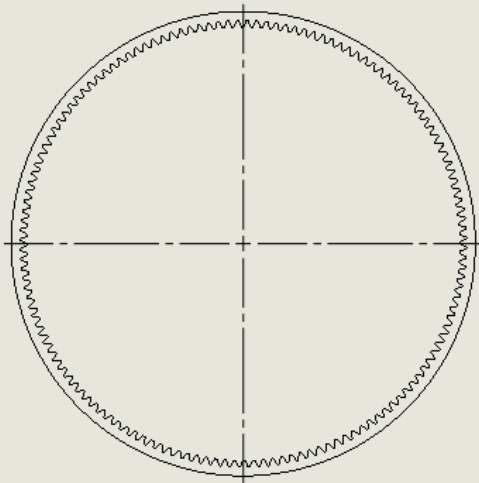
5

4

3

2

1



DATA FOR SPUR GEAR (RING)		
TYPE OF DATA	VALUE	DATA
BASIC SPECIFICATIONS	144	NUMBER OF TEETH
	24	DIAMETRAL PITCH
	20°	PRESSURE ANGLE
	6	STANDARD PITCH DIAMETER
	STANDARD	TOOTH FORM
	.12083	MAX. CALC. CIRCULAR THICKNESS ON STD. PITCH CIRCLE
MANUFACTURING AND INSPECTION	12	A.G.M.A. QUALITY CLASS
	D	BACKLASH DESIGNATION
	0.0001	ALLOWANCE, PER GEAR, INCH
	0 TO .0001	TOLERANCE, PER GEAR, INCH
	0.0003	MAX. TOOTH-TO-TOOTH COMPOSITE ERROR
	0.0007	MAX. TOTAL COMPOSITE ERROR
		OUTSIDE DIAMETER (SHOWN ON DRAWING)
	142.6679	MIN MEAS. OVER TWO .XXX DIA. PINS
	142.6706	MAX MEAS. OVER TWO .XXX DIA. PINS
ENGINEERING REFERENCE	60	NUMBER OF TEETH IN MATING GEAR



NOTES:	SCALE: 1:2	TITLE:
	MATERIAL	SIZE A UW - MADISON PART NUMBER 217e-320-06
		WEIGHT: LBS SHEET 2 OF 2

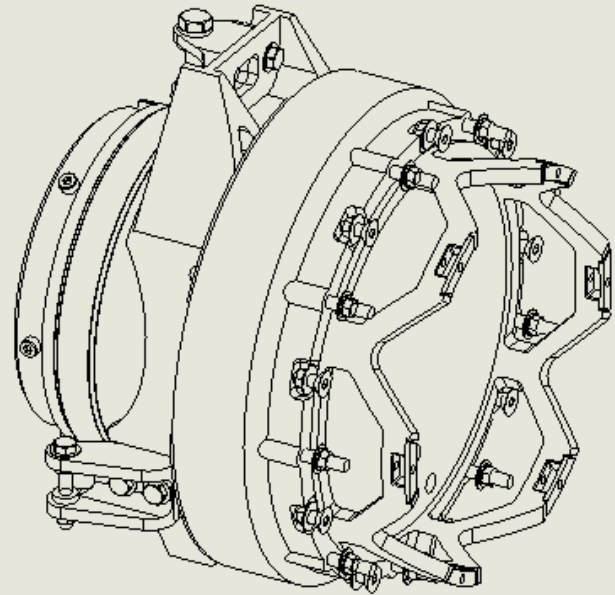
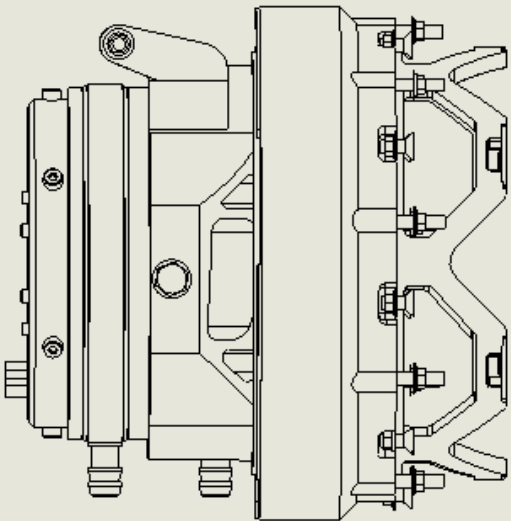
5

4

3

2

1



NOTES:

SCALE 1:5

TITLE:

MATERIAL

SIZE LW - MADE ON PART NUMBER

2 ★ E-241-00-01 Front Upright Assembly

WEIGHT: LBS

SHEET 1 OF 2



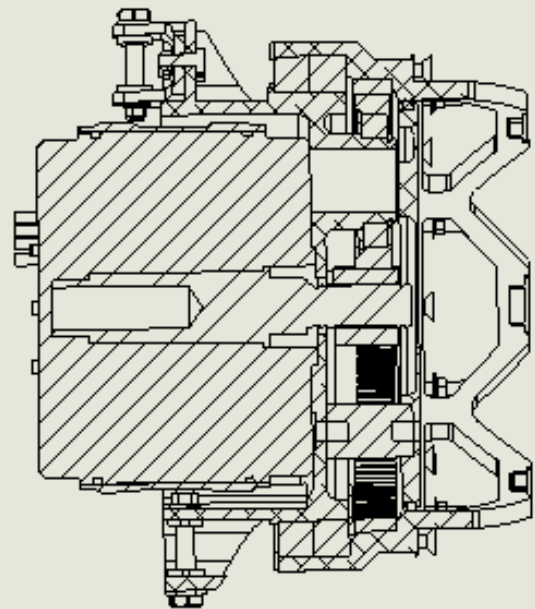
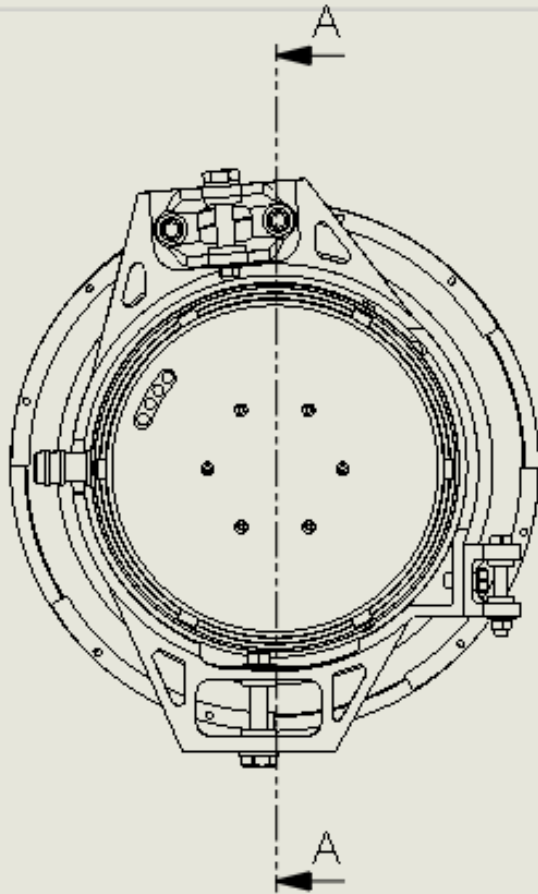
5

4

3

2

1



SECTION A-A
SCALE 1 : 2

NOTES:

SCALE: 1:2

TITLE:

MATERIAL

SEE UW-MADISON PART NUMBER

214 E-241-00-01 Front Upright Assembly

WEIGHT: LBS

SHEET 5 OF 5



5

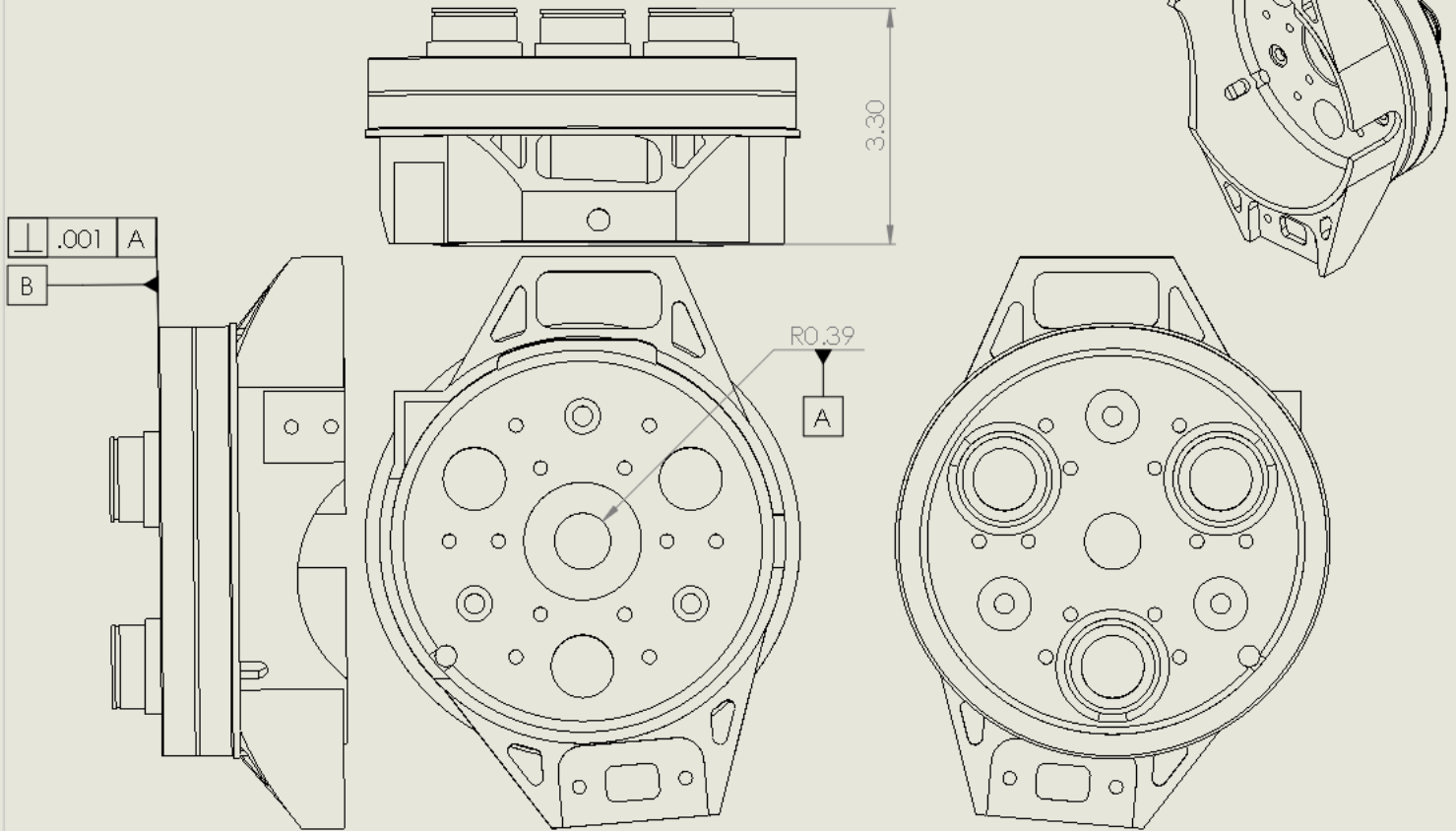
4

3

2

1

1. THIS IS A MINIMAL DIMENSION DRAWING. REFER TO SOLID MODEL FILE UNLESS OTHERWISE SPECIFIED
 2. GENERAL PROFILE TOLERANCE Δ .010 A B



NOTES: CONTACT: BILLY KUCINSKI C: (715) 307 - 3266 E: KUCINSKI@GO.UWRACING.COM	SCALE: 1:5	TITLE:
	MATERIAL 7075-T6	SIZE UW-MADISON PART NUMBER A 217e-241-01-04L Front Upright WEIGHT: LBS SHEET 1 OF 3



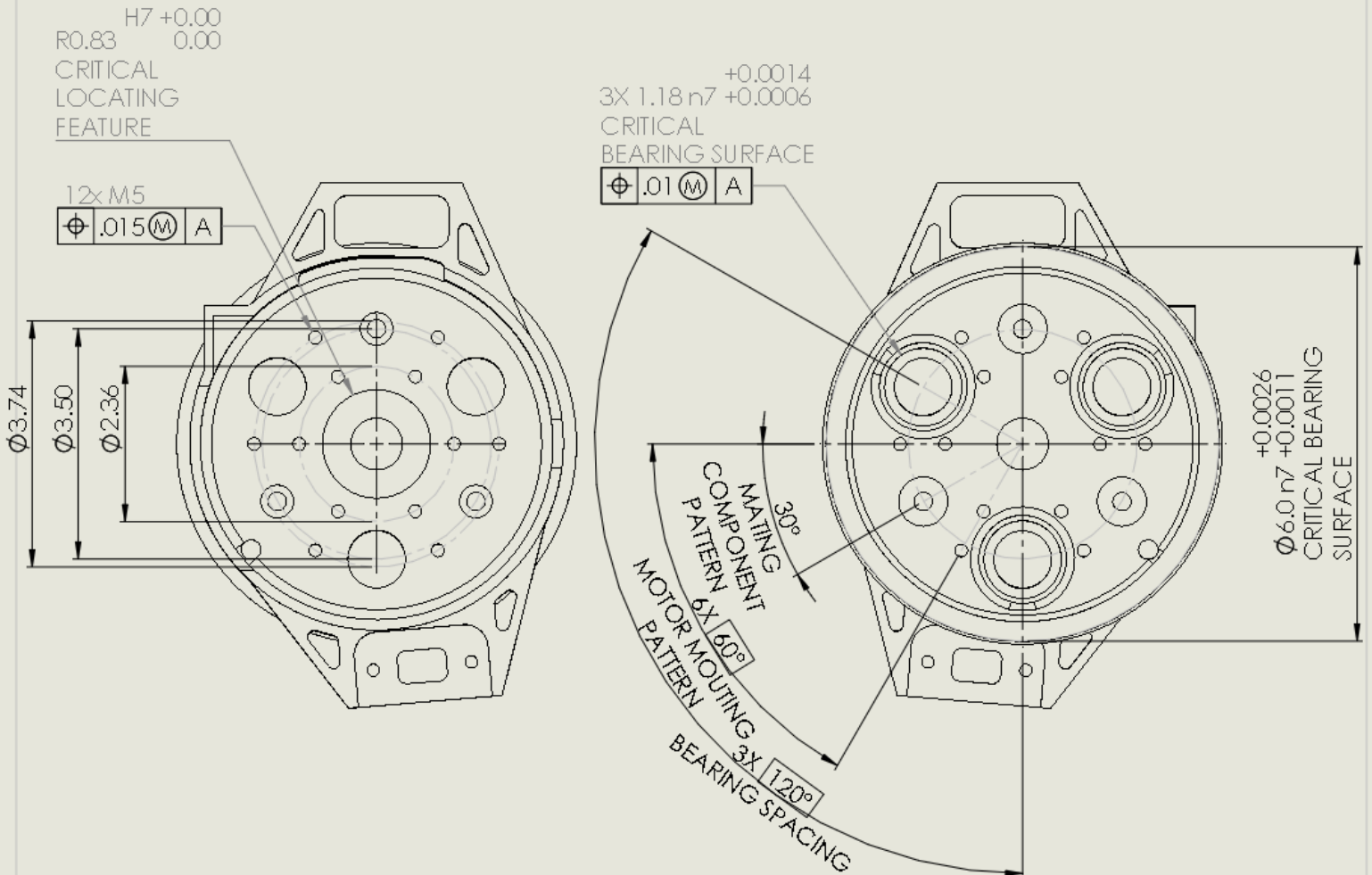
5

4

3

2

1



NOTES:

SCALE: 1:1

TITLE:



MATERIAL

SIZE UW-MADISON PART NUMBER

A 217e-241-01-04L Front Upright

WEIGHT: LBS

SHEET 2 OF 3

5

4

3

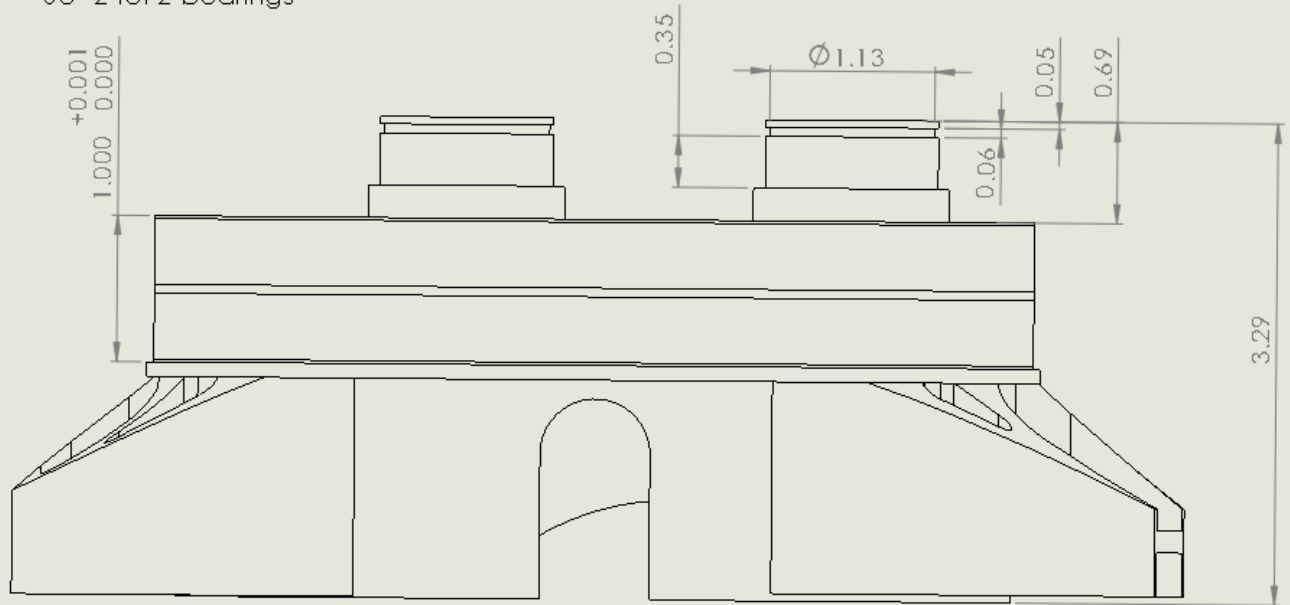
2

1

$1.00 - (.0005 * 2) = .99$
 For SD060BROK

K gives negative
 axial clearance of -
 0.0005 per bearing

So *2 for 2 bearings



NOTES:

SCALE: 1:5

TITLE:



MATERIAL

SIZE UW-MADISON PART NUMBER

A 217e-241-01-04L Front Upright

WEIGHT: LBS

SHEET 3 OF 3

5

4

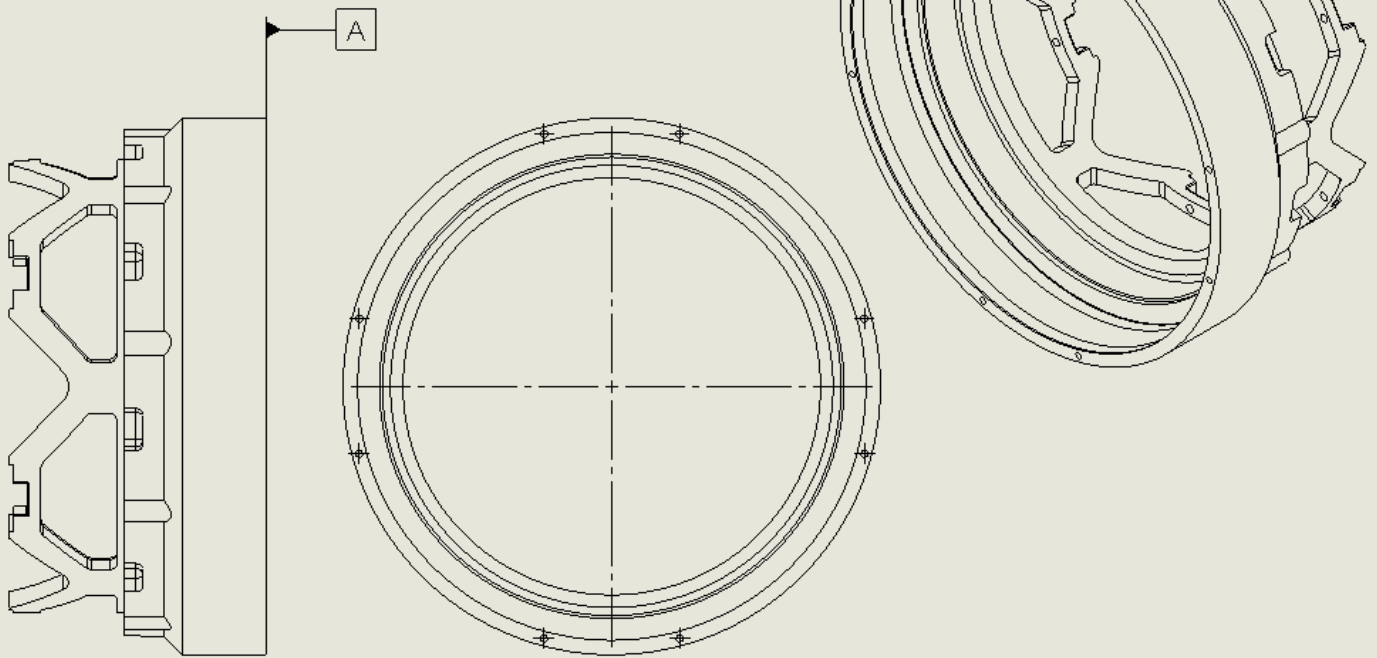
3

2

1

1. THIS IS A MINIMAL DIMENSION DRAWING. REFER TO SOLID MODEL FILE UNLESS OTHERWISE SPECIFIED

2. GENERAL PROFILE TOLERANCE $\triangle .015$ A B



NOTES:
MINIMAL DIMENSIONS
FOR COMPONENT
ASSESSMENT

SCALE: 1:5

MATERIAL 7075-T6

TITLE:

SIZE
A

UW -MADISON PART NUMBER

271 E-247-wheel center

WEIGHT: LBS

SHEET 1 OF 3

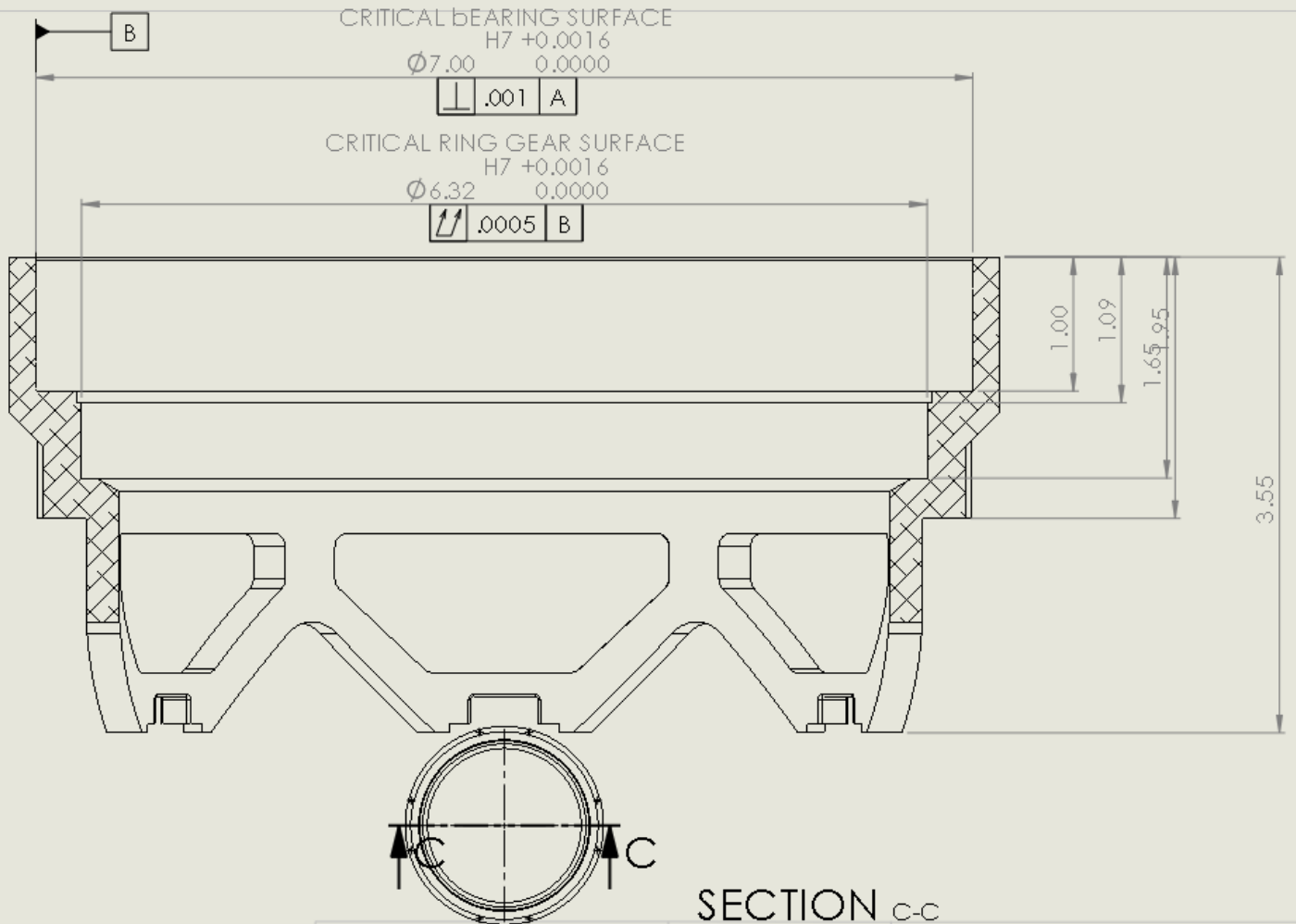
5

4

3

2

1



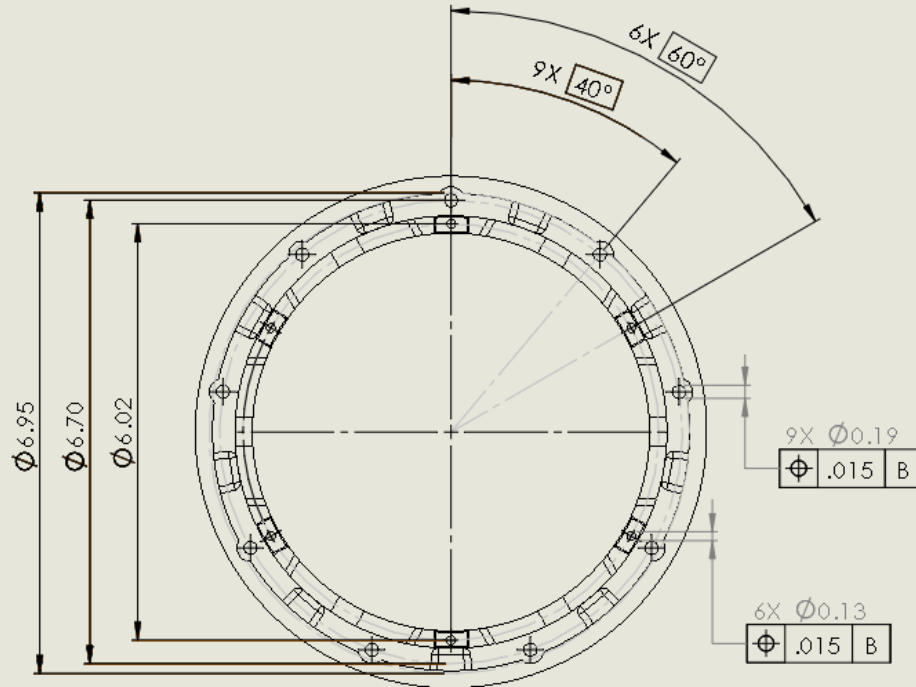
NOTES:

SECTION C-C
SCALE 1:1



MATERIAL	SIZE A	UW - MADISON PART NUMBER
		271 E-247-wheel center
	WEIGHT: LBS	SHEET 2 OF 3

5 4 3 2 1



NOTES:

SCALE: 1:5

TITLE:



MATERIAL

SIZE

A

UW-MADISON PART NUMBER

271 E-247-wheel center

WEIGHT: LBS

SHEET 3 OF 3

5

4

3

2

1



Sources

1. 410 Stainless Steel. (n.d.). Retrieved December 11, 2016, from <http://www.pennstainless.com/stainless-grades/400-series-stainless/410-stainless-steel/>
2. What is sintering - EBC Brakes. (n.d.). Retrieved December 11, 2016, from <http://ebcbrakes.com/what-is-sintering/>
3. Motion & Control NSK Roller Bearing CatalogNo. E110g 2003E-8 Printed in Japan NSK Ltd. 1996
4. Oberg, Eric, 1881 - 1951 Machinery's Handbook. ISBN 0-8311-2492-X
5. A Four Wheel Drive System for a Formula Style Electric Racecar, Peder August Aune, Norwegian University of Science and Technology.

Pictures:

EBR: <http://www.motorcycle.com/manufacture/buell/2014-eb-1190rx-review-first-ride.html>

Delft: <http://www.racecar-engineering.com/wp-content/gallery/delft/zuptud2.jpg>



Appendix

ME 351 - Formula Electric Drivetrain Product Design Specification Formula SAE Electric



WISCONSIN
UNIVERSITY OF WISCONSIN-MADISON

University of Wisconsin - Madison

Authors: William Kucinski, Rocky Liang, Chad Davis, Matt Masucci

Issue 1 – 4/10/2016

Contents

Function	104
Client Requirements	104
Design Requirements	104
Physical and Operational Characteristics	



1.0 Performance Requirements	104
2.0 Safety	105
3.0 Accuracy, Quality and Reliability	105
4.0 Life in Service	105
5.0 Shelf Life	105
6.0 Operating Environment	105
7.0 Ergonomics	106
8.0 Size	106
9.0 Weight	106
10.0 Materials	106
11.0 Aesthetics, Appearance and Finish	106
Production Characteristics	
12.0 Quantity	106
13.0 Target Product Costs	106
14.0 Testing	107
Miscellaneous	
15.0 Standards and Specifications	107
16.0 Customer Requirements	107
17.0 Competition	108

Function

Design, testing and implementation of an all-wheel drive electric drivetrain. The drivetrain is to include the front corner assembly with integrated Nova 15 motors and a planetary gear reduction of 6.5:1. The rear drivetrain is to incorporate a single speed gearbox to properly mount the motors and place the output shafts in proper alignment with the rear corners while achieving a 4.5:1 reduction.

Client Requirements

The system is to minimize mass and occupied volume, while adequately supporting the load cases and passing the 2017 Formula SAE Electric rules. The design must be adequately documented and training of new Wisconsin Racing members must be conducted to insure proper knowledge transfer. The senior design is to be the stepping stone for Wisconsin Racing to build a solid foundation for the current and future Formula Electric team.

Design Requirements

Physical and Operational Characteristics

1.0 Performance Requirements

<u>Front Drivetrain</u>	<u>Rear Drivetrain</u>
Power to be delivered: 15 kW	30 kW
Input speed: 10,000 rpm	6,000 rpm



Output Speed: 1336 rpm	1336 rpm
Max Vehicle Speed: 70 mph	-same-
Brushless DC Motors	-same-
Low maintenance	-same-
Face mounted Motor	-same-
Liquid cooled	-same-
Regenerative Capability	

Front Brake System

Lock all four tires without tractive system active

2.0 Safety

Set by the Society of Automotive Engineers Formula SAE Electric Competition

Link: <http://students.sae.org/cds/formulaseries/rules/>

Rules for Brakes:

Article 7: Brake System

- EV 2.5
- EV 4.10.2
- EV 5.1.1/ 5.1.7/ 5.1.11/ 5.4/ 5.6
- S2.7.2/ S2.7.3
- S4.18.3
- T7.2
- D1.1.2/ D12.1.3/ D13.1.1

Rules for Drivetrain:

3.0 Accuracy, Quality and Reliability

Proper tolerancing of assembly is crucial to successful operation. Bearing surfaces, motor and planetary transmission alignment, gear meshing and brake caliper piston to rotor alignment will all significantly impact performance. Improper tolerancing of the system can lead to catastrophic failure.

4.0 Life in Service

<u>Front Drivetrain</u>	<u>Rear Drivetrain</u>
Motors: 5 Years	-same-
Transmission: 2 years	-same-
Uprights: 2 years	N/A
Brakes: 2 years	N/A



5.0 Shelf Life

N/a

6.0 Environment

Location: Lincoln Nebraska

Climate: Hot and Humid

Air Temperature: 30 degrees Celsius

Track Surface Temperature:

7.0 Ergonomics

Noise: Gears meshing

Vibration: Minimize transmission vibration. Minimize torque ripple

Responsiveness: To accelerator pedal and brake pedal

8.0 Size

Front Corner Assembly

Width: Fit inside wheel and avoid impact with suspension members

Wheel Center

Inside diameter: Must be toleranced for material expansion fit with ring gear and bearings

Outside diameter: Must be smaller than bolt pattern of wheel shell to allow insertion of mounting fasteners

Brakes

Max outside diameter: must fit within wheel shell bore to allow proper removal

Width: Assembly should be kept as close to the vehicle centerline plane as possible.

Caliper housing: Should be as small as possible to house pistons and fluid routing

Planetary

Sun Gear: Inside spline must be large enough to allow adequate motor shaft size with mating spline sized to prevent failure or slippage;

Motor Spline:

Spline: Must be large enough such that min diameter is greater than the min shaft diameter.

Min shaft diameter: sized to motor torque times a 1.5 safety factor.

Spline Teeth: sized to react motor torque

Ring Gear: Outside diameter must be small enough to allow wheel center press fit without mounting fastener interference.



9.0 Weight

Design architecture, component selection and material selection should all be targeted to minimize mass. Outboard corner mass is a critical parameter for the vehicle dynamics.

Motor: 5.5 lbs

Upright: Less than 1.5 lbs

Brake System: Less than

Overall front hub system mass is to be under 12 lbs

10.0 Materials

Aluminium 7075: Upright, Wheel Center, Brake Hat, Bearing retainers, pillow blocks, caliper housing

Steel: Gears 4140

Brakes:

Magnesium: Brake pistons

Brake Seals:

Bearings: Stainless Steel

Lubrication:

11.0 Aesthetics, Appearance and Finish

The design is to be aesthetically appealing as to inspire confidence in the competition judges. Proper surface finish must be incorporated for all mating surfaces, material treatment must be applied to gears, upright, wheel center and brake hat. Color selection of heat treatment is to be determined by the vehicle livery, information is to be supplied by Wisconsin Racing leaders.

Production Characteristics

12.0 Quantity

Two front hub motor drivetrain assemblies and one rear drive units must be completed. Various components: gears, brake calipers, etc.. will require extra test components. Test components do not need to be one hundred percent representative. Only key parameters must be competition representative.



13.0 Target Product Costs

The drivetrain estimated product cost is \$27,118. Assembly costs include the following. The high initial cost is due to the purchase of four motors and controllers. A price that can be considered as a longer term investment in the formula electric program. The distribution of the motor price over a 4-5 year design cycle decreases the motor and controller cost to \$5,000 per year.

Powertrain				
	Item Description	Total Cost	Sponsorship	Amount Needed
Plettenberg	Nova 15 x2	\$ 4,600.00	\$ -	\$ 4,600.00
	Nova 30 x 2	\$ 9,800.00	\$ -	\$ 9,800.00
	4 Motor Controllers	\$ 6,800.00	\$ -	\$ 6,800.00
Cooling	Spal	\$ 300.00	\$ 300.00	\$ -
	Water Pump	\$ 400.00	\$ 400.00	\$ -
	Cooling Lines	\$ 100.00	\$ -	\$ 100.00
	Coolant Line adapters	\$ 50.00	\$ 50.00	\$ -
Driveline	Planetary Gear Edgerton	\$ 2,000.00	\$ -	\$ 2,000.00
	Rear Transmission Gearing	\$ 2,000.00	\$ -	\$ 2,000.00
	Tripod Housings (2)	\$ 450.00	\$ -	\$ 450.00
	Tripod boots (2)	\$ 18.00	\$ -	\$ 18.00
	Half shafts (2)	\$ 450.00	\$ -	\$ 450.00
Misc.	Fasteners	\$ 100.00	\$ -	\$ 100.00
Lubrication	Planetary Gear lubrication	\$ 50.00	\$ 50.00	\$ -
	TOTAL	\$27,118.00		\$26,318.00

14.0 Testing

Testing should be completed on a component and assembly basis.

Brake System

Max caliper pressure test

Bearing Assembly

Deflection Testing at operating load



Rotor thermal testing
Caliper brake dyno testing

Press fit will be tested upon insertion

Upright
Testing on vehicle during operation

Planetary Assembly
Testing on vehicle during operation

Miscellaneous

15.0 Standards and Specifications

Set by the Society of Automotive Engineers Formula SAE Electric Competition

Link: <http://students.sae.org/cds/formulaseries/rules/>

16.0 Customer Requirements

As per the customer the drivetrain should:

1. minimize the weight of the design
2. minimize gear noise
3. Minimize occupied volume
4. Motors are to be liquid cooled
5. Transmission is to be lubricated
6. System is to be compliant to FSAE Electric rules through 2017
7. Senior design team is to provide adequate documentation and training to FSAE Electric team to insure knowledge transfer. The senior design team is to be a building block to aid in the sustainability for Wisconsin Racing's Electric program.

17.0 Competition

Formula SAE/Formula Student

An extensive competition analysis has been conducted domestically and internationally. Two competitors, one domestic and one internationally have been identified. The University of Michigan-Ann Arbor Formula hybrid team is utilizing the Nova 15 motors for an in-hub assembly. Student designer Jason Hoving is in collaboration with our William Kucinski for the development of the Nova 15 in-hub assembly.

Delft University in the Netherlands was the first Formula Student team to utilize the inverted caliper design with exterior mounted brake system. The university utilized a custom caliper



modeled after the ISR calipers, as the Wisconsin Racing team will model the calipers after a Hayes Performance caliper.

Industry

Industry has multiple in-hub motor assemblies, however their application design specifications and requirements do not lie within the same scope as the FSAE electric vehicles. The patents and designs are useful for comparison but provide less usable designs as compared to the Formula compressions along sharp edges. Additionally, we were able to remove material from the caliper between the piston bores, making the assembly lighter, and compensating for some the mass we added in thickening up the supports. After going through multiple iterations of the caliper housing, we were able to verify that the housing is below the yield strength in all areas during both the normal and the panic braking scenarios; as an added factor of safety, the FEA showed that the caliper housing could withstand a panic braking scenario without taking into account slip of the tire, which would significantly reduce the actual torque seen by the caliper during a hard braking situation.

Safety

Safety is the top priority of this custom build, and, as such, once the custom in-hub assembly is completed extensive testing will be performed on each system.